

**SEQUENCE STRATIGRAPHIC INTERPRETATION METHODS FOR LOW-
ACCOMMODATION, ALLUVIAL DEPOSITIONAL SEQUENCES:
APPLICATIONS TO RESERVOIR CHARACTERIZATION OF
CUT BANK FIELD, MONTANA**

A Dissertation

by

RAHILA RAMAZANOVA

Submitted to the Office of Graduate Studies of
Texas A&M University
in partial fulfillment of the requirements for the degree of

DOCTOR OF PHILOSOPHY

December 2006

Major Subject: Geology

**SEQUENCE STRATIGRAPHIC INTERPRETATION METHODS FOR LOW-
ACCOMMODATION, ALLUVIAL DEPOSITIONAL SEQUENCES:
APPLICATIONS TO RESERVOIR CHARACTERIZATION OF
CUT BANK FIELD, MONTANA**

A Dissertation

by

RAHILA RAMAZANOVA

Submitted to the Office of Graduate Studies of
Texas A&M University
in partial fulfillment of the requirements for the degree of

DOCTOR OF PHILOSOPHY

Approved by:

Co-Chairs of Committee,	Walter B. Ayers, Jr Philip D. Rabinowitz
Committee Members,	Jerry L. Jensen Duane A. McVay Richard L. Gibson
Head of Department,	John H. Spang

December 2006

Major Subject: Geology

ABSTRACT

Sequence Stratigraphic Interpretation Methods for Low-Accommodation, Alluvial
Depositional Sequences: Applications to Reservoir Characterization of
Cut Bank Field, Montana. (December 2006)

Rahila Ramazanova, B.S., Azerbaijan Oil Academy;

M.S., Texas A&M University

Co-Chairs of Advisory Committee: Dr. Walter B. Ayers, Jr.
Dr. Philip D. Rabinowitz

In South Central Cut Bank Sand Unit (SCCBSU) of Cut Bank field, primary production and waterflood projects have resulted in recovery of only 29 % of the original oil in place from heterogeneous, fluvial sandstone deposits. Using high-resolution sequence stratigraphy and geostatistical analysis, I developed a geologic model that may improve the ultimate recovery of oil from this field.

In this study, I assessed sequence stratigraphic concepts for continental settings and extended the techniques to analyze low-accommodation alluvial systems of the Cut Bank and Sunburst members of the lower Kootenai formation (Cretaceous) in Cut Bank field. Identification and delineation of five sequences and their bounding surfaces led to a better understanding of the reservoir distribution and variability.

Recognition of stacking patterns allowed for the prediction of reservoir rock quality. Within each systems tract, the best quality reservoir rocks are strongly concentrated in the lowstand systems tract. Erosional events associated with falling base-level resulted in stacked, communicated (multistory) reservoirs. The lowermost Cut

Bank sandstone has the highest reservoir quality and is a braided stream parasequence. Average net-to-gross ratio value (0.6) is greater than in other reservoir intervals. Little additional stratigraphically untapped oil is expected in the lowermost Cut Bank sandstone. Over most of the SCCBSU, the Sunburst and the upper Cut Bank strata are valley-fill complexes with interfluves that may laterally compartmentalize reservoir sands. Basal Sunburst sand (Sunburst 1, average net-to-gross ratio ~0.3) has better reservoir quality than other Sunburst or upper Cut Bank sands, but its reservoir quality is significantly less than that of lower Cut Bank sand.

Geostatistical analysis provided equiprobable representations of the heterogeneity of reservoirs. Simulated reservoir geometries resulted in an improved description of reservoir distribution and connectivity, as well as occurrences of flow barriers.

The models resulting from this study can be used to improve reservoir management and well placement and to predict reservoir performance in Cut Bank field. The technical approaches and tools from this study can be used to improve descriptions of other oil and gas reservoirs in similar depositional systems.

To my family...

ACKNOWLEDGEMENTS

I wish to express my sincere gratitude to my advisor, and co-chair of my committee, Professor Walter B. Ayers, Jr. for his expert guidance, stimulating suggestions, advice and evaluation in putting together this thesis and for his tremendous support throughout the course of this study. Special thanks, also, go to Professor Philip Rabinowitz, for his support, for serving as a co-chair of my committee, and for his unforgettable kindness during my stay in College Station. Moreover, I would like to express my appreciation to professors Duane McVay, Jerry Jensen, and Richard Gibson for their contributions, and feedback, and for giving me the opportunity to be part of their Reservoir Studies group together with Professor Ayers, use their lab and resources and for serving as committee members. This research benefited from the group's studies on Cut Bank field, and financed part of my study as a graduate research assistant.

I, also, would like to thank the staff of the Department of Geology and Geophysics at Texas A&M University for their partial financial support through a teaching assistantship and several fellowships and for their help in making this research project reach the final stage. Also, I am honored that ConocoPhillips Petroleum Corp. awarded me the ConocoPhillips Spirit Scholarship and I wish to thank them for the financial assistance it gave me to complete my degree work.

I thank Quicksilver Resources Co., who made this study possible by the donation of their digital data and access to their hard copy files and cores. Special thanks to Mr. Peter Bastian for gathering the data set and other supporting material on the field and for helping me understand it. These contributions represent an integral part of this study.

I could not go through this process without the never ending support and encouragement from my dear husband, Dr. Masoud Hajiaghajani. I wish to express my utmost gratitude to him and to acknowledge that this dissertation would have been impossible without his assistance, care and love. My daughter, Mariam, has been wonderful blessing and an inspiration to further my studies. I would like to extend my thanks and admiration to my parents, brothers and sisters for their invaluable support through this endeavor of mine.

Many thanks to the teachers of the Department of Geology and Geophysics and to Texas A&M University for being a good host. Finally, my thanks go to all of my friends and colleagues for sharing both the tough and the sweet moments at Texas A&M University.

TABLE OF CONTENTS

	Page
ABSTRACT	iii
DEDICATION	v
ACKNOWLEDGEMENTS	vi
TABLE OF CONTENTS	viii
LIST OF FIGURES	x
LIST OF TABLES	xix
 CHAPTER	
I INTRODUCTION	1
1.1 Research Objectives	6
1.2 Methodology	6
II GEOLOGICAL OVERVIEW OF CUT BANK FIELD, MONTANA	11
2.1 Location of Study Area	11
2.2 Field Overview	15
2.2.1 Reservoir Properties	15
2.2.2 Field History	17
2.3 Lithologic and Stratigraphic Framework	20
2.4 Provenance	27
2.5 Depositional Environment	28
2.6 Framework Composition and Texture	32
2.6.1 Composition	32
2.6.2 Sedimentary Structures	35
2.7 Hydrocarbon System	36
III EVALUATION AND LIMITATION OF DATA	39
3.1 Database	39
3.2 Assessing Data Quality	40
3.3 Evaluation of Previous Geological Maps	43
3.4 Porosity Calculation	46

CHAPTER	Page
3.5 Integration of Seismic and Well Log Data	53
IV FACIES ANALYSIS	64
4.1 Lithofacies Interpretation	64
4.2 Lithofacies Descriptions from Cores.....	65
4.3 Depositional Model	71
4.4 Channel Geometry.....	74
V SEQUENCE STRATIGRAPHY	80
5.1 Sequence Stratigraphy Model	80
5.2 Sequence Stratigraphic Surfaces	87
5.3 Sequence Stratigraphic Interpretation	92
5.4 Stacking Pattern.....	103
5.5 Description of the Conceptual Low Accommodation Alluvial System Sequence Stratigraphic Model	105
5.6 Reservoir Geometry and Compartmentalization.....	107
VI GEOSTATISTICAL MODELING	110
6.1 Reservoir Geostatistical Model	110
6.2 Vertical Proportion Curve	119
6.3 Variogram Computation.....	121
VII INTEGRATING PRODUCTION TRENDS WITH THE RESERVOIR MODEL.....	125
VIII DISCUSSION	136
IX CONCLUSIONS AND RECOMMENDATIONS	139
REFERENCES CITED	143
VITA	154

LIST OF FIGURES

	Page
Figure 1. Cut Bank field is located in Glacier, Pondera, and Toole Counties, northwest Montana (from, DeAngelo and Hardage (2001)).	2
Figure 2. Cut Bank Field – Stratigraphic section (modified from Dolson and Piombino, 1994).	3
Figure 3. Location of Cut Bank field relative to major structures (Modified from Balster et al., 1976).	12
Figure 4. Generalized structure top of Ellis Group, Cut Bank field. Shaded area corresponds to oil leg. Outlines are Cut Bank Units and 3-D seismic survey area. A-A' shows the location of diagrammatic well cross section (modified from Gully, 1984).	13
Figure 5. Structure map of the base of the Cut Bank sandstone (top of Ellis Group) in SCCBSU area (Datum is mean sea level).	14
Figure 6. Diagrammatic cross section A-A', Cut Bank field. See Figure 3 for location (Modified from Gully, 1984).	16
Figure 7. Oil production history of the Cut Bank Field from year 1932 to 1962 (Cupps and Fry, 1967).	18
Figure 8. SCCBSU water flood expansion history (from Quicksilver Resources, 2002).	19
Figure 9. SCCBSU production and injection history from year 1969 to 1998 (data from Quicksilver Resources, 2002).	20
Figure 10. Cut Bank field – Type Log, Well SCCBSU #51-6. GR –gamma ray, NØ-neutron porosity, DØ-density porosity.	21
Figure 11. South Central Cut Bank Sand Unit (SCCBSU) well base map. Green shaded area corresponds to Lower Cretaceous Gorge where the “Tinroof” is absent (from Quicksilver Resources, 2002).	24

	Page
Figure 12. Stratigraphic cross section A-A' (See Figure 11 for location). Vertical Exaggeration=10.6667.....	25
Figure 13. West to east seismic section (See Figure 11 for location). Tinroof is cut by incised valley-Lower Cretaceous Gorge.....	26
Figure 14. Cut Bank field – depositional setting (after Dolson and Piombino, 1994).....	30
Figure 15. Cut Bank Field -Ternary plot of framework composition of Cut Bank sandstone. Sandstone framework composition is composed of quartz, silicified carbonate clasts, and argillaceous chert clasts (from Horkowitz, 1987).....	33
Figure 16. Cut Bank Field - Relationship between grain size and composition of Cut Bank sandstone: a) quartz content; b) silicified carbonate clast content (Chert-B); c) siliceous mudstone clast content (Chert-A) (from Horkowitz, 1987).....	34
Figure 17. Migration routes of Bakken oil through Mississippian strata and lowermost Jurassic Sawtooth strata (arrows). Structure, top of Sun River Dolomite (in feet) (uppermost Medison Group) (Dolson and Piombno, 1994).....	38
Figure 18. Plot of types of logs in the well logs database.....	39
Figure 19. SCCBSU well base map with log data. Red are wells with core data. Well 54-8 has VSP data.....	40
Figure 20. QRI/BEG net sand thickness (Quicksilver Resources, 2002) contours >15 ft superposed on the average absolute seismic amplitude map. Generally, higher average absolute amplitude corresponds to greater net sand thickness.	44
Figure 21. There is no correlation between net sand thicknesses from well logs (based on 60% GR and 10% porosity cutoff) and average absolute seismic amplitude.	45
Figure 22. Well 37-7 - Core-well log porosity calibration for lower Cut Bank Sand.....	48

	Page
Figure 23. Core porosity-permeability crossplot. There is no relationship between permeability and porosity less than 10% porosity line (low porosity and permeability usually are in fine-grained sand). It appears there is a relationship above this line. The trend lines are hand drawn.....	49
Figure 24. Core vs. density porosity comparison for all cored wells in the Cut Bank Sand.	51
Figure 25. Neutron-density average porosity values for net pay in the lower Cut Bank Sand. Net pay is based on a 10% porosity cutoff.....	52
Figure 26. Seismic inline 145 displaying upper, middle , and lower bounding stratal surfaces the resolution of seismic data in the interval between Tinroof shale and Ellis group at the VSP well. Red curve is GR log.....	54
Figure 27. Relation between the log neutron-density average porosity and 3-D seismic amplitude at the well ties. Each point represent a well with a given single character name. The empty squares are the excluded wells. Significance F =0.000706847 or 0.0707%.	57
Figure 28. Maximum amplitude of lower Cut Bank horizon. Red is highest amplitude and blue is lowest. Red polygons around wells 49-10 and 39-4 are areas of mismatch	58
Figure 29. Seismic inline 286 displaying upper, middle , and lower bounding stratal surfaces. Notice the bottom of lower Cut Bank interval, or top of Ellis, is at the zero crossing above the positive amplitudes (Location on Figure 28).....	59
Figure 30. Seismic inline 163 displaying upper, middle , and lower bounding stratal surfaces. Maximum amplitude at Well 49-10 is anomalously high compared to the average log porosity value. One reason for that may be inconsistent interpretation of the bottom of the lower Cut Bank strata in this area. This surface is at the zero crossing above the positive amplitudes all over the seismic survey (see Figure 29) except in the problem area (Location on Figure 28).	60

- Figure 31. Seismic inline 235 displaying upper, middle, and lower bounding stratal surfaces. In Well 39-4 the maximum amplitude value under-predicts the porosity. One of the reason may be inconsistency of interpretation of lower Cut Bank interval in well log and seismic intepretation. Middle of Cut Bank interval in seismic does not correspond to the top of lower Cut Bank interval (Location on Figure 28). 61
- Figure 32. Log-pattern (electrofacies) facies overlain on Quicksilver Resources gross thickness map of lower Cut Bank sand (Quicksilver Resources, 2002). Red curve is GR log increasing from 0 to 150 API from left to right, light blue is cased GR, dark blue is old GR logs. Log patterns are blocky in the mid-channel deposits and upward fining or serrated at the channel margins. Thickness decreases markedly, and the log patterns are serrated or sometimes upward-fining in interchannels. 66
- Figure 33. Calibration of the well log signature of lithofacies to the core, Well 37-7. Six of the seven lihofacies identified in cores were found in cores and calibrated to log data in this well. For lithofacies 7 see Figure 34. Numbers in white boxes on each core photograph correspond to lithofacies number in Table 2. 68
- Figure 34. Calibration of the well logGR signature of lithofacies 7 to the core, Well 33-5. 69
- Figure 35. Analog field-reconstruction of the depositional environments in Chaunoy field (from Lemouzy et al., 1995). 73
- Figure 36. West to east well log stratigraphic cross section B-B' from the north of SCCBSU area (See figure 11 for location). Vertical Exaggeration=10.6667..... 75
- Figure 37. Frequency distribution of lower Cut Bank sandbody thickness to define the single story channel thickness..... 78
- Figure 38. Log patterns of lower Cut Bank sandstone bodies: a) the GR log pattern in 5-20 ft thickness interval is mostly blocky; b) the sandbodies above 20 ft thick are multistory, with complex stacking pattern. In some cases thin shale interlayers are observed, clearly showing vertical stacking of several channels. 78

Figure 39. Conceptual framework for bounding surface development driven by cyclic base-level fluctuation. (1) Base-level fall leads to the development of a regional erosion surface with incised valleys, sequence boundary 1 (SB1). (2) Low rates of base-level rise/aggradation and confinement of rivers within the valley produce a sand-rich valley fill that can be capped by a significant base-level rise or flooding surface 1 (FS1). (3) Higher rates of base-level rise/aggradation and a wide, nonconfined alluvial plain leads to the preservation of isolated channels within mudstone-rich overbank deposits. (4) Renewed base-level fall causes the development of the next regional erosion surface (SB2), and so on (from MacDonald et al (1998) after Shanley and McCabe (1991)).....	82
Figure 40. Core description, well log profile and sequence interpretation of Well 38-11.	84
Figure 41. Stratigraphic cross section along line 13 (location on Fig. 42) showing the two-part subdivision of sequences. A sheet-like sandbody comprises the base of the succession, whereas the upper part consists of overbank mud.	85
Figure 42. Locations of the cross sections lines (there are 18 lines, line numbers increase from north to south) overlain on thickness map from Tinroof to Ellis.	88
Figure 43. Synthetic reconstruction of the reservoir geometry in SCCBSU with short term base-level cycle interpretation. FS1-FS5 are flooding surfaces. Red square at the top of the well shows there are core data for that well. Green correlation line is Tinroof shale that correspond to FS5 or maximum flooding surface (MFS). Correlation is illustrated by GR (on the left) and porosity logs (on the right red density porosity, green neutron porosity).....	89
Figure 44. Sequence stratigraphic correlation/interpretation along Line 13. Five sequence boundaries and four flooding surfaces were identified between Tinroof and Ellis Group. Color filled part of each sequence corresponds to “VF” (valley fill), and white is “HS” (highstand). Valley fills are amalgamated, continuous channel fills, therefore have best reservoir quality and connectivity. Highstands consist of channel fills isolated within flood plain shales.	90

- Figure 45. Cross section showing interpretation of sequence stratigraphic surfaces and cored interval (thick black vertical lines). There is no horizontal scale because the section was constructed using equal distance between wells, just to show all cored wells on the same cross section. Map on the right shows the location of cross section. Available core data is mostly from valley fill of Sequence 1 (VF1), except well 33-5. 91
- Figure 46. Isopach map of valley fill of Sequence 1 (VF1, gross thickness from FS1 to SB1). Points indicate location of wells used to draw the map. Contour interval is 2.5 ft. 93
- Figure 47. Net-to-gross ratio map of the valley fill of Sequence 1 (VF1, gross thickness from FS1 to SB1) (lower Cut Bank). Contour interval is 0.1. 94
- Figure 48. Isopach map of valley fill of Sequence 2 (VF2, gross thickness from FS2 to SB2). Points indicate location of wells used to draw the map. Contour interval is 2.5 ft. 96
- Figure 49. Net-to-gross ratio map of valley fill of Sequence 2 (VF2, gross thickness from FS2 to SB2) (upper Cut Bank). Contour interval is 0.1. 97
- Figure 50. Isopach map of valley fill of Sequence 3 (VF3, gross thickness from FS3 to SB3). Points indicate location of wells used to draw the map. Contour interval is 2.5 ft. 99
- Figure 51. Net-to-gross ratio map of valley fill of Sequence 3 (VF3, gross thickness from FS3 to SB3) (Sunburst 1). Contour interval is 0.1. 100
- Figure 52. Isopach map of valley fill of Sequence 4 (VF4, gross thickness from FS4 to SB4). Yellow dots indicate location of wells used to draw the map. Contour interval is 2.5 ft. 101
- Figure 53. Isopach map of valley fill of Sequence 5 (VF5, gross thickness from Tinroof to SB5). Points indicate location of wells used to draw the map. Contour interval is 2.5 ft. 103

Figure 54. Stratigraphy developed in low accommodation alluvial setting. Deposits of lowstand or valley fill are dominated by both vertically and laterally amalgamated units. Base-level fall leads to closely spaced unconformities which corresponds to base of these amalgamated units , sequence boundaries (SB1, SB2, SB3). Low rates of base-level rise produce a sand-rich valley fill that is capped by a significant base-level rise or flooding surface 1 (FS1). Higher rates of base-level rise leads to the preservation of isolated channels within mudstone-rich overbank deposits. Renewed base-level fall causes the development of the next erosion surface (SB2, SB3), and so on.	106
Figure 55. North-south and west-east cross section showing sequence stratigraphic correlation in the interval between Ellis top at the bottom and combined Tinroof and Lower Cretaceous surface at the top. VF-valley fill, HS-highstand.	113
Figure 56. 3D Sgrid model bounded by combined Tinroof and Lower Cretaceous Gorge base surface at the top and Ellis at the bottom.	114
Figure 57. North-south and west-east cross sections of the facies realization (vertical exaggeration= 20).	116
Figure 58. 3-D view of the facies realization in valley fill of Sequence 1 (VF1), lower Cut Bank (vertical exaggeration= 50).	116
Figure 59. North-south and west-east cross section of the porosity realization (vertical exaggeration=20).	118
Figure 60. 3-D view of the porosity realization in valley fill of Sequence 1 (VF1), lower Cut Bank (vertical exaggeration=50).	118
Figure 61. Vertical proportion curve of lithotypes computed with 169 wells for the whole series. The five cycles are clearly shown in the curve, with sandstone peaks grading to mudstone peaks. Reservoir units correspond to the series between two mudstone spikes, corresponding to the maximum flooding surface of the base-level cycles.	120

Figure 62. Lithofacies vertical and areal variogram model for study interval (UVW coordinate and indicator transformation applied). UVW transformation was used for SGrid. UVW are local coordinates of SGrid and these coordinates are different than XYZ coordinates. Short-scale variance represents a nugget effect; intermediate-scale variance represents geometric anisotropy; and large-scale variance represents zonal anisotropy.....	122
Figure 63. Lower Cut Bank net sand thickness map (QRI/BEG) (from Quicksilver Resources, 2002) overlain by cumulative production bubble map (McVay et al., 2004). There is a clear correlation between cumulative production and reservoir net thickness, i.e. high production trend correspond to high net-reservoir thickness in most areas excluding the highlighted wells.....	127
Figure 64. Lithofacies map realization at valley fill of Sequence 1 (VF1) overlain by cumulative production bubble map.....	128
Figure 65. Porosity map realization of valley fill of Sequence 1 (VF1) overlain by cumulative production bubble map. White areas correspond to porosity values less than 8%.....	129
Figure 66. Lower Cut Bank cumulative production vs VF1 facies realization times porosity realization (facies*porosity). There is a general increasing trend of cumulative production with the increase of facies*porosity, with a large scatter.....	130
Figure 67. Lower Cut Bank cumulative production vs QRI/BEG net thickness [(net thickness data were estimated from QRI/BEG net thickness map (Quicksilver Resources, 2002)]. The general trend between QRI/BEG net thicknesses and lower Cut Bank cumulative production is expressed weaker and the scatter is larger than lower Cut Bank cumulative production vs facies*porosity (Fig. 66).....	131
Figure 68. Lithofacies map realization at valley fill of Sequence 1 (VF1) overlain by arrow plots. λ (fraction of flow in a producer attributable to flow at an injector) is large in sand zones and small in shale zone.....	132
Figure 69. Porosity map realization at valley fill of Sequence 1 (VF1) overlain by arrow plots. White area corresponds to porosity values less than 8%.....	133

Figure 70. Lithofacies map realization at valley fill of Sequence 1 (VF1) overlain
by net-to-gross ratio contours of VF1 constructed using well logs. 135

LIST OF TABLES

	Page
Table 1. Summary of core porosity and density porosity calibration through cross-plotting.	47
Table 2. Main Cut Bank Sandstone lithofacies characteristics from core data from 6 wells, my description of four cores (wells 38-11, 36-5, 33-5 and 39-1X) , and two core descriptions (wells 37-7 and 22-6) obtained from QRI.	67
Table 3. Dimensions of the geostatistical GOCAD model.	112

CHAPTER I

INTRODUCTION

1.1 Statement of Problem

A stripper oil well is an oil well that produces less than 10 barrels (10 bbl) of oil per day (Remson, 2005). In the United States, 400,000 stripper wells produce 300 million bbl of oil annually and account for 15% of the U.S. domestic oil production (DOE, 2005).

Opportunities for oil reserves growth occur in depleting reservoir stripper well fields owing to heterogeneities that prevent mobile hydrocarbons from migrating to well bores. At the South Central Cut Bank Sand Unit (SCCBSU) of Cut Bank Field, Montana (Fig. 1), primary production and waterflood projects have resulted in production of only 29 % (43 million bbls of the original 150 million bbls) of oil in place in complex, heterogeneous sandstone reservoirs. Part of this research was funded by Quicksilver Resources, Inc., who seeks to develop a list of infill and recompletion candidate wells and production enhancement strategies in SCCBSU. Oil production at SCCBSU is from fluvial channel-fill sandstone of the Cut Bank and Sunburst members of the Kootenai Formation (Fig. 2). The Cut Bank and Sunburst members are composed of sedimentary alluvial sequences with multiple scales of heterogeneity that give rise to complex sedimentary facies distributions that often appear to be chaotic and unpredictable. To optimize oil production from Cut Bank and Sunburst reservoirs requires a detailed

This dissertation follows the style and format of the Bulletin of American Association of Petroleum Geologists (AAPG).

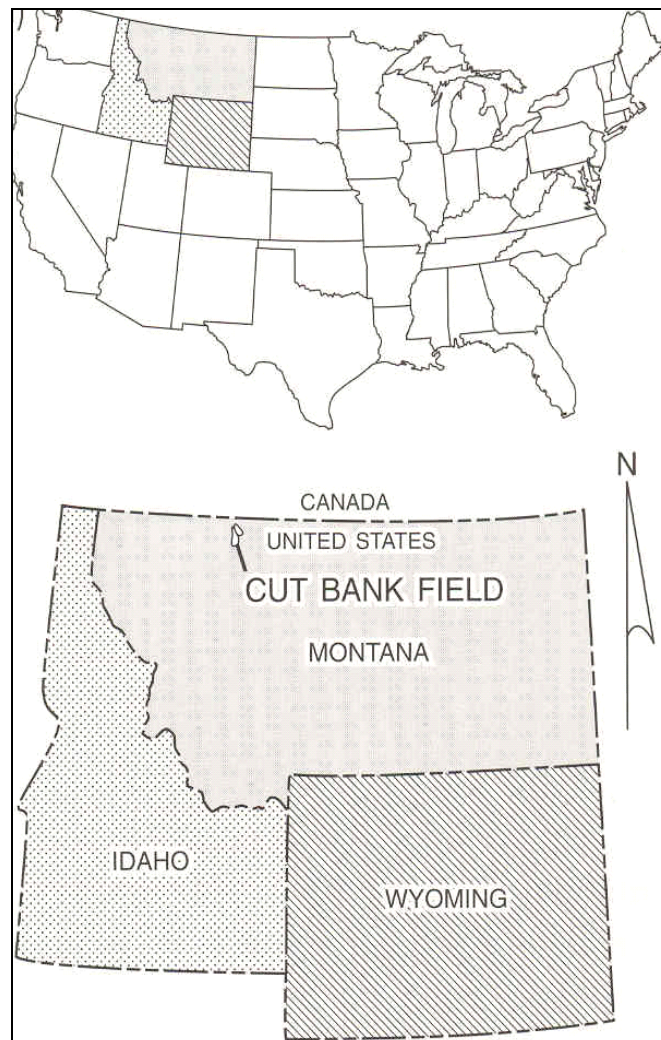


Figure 1. Cut Bank field is located in Glacier, Pondera, and Toole Counties, northwest Montana (from, DeAngelo and Hardage (2001)).

reservoir model that allows prediction of (a) reservoir shape and size, (b) lateral continuity and degree of interconnectedness of sandstones and interbedded mudrocks, and (c) the internal heterogeneity of reservoir sand bodies using geophysical, geological and engineering data. However, it is difficult to model such reservoirs accurately,

Mesozoic	Lower Cretaceous	Kootenai Fm.	Flood Ss.
			Fuson Shale
			Calcareous Mbr.
			Moulton Ss. ● ●
			Sunburst Ss. ● ●
	Cutbank Ss. ● ●		
	Jurassic	Ellis Group	Morrison Fm.
			Swift Fm.
			Rierdon Fm.
			Sawtooth Fm.
Paleozoic	Mississippian	Madison Group	Sun River Dol.
			Mission Canyon Ls.
			Lodgepole Ls.
			Bakken/Exshaw
	Devonian		Three Forks Fm.
			Potlach Fm.
			Nisku Fm.
	Duperow Fm.		
	Souris River Fm.		

Figure 2. Cut Bank Field – Stratigraphic section (modified from Dolson and Piombino, 1994).

because individual channel units are thin and discontinuous, which causes well-to-well correlations to be problematic and the geometry of individual channels nearly impossible to estimate. Also, seismic resolution was insufficient to define individual channels.

An approach to evaluating complex stratigraphic units is to use high-resolution stratigraphy to provide a stratigraphic framework that may reduce the risk of miscorrelations between different genetic units. These detailed stratigraphic models can be used to predict reservoir extent and architecture (Gardner and Cross, 1994). However, sequence stratigraphic principles and techniques were developed for marine strata. The application of sequence stratigraphy to nonmarine strata is the topic of intense debate and controversy, and many fundamental concepts are still being developed (Schumm, 1993; Shanley and McCabe, 1994; Blum, 1994; Aitken and Flint, 1995; Currie, 1997; Zaitlin et al., 2002). Recognition of sequences in alluvial settings is difficult because of the scarcity of marker horizons, the lack of biostratigraphic aids, the discontinuous nature of alluvial strata, and the lack of regionally extensive outcrops. Efforts to extend the sequence stratigraphic concepts inland to continental sediments have succeeded only where the fluvial strata were located relatively near coastal marine environments (Wood, 1996; Zaitlin et al., 2002). This research strives to apply sequence stratigraphic analysis to the Cut Bank and Sunburst members of the Kootenai formation. These strata are braided-to-meandering fluvial sediments that were deposited as incised valley fill in an accommodation-limited alluvial setting (Shelton, 1967; Weimer and Tillman, 1982; Berkhouse, 1985; Horkowitz, 1987; and Hopkins, 1993). This setting is characterized by a paucity of marine deposits, low sedimentation rates and closely spaced unconformities. Therefore, the challenge in this study was to establish a stratigraphic framework upon which interpretation and extrapolation of reservoir facies could be based. The approach that I present here, is to build on an existing conceptual stratigraphic framework, based

on base-level variation, that can determine sequence boundary and systems tract geometries. Prediction of facies distributions within each sequence is possible, because specific depositional patterns are expected to occur in predictable positions within the sequence. Well log sequence stratigraphy helps to clarify the geometry, continuity and distribution of the reservoir sands both vertically and laterally.

In many cases, conceptual models at the scale of the reservoir unit are essential, but their accuracy commonly is insufficient to predict the distribution of internal heterogeneities within reservoir units (Haldorsen and Damsleth, 1990). Furthermore, fluid-flow modeling requires a gridded representation of the facies distribution, which must be further transformed to represent petrophysical properties. Stochastic approaches are now more frequently applied to simulate the distribution of small-scale sedimentary bodies and internal reservoir heterogeneity (MacDonald et al., 1998). Geostatistical approaches also rapidly provide equiprobable realizations of the heterogeneity distribution. Multiple realizations can be used to evaluate the impact of different possible facies distributions on fluid-flow simulation, which can help to optimize a field development plan.

The issues discussed above motivated me to apply an integrated approach, combining both deterministic and geostatistical approaches to build a realistic model of the reservoir. This study combines both deterministic and geostatistical approaches. Sedimentological and sequence stratigraphic analyses were performed first and contributed to defining the reservoir layers. Within this framework, geostatistical simulations provided different realizations of the small-scale geological heterogeneities.

1.2 Research Objectives

The overall objective of this study was to improve ultimate recovery of oil from Cut Bank sandstone by characterizing reservoir heterogeneity. Specific objectives for this research were to:

- A. develop and assess a technique to apply sequence stratigraphic analysis in low-accommodation alluvial settings and perform a high-resolution sequence stratigraphic analysis of the Cut Bank and Sunburst sands;
- B. identify sedimentary structures and hierarchies to recognize potential reservoir compartments within the low-accommodation stratigraphic sequence framework using core and well log data and publications;
- C. predict the spatial distribution of petrophysical properties and reservoir connectivity by modeling reservoir facies using conceptual stratigraphic concepts and geostatistical simulations; and
- D. integrate results of the geologic assessment with previous results of production analysis to evaluate geological controls on reservoir performance and potential for improved oil recovery.

1.3 Methodology

This study involved building a detailed earth model to accurately define the geologic framework. The stratigraphy of the reservoir was defined using high-resolution sequence stratigraphic analysis and facies modeling.

- A. High-resolution sequence stratigraphy.

I performed a high-resolution sequence stratigraphic analysis of the lower Cut Bank, upper Cut Bank, and Sunburst members of the Kootenai formation based on analysis of high-frequency fluctuations of base-level. As part of this study, I correlated well logs from 144 wells to assess relationships between base-level variations and channel amalgamation. In low-accommodation settings, the style of depositional fill is marked by abrupt stratigraphic and spatial change, in comparison to high-accommodation settings. Individual sequences can be differentiated by their texture and composition (different fill patterns). Sequence boundaries are immediately overlain by laterally amalgamated fluvial sheet deposits that have high percentages of interconnected, coarser-grained, channel-fill sandstone. I investigated amalgamated units, erosional truncation by the overlying strata, and presence of soil horizons to identify the multiple, closely spaced unconformities. My approach of establishing a reliable high-resolution, reservoir stratigraphy is based on the following specific steps:

1. identification of chronostratigraphic surfaces;
2. determination of the correlatable thin shale units and their relative stratigraphic positions; and
3. identification of the bounding hiatal surfaces that separate genetic units and record significant interruptions in basin depositional history, such as shut-off of sediment supply or switch of sediment source, owing to avulsion on floodplain, a rapid climate change, or base-level shift.

The method I used to realize high-resolution stratigraphic correlations consists of (1) establishing sedimentary facies, facies associations, and facies successions from cores

and well logs, (2) inferring depositional processes from the facies, (3) interpreting sedimentary environments from the combinations of inferred processes, (4) identifying individual genetic sequences and their well-log signatures, and (5) reconstructing the genetic sequence stacking pattern. Reservoir stratigraphic analysis can be used to constrain simulations of facies or petrophysical architecture within each stratigraphic unit.

B. Internal sedimentary structures and hierarchies

Continental clastic reservoirs are commonly highly heterogeneous, with marked barriers or baffles to fluid flow. These barriers and baffles can be simple or highly complex in terms of three-dimensional geometries. Therefore, it is important to analyze internal sedimentary structures and hierarchies, which elucidate presence of barriers and baffles, to assess potential reservoir compartments. Depositional processes result in predictable facies and spatial patterns of reservoir properties (thickness, porosity, and permeability) in clastic sedimentary rocks. Moreover, each facies exerts a characteristic influence on fluid flow through the rock. Knowledge of these characteristics can help geologists and reservoir engineers determine the most appropriate ways of representing permeability in numerical simulations in order to predict reservoir performance. To clarify facies characteristics, I used the following approach.

1. I analyzed 200 ft of core from 6 wells, well logs, and publications to assess the depositional processes, grain size and types, sedimentary structures, hierarchies with the objective of recognizing evidence of potential compartments and interchannel strata as well as intrachannel permeability barriers.

2. I integrated seismic and well log data to determine which seismic attributes can be used to map reservoir properties. At Cut Bank field, seismic attributes were compared with well log porosities to establish a correlation and to model the porosity distribution throughout the field. The nature and strength of the relationship were investigated by plotting the porosity at each well against the seismic attributes at that well. Issues to be addressed when employing the seismic-guided log property mapping technique include the scarcity of available porosity values from well logs (in the Cut Bank dataset, neutron-density average porosity is most reliable) and the low resolution of seismic data makes it tenuous to use for mapping reservoir parameters.

C. Spatial distribution of petrophysical properties

To predict the spatial distribution of petrophysical properties, and to address the issues of reservoir connectivity, I built a geological model populated with reservoir parameters and used geostatistical studies to provide equiprobable representations of the geological heterogeneity of the main reservoir units.

D. Integrating trends in fluid flow with reservoir architecture

Integrating production behavior and fluid flow trends with reservoir architecture are critical steps to identifying heterogeneities within the reservoir and developing three-dimensional flow-unit models that can be used to predict untapped compartments. Coincidences among the spatial positions of reservoir quality, structural setting, and production trends are key to recognizing heterogeneities and controls on production. For Cut Bank field, this comparison was accomplished by relating production performance

maps with geologic and reservoir-quality maps. Areas of high reservoir quality predicted by the geologic analysis should coincide with fairways of high transmissivity of fluids and high production rates. Breaks in production trends that coincide with facies changes or structural discontinuities confirm the integrity of the model. To detect reservoir heterogeneities and test the validity of the geologic model, I integrated maps of the geologic parameters at the genetic-unit level with the production performance analysis results from previous studies by Texas A&M University (McVay et al., 2004).

CHAPTER II

GEOLOGICAL OVERVIEW OF CUT BANK FIELD, MONTANA

2.1 Location of Study Area

Oil and gas production in Cut Bank field is from shallow Cretaceous sands on the west flank of the Sweetgrass arch, approximately 25 mi west of the crest of Kevin-Sunburst dome (Fig. 3) (Blixt, 1941). The gentle dip (1° SW) of strata on the west flank of the Kevin-Sunburst dome is illustrated by the structure of the top of the Ellis Formation (base of the Cut Bank sandstone) in the field area (Fig. 4). Dip is 80 to 100 ft per mile to the west-southwest. There is no evidence of faults in the field. Because the Cut Bank sand erosionally overlies the Ellis formation, the map shows minor irregularities of Ellis topography as well as local folds (Fig. 5).

Cut Bank Field is a long, narrow oil-leg on the downdip (west) side of a larger stratigraphic trap. The oil producing leg is 30 miles long and ranges in width from less than 2 miles near the northern end to about 6 miles near the southern end. Probably less than 80 percent of this area can be considered oil productive, because many dry holes and abandoned wells are interspersed with producing wells. The gas-oil contact of the Cut Bank sandstone is at approximately 1,040 ft. The Cut Bank water contact is tilted, cutting across structural contours from 600 ft on the west to 1,300 ft on the northeast (Fig. 4) (Gully, 1984). Origin of tilted water contact is not understood and is not investigated in this study because it is not part of research, owing to lack of data.

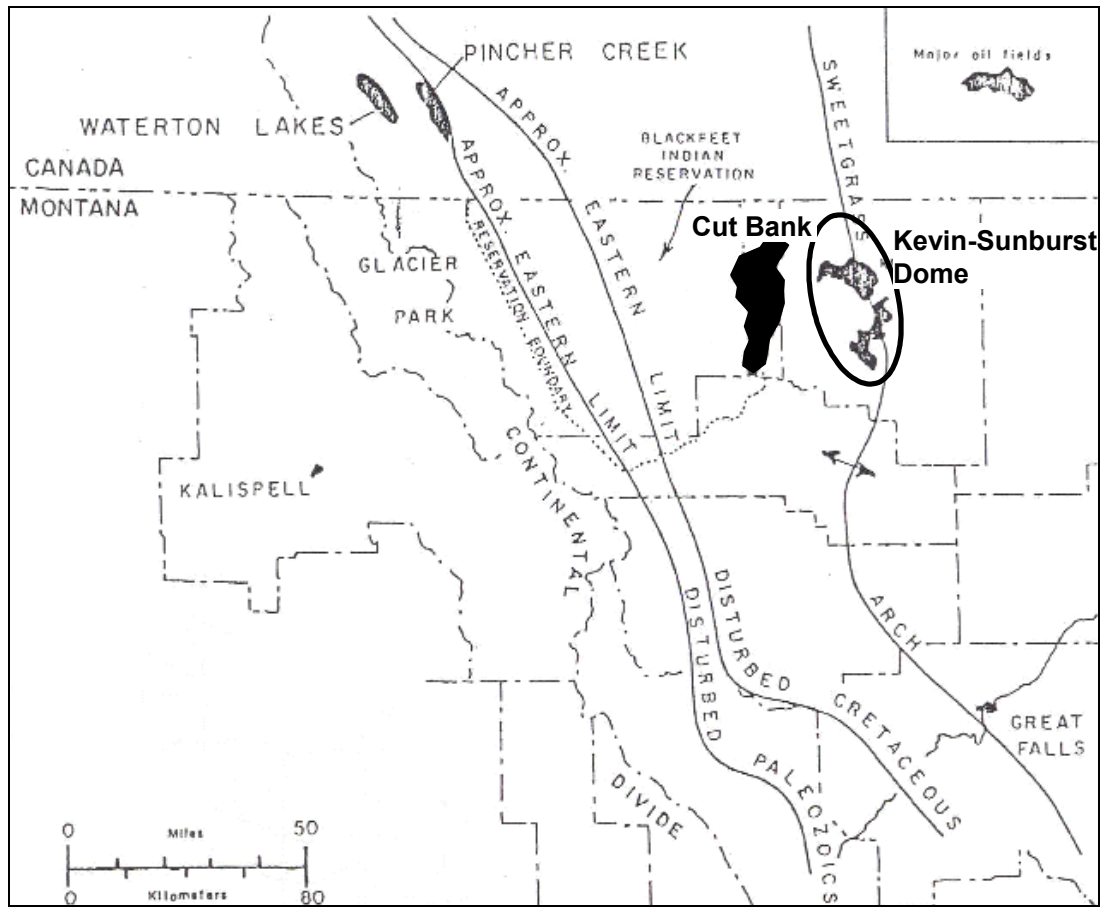


Figure 3. Location of Cut Bank field relative to major structures (Modified from Balster et al., 1976)

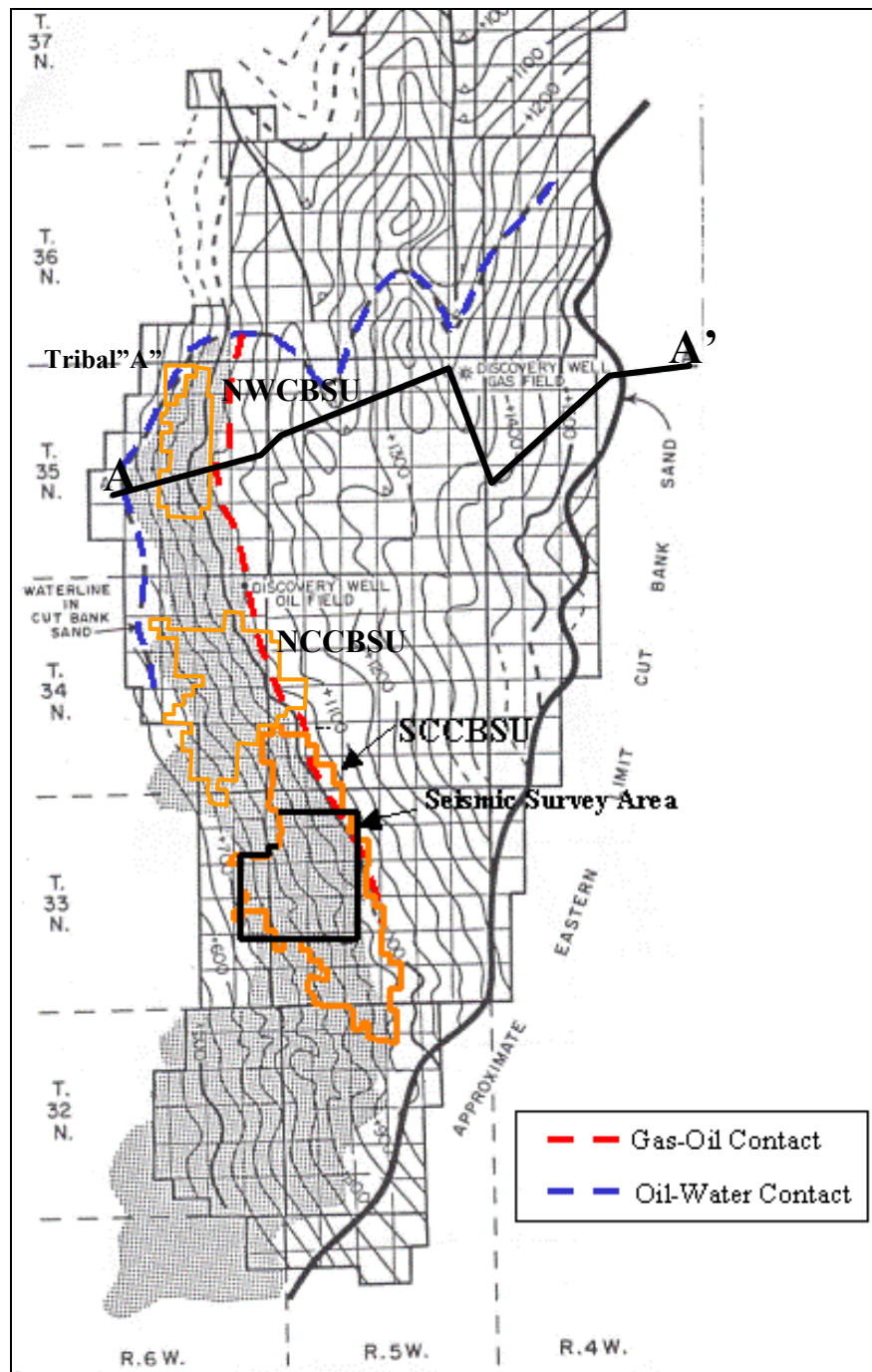


Figure 4. Generalized structure top of Ellis Group, Cut Bank field. Shaded area corresponds to oil leg. Outlines are Cut Bank Units and 3-D seismic survey area. A-A' shows the location of diagrammatic well cross section (modified from Gully, 1984).

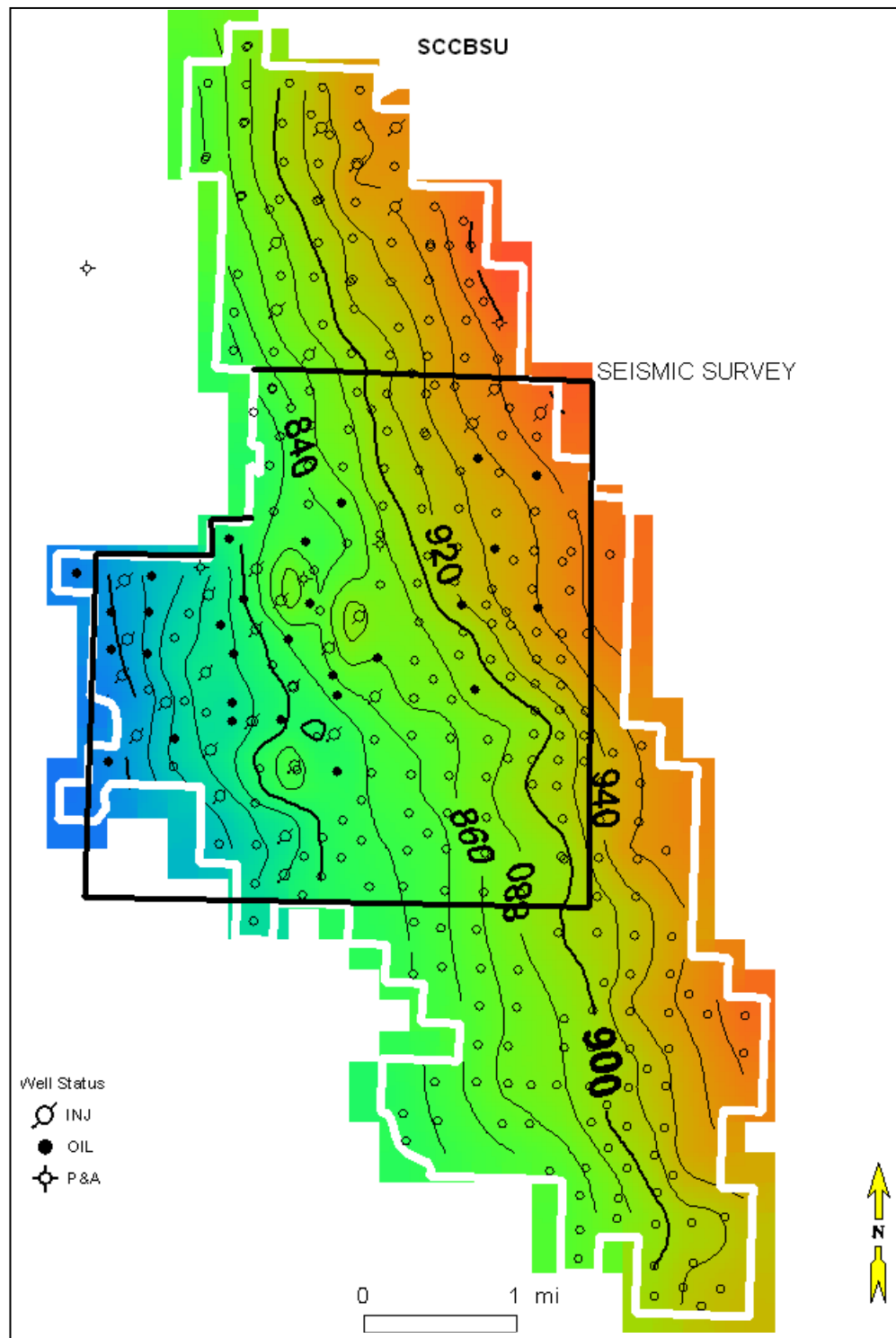


Figure 5. Structure map of the base of the Cut Bank sandstone (top of Ellis Group) in SCCBSU area (Datum is mean sea level).

2.2 Field Overview

2.2.1 Reservoir Properties

The three productive members of the Lower Cretaceous Kootenai Formation are the: (1) Cut Bank member at the base (averaging about 47 feet thick); (2) Sunburst member in the middle (about 50 feet thick); and (3) Moulton member at the top (about 100 feet thick) (Fig. 2). The Cut Bank member is the most important producing unit. The average depth to Cut Bank sandstone is 2,950 ft. The sand varies in thickness and pinches out against the Ellis Group on the east, forming a stratigraphic trap (Fig. 6). Thickness ranges from the pinchout on the east to more than 80 ft. The Cut Bank sandstone is divided into two members, the upper and lower Cut Bank. The boundary between the upper and lower sands varies from gradational to abrupt. The lower sand is the main oil producing horizon. The upper Cut Bank sand produces only locally. The lower sand is laterally more extensive and averages approximately 17 ft thick. The average porosity of the pay section is 14%, and the permeability ranges from 10 md to 1,500 md, with the average being approximately 50 md (Matthies, 1962).

Water saturation is 38 %, original formation volume factor was 1.009, reservoir temperature is 82°F and initial reservoir pressure was 750 psi (Gully, 1984).

Gas has been developed and produced from the primary gas cap up structure. The oil pool is bordered by edgewater downdip to the west, but this water is not encroaching. The gas cap does not contribute significantly to the recovery. Oil production from the Cut Bank sand is attributed to solution gas drive (Matthies, 1962).

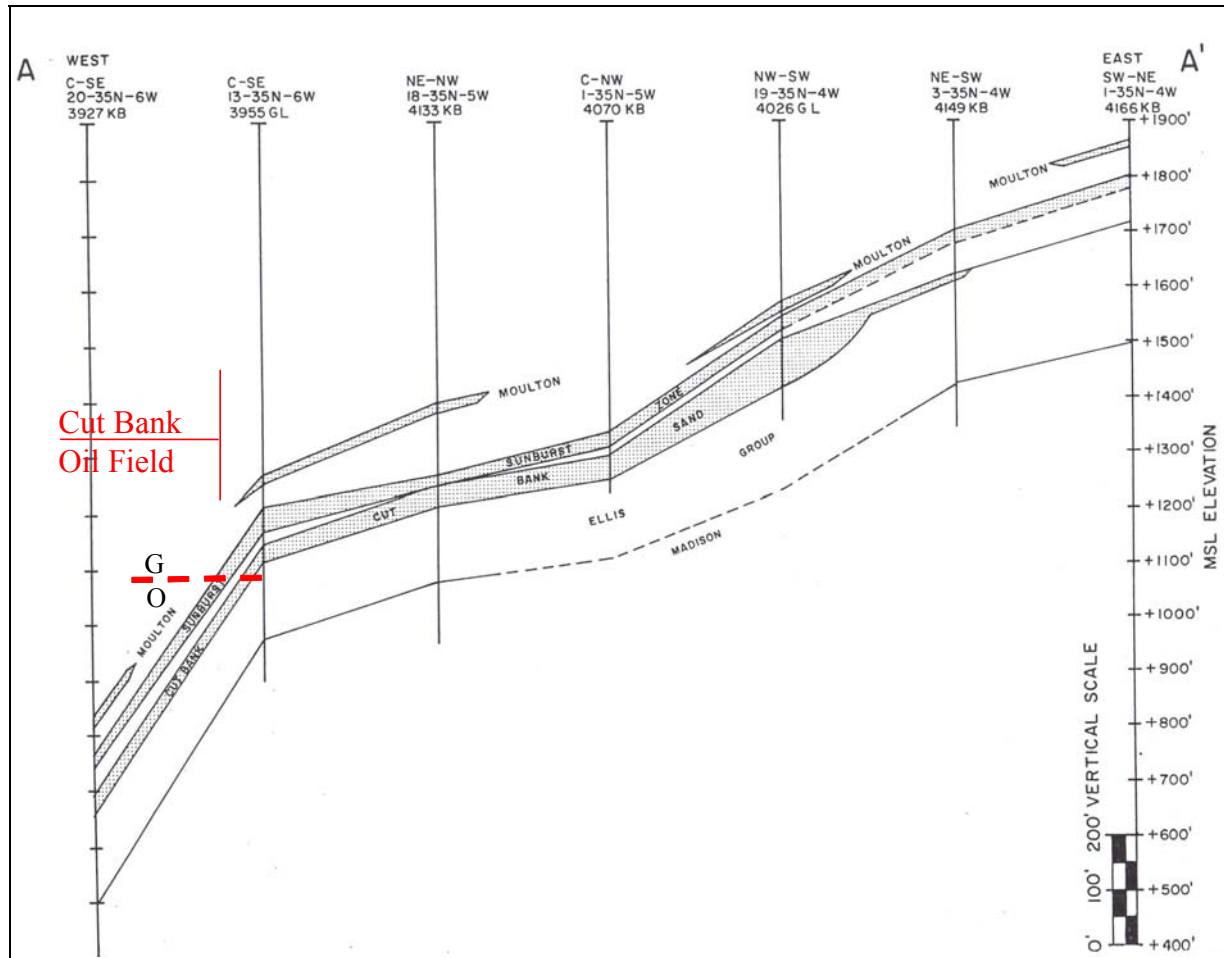


Figure 6. Diagrammatic cross section A-A', Cut Bank field. See Figure 3 for location (Modified from Gully, 1984)

Oil is produced from the Sunburst and Moulton members locally in the north part of the field. The Sunburst member is a better reservoir than the upper Cut Bank, but it is not nearly as good as the lower Cut Bank. Sunburst porosity values average 12 %, but range from near 0% to 18%. Net thickness, based on a 10% porosity cut-off, is commonly 4 to 8 feet. Permeability is usually low due to the silty and shaly nature of the sand. Although the Sunburst sand produces oil in economic amounts in SCCBSU, but it is not included in the present waterflood.

2.2.2 Field History

Oil was discovered in Cut Bank field in 1931, and by 1963, about 77 million bbl of oil had been recovered from the 54,250-acre field. Initial production declines were steep, but new wells more than offset the decrease of field production rates until 1942 (Cupps and Fry, 1967). Thereafter, the field-wide production declined at an annual rate of about 14% until 1950, when an active re-work program somewhat arrested the decline (Fig. 7). In 1961, the average daily production of the entire field was about 4,500 bbl of oil from 1,038 wells (Matthies, 1962). The oil is produced as a result of solution gas drive with little or no help from the edgewater to the west of the field or the gas cap to the east of the field.

In the early 1970's, waterflooding was initiated in South Central Cut Bank Unit area. This unit has 43 MMBO cumulative oil production. The waterflood development history and production history of this period is shown in Figures 8 and 9 respectively.

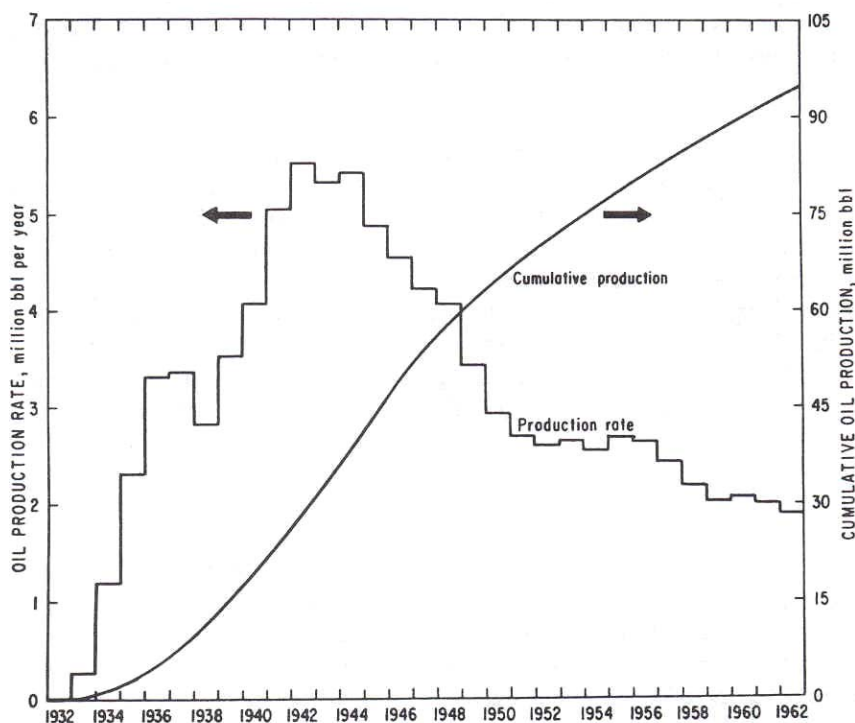


Figure 7. Oil production history of the Cut Bank Field from year 1932 to 1962 (Cupps and Fry, 1967).

In 1998, a 3-D seismic survey was acquired over an 8-mi² section of Cut Bank field, with the objective of improving the ongoing waterflood performance (Fig. 5). The 3-D seismic data revealed that reservoir compartmentalization is controlled by lateral and vertical facies changes, not by faults. Attribute analysis identified sinuous features associated with siliciclastic depositional environments, which were missed by offset drilling programs. Five new proof-of-concept wells were drilled in strategic locations to exploit previously untapped reservoir compartments. Four of five wells encountered reservoir-quality sands. However, these sands were already swept of oil as a result of secondary recovery efforts, leaving significant hydrocarbons trapped within only the upper portions of the reservoir (DeAngelo and Hardage, 2001).

Presently, there are 277 wells in South Central Unit area; 54 are producers, 29 are injectors and 194 are idle.

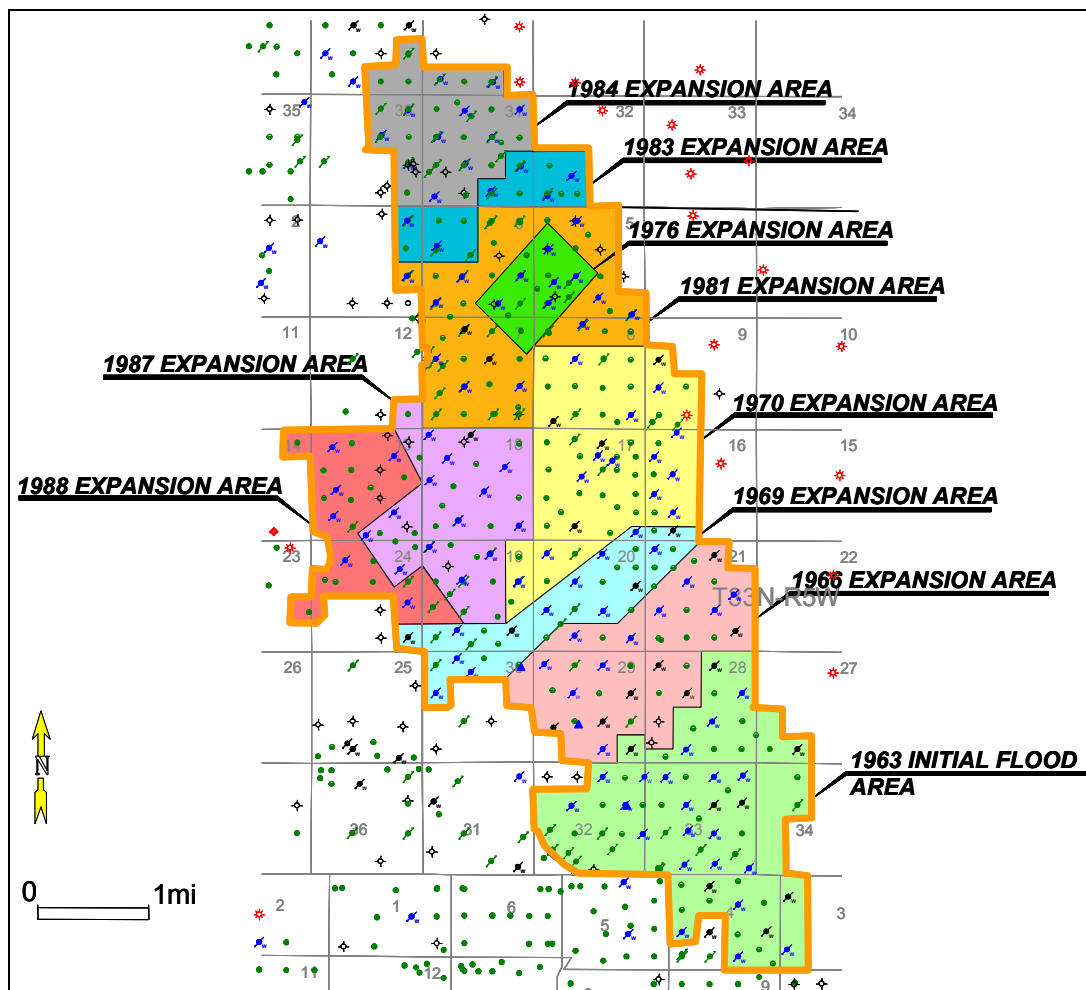


Figure 8. SCCBSU water flood expansion history (from Quicksilver Resources, 2002).

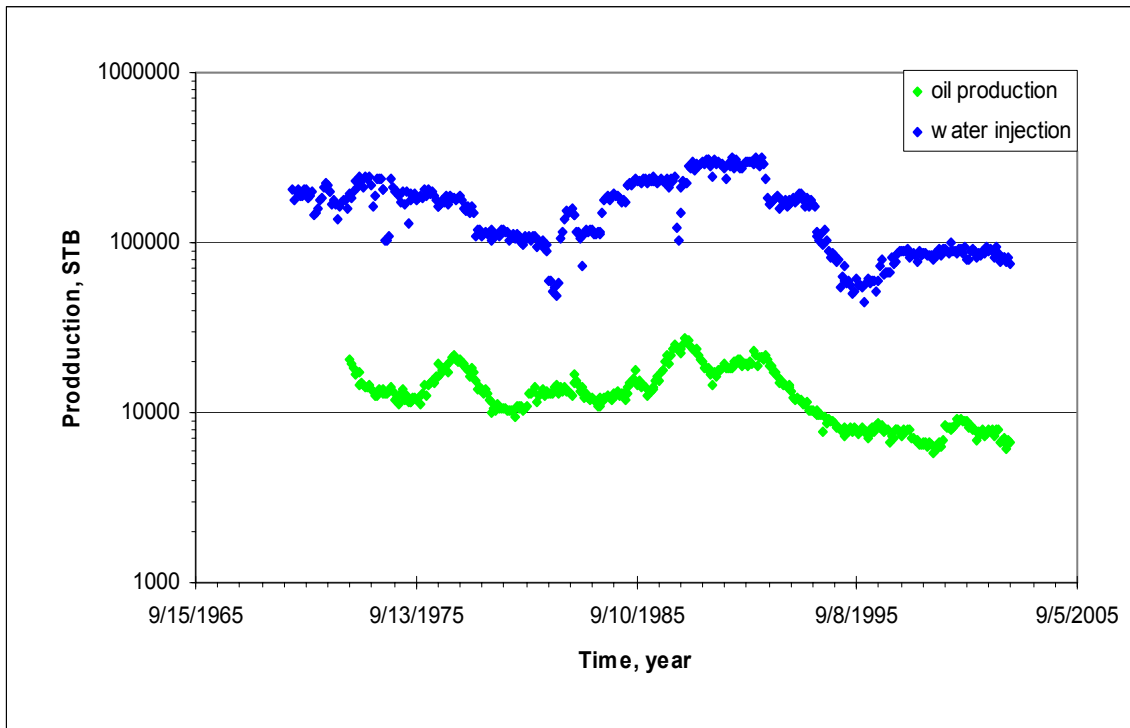


Figure 9. SCCBSU production and injection history from year 1969 to 1998 (data from Quicksilver Resources, 2002).

2.3 Lithologic and Stratigraphic Framework

Correlation of the Cut Bank, Sunburst, and Moulton intervals (Fig. 10) is difficult and imprecise. The Cut Bank sandstone unconformably overlies the siderite-cemented, black Ellis shale (Dolson and Piombino, 1994).

In the western part of the area, Callagher (1957) described a basal Cut Bank chert-quartz conglomerate averaging ten feet thick. This basal conglomeratic zone thins eastward, and throughout most of the area, it is only of a few inches thick.

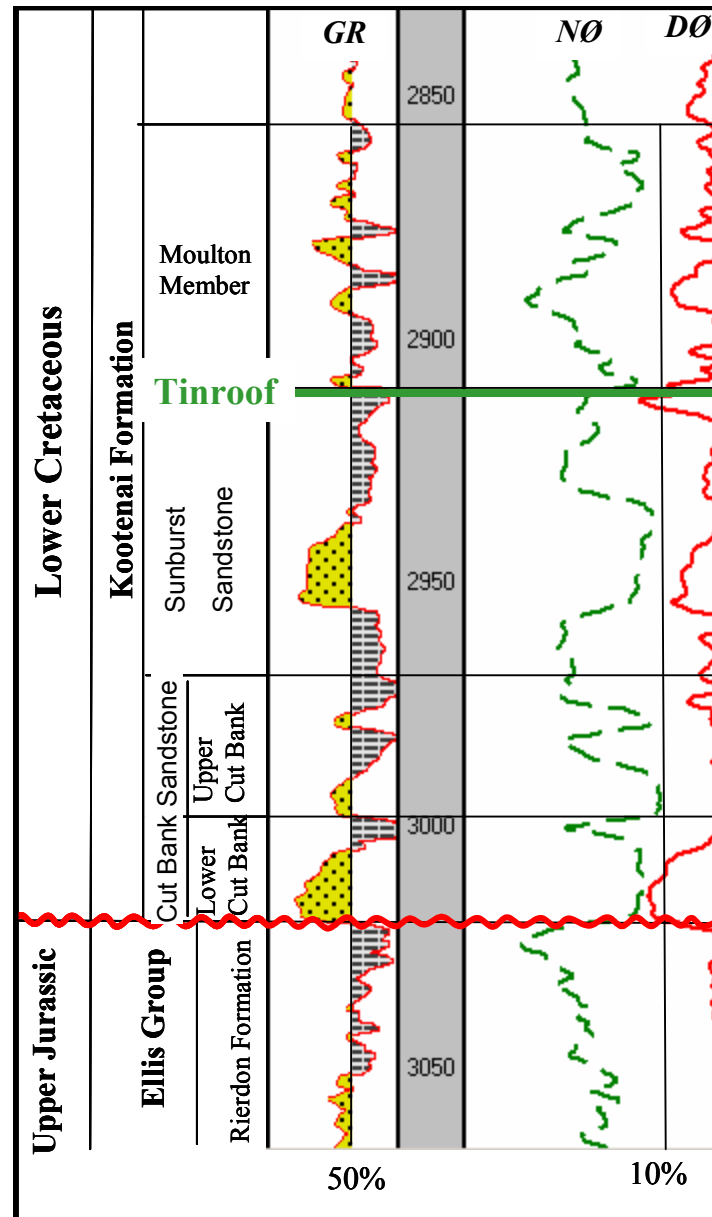


Figure 10. Cut Bank field – Type Log, Well SCCBSU #51-6. GR –gamma ray, NØ–neutron porosity, DØ–density porosity.

Blixt (1941) arbitrarily subdivided the Cut Bank sandstone into upper and lower units on the basis of chert content, which is highest in the lower unit. The boundary

between upper and lower sands may be gradational or abrupt. Principal detrital constituents of the Cut Bank sandstone include quartz, silicified carbonate clasts, and argillaceous chert clasts (Horkowitz, 1987). Texture ranges from conglomerate to fine-grained sand.

From outcrop studies, Horkowitz (1987) identified two sandstone subfacies within the lower Cut Bank sand. These are massive, lenticular sandstones and epsilon cross-bedded sandstones. Also, there are clay-filled abandoned channel plugs within these two sandstone facies. Porosity and permeability vary appreciably, both laterally and vertically. Cupps and Fry (1967) indicated that the highest porosity and permeability occur in medium-grained, conglomerate-free, cherty sand. Because of wide variation in porosity, oil saturation is very irregular.

Interpretation of the upper Cut Bank sandstone is based mainly on log analysis. It is composed of a fairly clean, uniform, fine- to medium-grained sand (Hill, 1989). Unlike the lower sand, a basal conglomerate is rare, and when present, it is quite thin. The upper Cut Bank sand is thinner and not as widespread as the lower sand. It is thickest at the north end of SCCBSU, where a two or more channel-fill deposits are amalgamated.

The Cut Bank-Sunburst contact is gradational and difficult to identify, but the Sunburst is considered to be a separate reservoir (Hill, 1989). The sands commonly exhibit a salt and pepper appearance due to the presence of dark-colored chert grains. Sunburst sands tend to be more shaly and silty than the Cut Bank sands. The Sunburst member contains as many as three sand lenses, depending on location. These lenses

average 10 to 15 feet in total thickness. The lowest Sunburst sand, in rare instances, is in contact with the upper Cut Bank sand making it difficult to distinguish between those two units.

Treckman (1996) identified a 2- to 4-ft thick bentonite layer named the “Tin Roof” at the base of the Moulton (top of Sunburst). This layer is absent over part of the SCCBSU, where a major incised valley is present (Figs. 11, 12, and 13). The incised valley is 1 to 1.5 miles wide and is at least 150 feet deep. The valley fill creates stratigraphic trapping potential in the Sunburst and possibly in the upper Cut Bank sands.

According to DeAngelo and Hardage (2001) the Tin Roof bentonite appears to dampen the seismic reflectors below it, resulting in reduced seismic clarity of the lower Cut Bank sand. Based on the 3-D seismic data, DeAngelo and Hardage (2001) used seismic attribute analysis to identify several sinuous features that may be shale-filled channels. They concluded that Cut Bank sandstone reservoir compartmentalization is controlled by lateral and vertical facies changes, not by faults.

Moulton sandstones are discontinuous, lenticular fluvial units comprised of fine-grained, cross-laminated sand. Gross thickness varies from 0 to 100 ft (Gully, 1984).

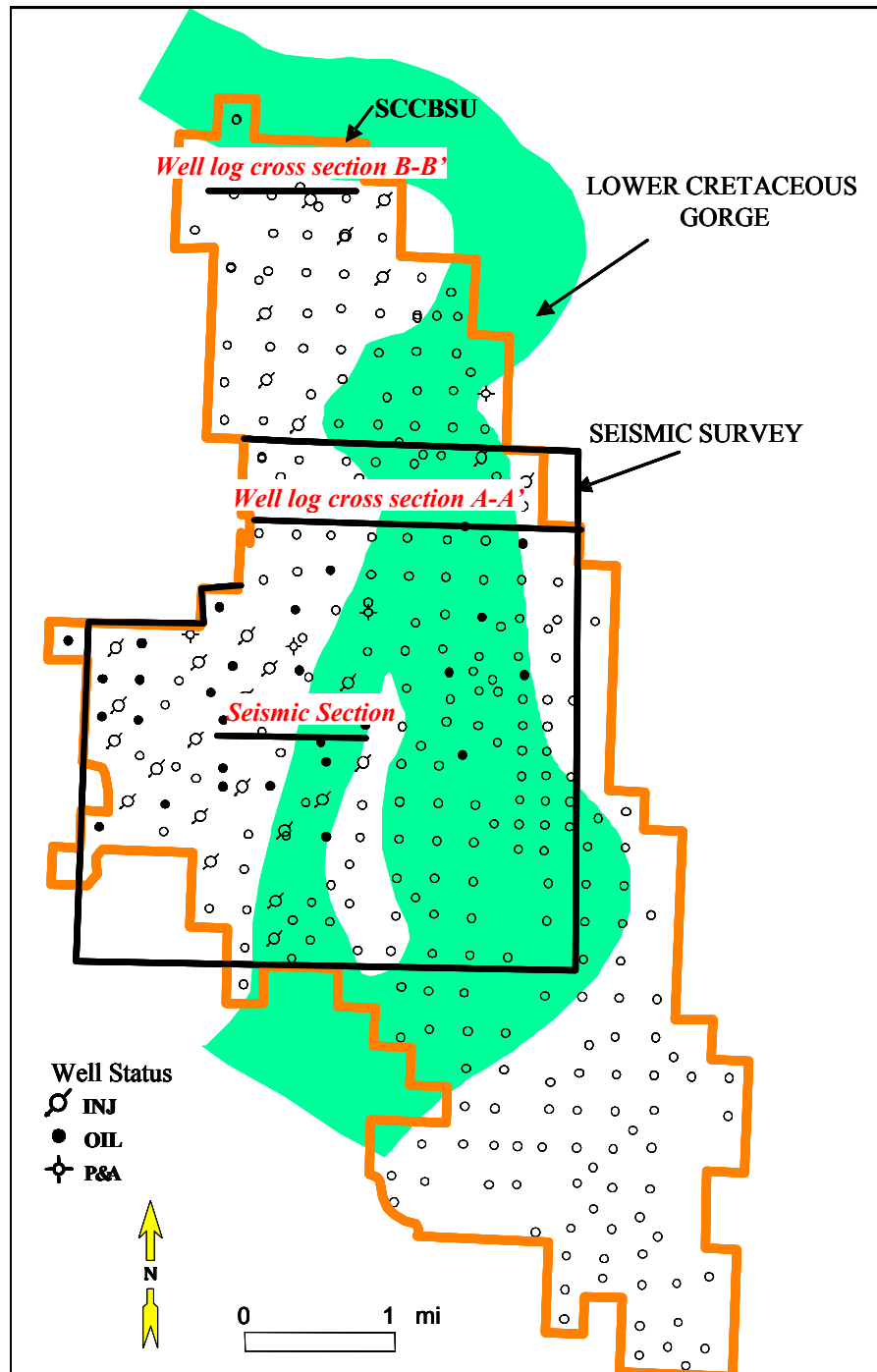


Figure 11. South Central Cut Bank Sand Unit (SCCBSU) well base map. Green shaded area corresponds to Lower Cretaceous Gorge where the “Tinroof” is absent (from Quicksilver Resources, 2002).

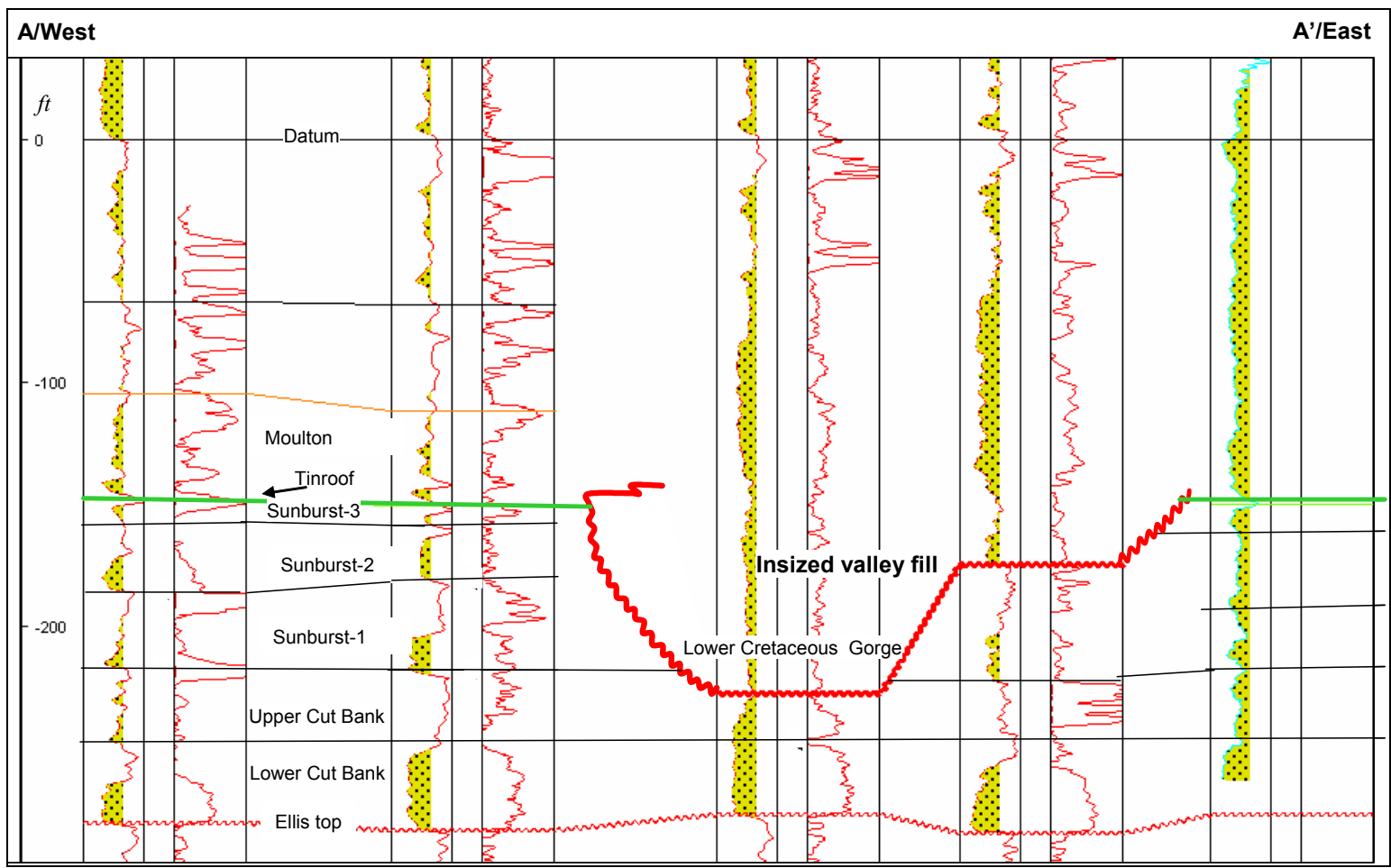


Figure 12. Stratigraphic cross section A-A' (See Figure 11 for location). Vertical Exaggeration=10.6667.

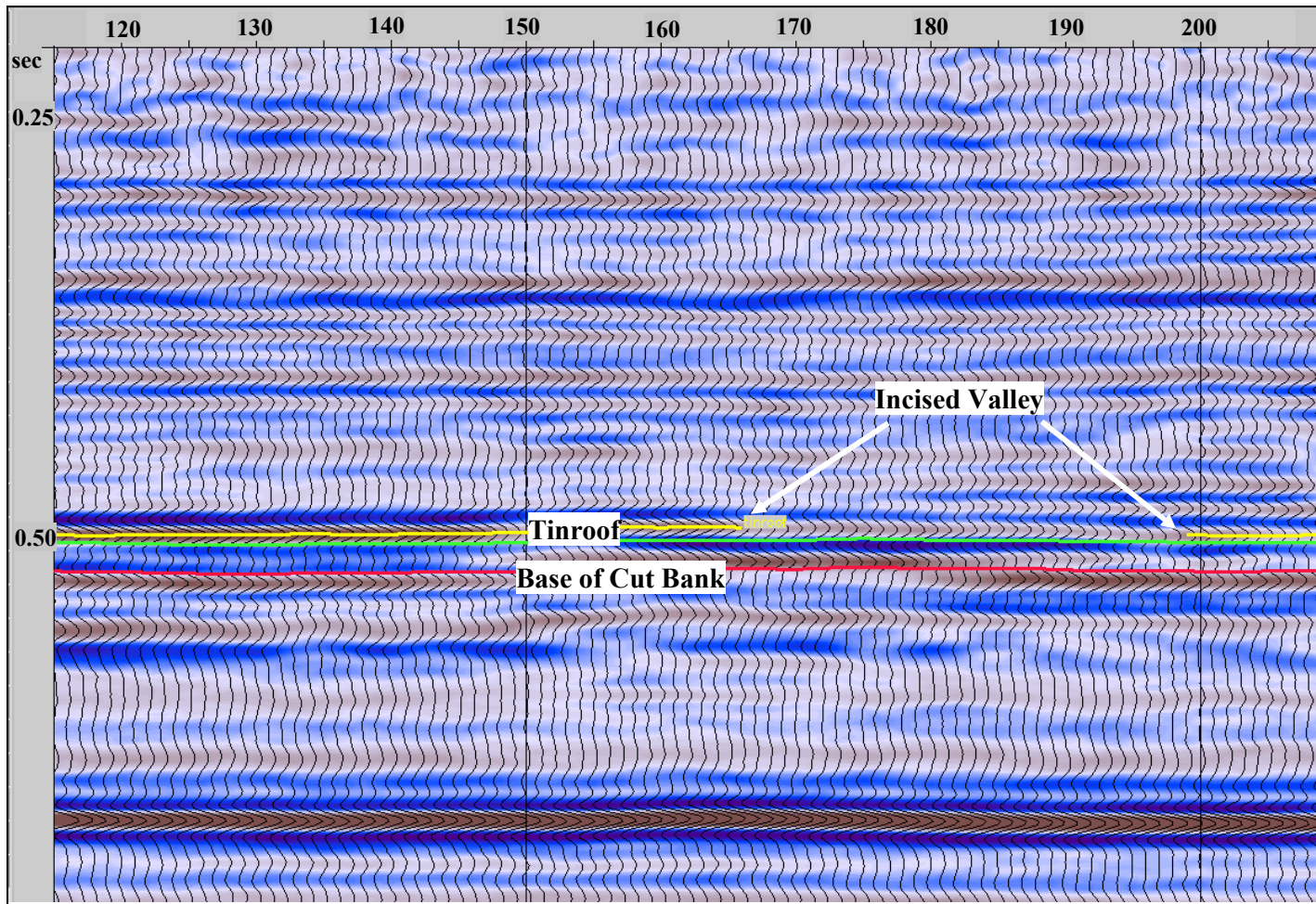


Figure 13. West to east seismic section (See Figure 11 for location). Tinroof is cut by incised valley-Lower Cretaceous Gorge.

2.4 Provenance

Within the study area, the Kootenai Formation reflects sedimentologic and petrologic responses to changing tectonic conditions. The Aptian Kootenai Formation in the Cut Bank area was deposited during a period of nonmarine sedimentation in the Sevier foreland basin of the northwestern United States (Berkhouse, 1985).

Hopkins (1993) summarized the regional paleogeography in Montana as follows. Sediment was supplied from the intermittently strongly positive Cordilleran Mountains and a broad, low-lying area to the northeast, which flanked the Canadian Shield. Local sedimentation patterns are the result of the dynamic relation between tectonism in positive and negative areas and the relative position of sea level with respect to the continent. Repeated advances and withdrawals of the sea against a background of general emergence marked the passage from dominantly marine sedimentation in the Jurassic to estuarine and continental sedimentation in the early Cretaceous. Cut Bank sandstones are generally medium- to coarse-grained litharenites in which composition of the lithic components are a wide range of chert and silicified sedimentary rock fragments. Their source lay to the west in Paleozoic carbonates.

Suttner (1969) suggested that clastic sedimentary rocks of Late Jurassic-Early Cretaceous age within the foreland basin in Montana and Alberta are dominantly composed of quartz and siliceous sedimentary rock fragments (chert and quartzite), reflecting derivation from Paleozoic sedimentary rocks involved in thrusting to the west. Virtually all of the sediment deposited in the foreland basin during the late Jurassic-early Cretaceous time was ultimately derived from the westward-adjacent orogenic belt,

implying primarily eastward sediment dispersal. Sediment supply from the craton to the east was negligible during this period, at least within the western regions of the foreland basin.

During the Aptian, the first major pulse of coarse, orogen-derived detritus into the eastward-adjacent foreland basin resulted in alluvial plain deposition of the Kootenai basal conglomerate and Cut Bank sandstone members of southwestern and northwestern Montana, respectively.

2.5 Depositional Environment

The onset of Kootenai sedimentation was marked by regional emergence and establishment of a north-trending drainage system that coincided with the influx of coarse clastic sediments from the rising Cordilleran Mountains to the west (Shelton, 1967; Weimer and Tillman, 1982; and Berkhouse, 1985). The sediment deposited by this system filled a paleo-valley cut into the Jurassic shale of the Ellis Group. The marine basin into which this fluvial system flowed was located in northern Alberta, Canada.

The depositional systems of the Kootenai Formation have long been debated. Walker (1974) indicated that coarse, chert-rich sandstones deposited by a north-flowing braided river system form the basal, Cut Bank sandstone. Hopkins (1993) supported this interpretation by describing Cut Bank sandstones that exhibit large-scale, unidirectional, tangential cross-stratification. He pointed out that the structures are typical of transverse bar bedforms generated in sandy, braided rivers.

Based on the character and assemblages of the sandstone subfacies, the distribution of shale, lateral and vertical subfacies associations observed at outcrops, and comparison of the Cut Bank sandstone with examples of modern meandering and braided rivers and ancient fluvial sandstones, Horkowitz (1987) considered the Cut Bank sandstone a two-part system reflecting deposition in a meandering-to-braided fluvial system. The meandering lower Cut Bank section filled the deeper parts of the shallow valley, and it was overlain by the braided, upper Cut Bank subfacies.

Cut Bank sandstones are generally medium- to coarse-grained litharenites in which the lithic component comprises a wide range of chert and silicified sedimentary rock fragments. Their source lay to the west in Paleozoic carbonates (Peterson, 1986). To the west of the Cut Bank field, Cut Bank sand and its equivalents thicken and are more conglomeratic.

Dolson and Piombino (1994) indicate that the Cut Bank strata illustrate an important variation on valley fill development in proximal positions to foreland uplifts, as a complete alluvial plain and fan assemblage lacking valley walls is preserved to the west of Cut Bank field (Fig. 14).

Ardies et al. (2002) and Zaitlin et al. (2002) did extensive research on the ancient valley systems of the lower Cretaceous “Basal Quartz” (BQ) member, the northern extension of Cut Bank sandstone in southern Alberta. The three-dimensional geometry of the valley networks in 100 km by 120 km of the densely drilled “BAT” (Bantry-Alderson-Taber) unit, which forms part of the “Basal Quartz” of Lower Cretaceous age in Southern Alberta was re-constructed in their studies. The authors showed that the

valley systems were fed from the west, south, and east by a network of tributaries. Eustatic sea level changes may have played a role in initiating river incision, but regional tectonic movements had an important influence on the history of accommodation change.

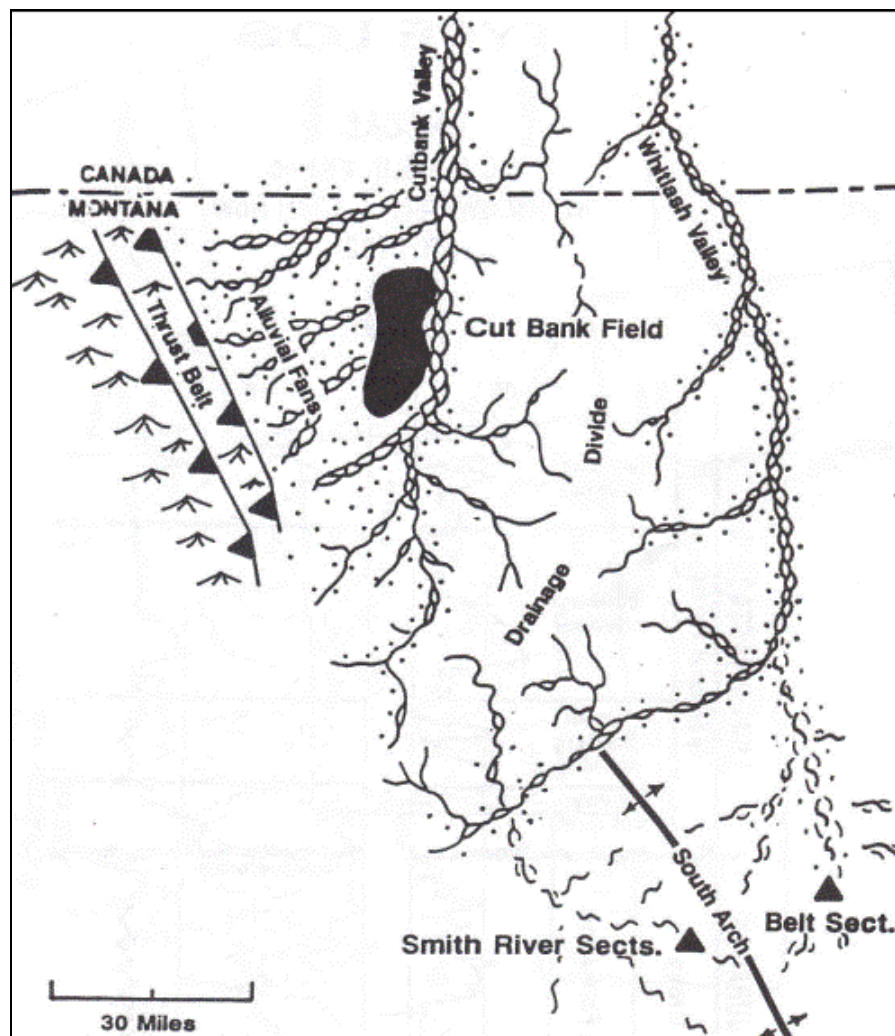


Figure 14. Cut Bank field – depositional setting (after Dolson and Piombino, 1994).

Periods of erosion appear to have been relatively brief, because the valleys are narrow, although confinement within cohesive, mudstone-rich paleosols of the underlying incised-valley deposits may have slowed valley widening. A relatively wet paleoclimate may also have contributed to the formation of narrow valleys by favoring the existence of single-channel rivers. The general morphology of the Alberta foreland basin, together with the distribution of unfilled relief associated with preceding valley system and/or less resistant, slightly older deposits, determined the location of trunk valleys. The trunk valley is significantly narrower and more deeply incised where it crosses the most pronounced uplifted block. Enhanced erosion at tributary junctions and valley bends produced localized areas (2-3 km in diameter) where the valley fill is up to five times thicker and considerably coarser grained than the adjacent valley deposits.

The high-resolution subdivision of the BQ clarifies changing BQ paleodrainage through time. The BQ is considered to be an accommodation-limited deposit due to general absence of marine deposits. BQ area was closer to the marine basin than was Cut Bank field, which favored the deposition and preservation of fluvial-estuarine deposits in a higher accommodation setting at BQ. It is easier to identify key bounding surfaces under higher accommodation conditions. Thus, a major challenge in the Cut Bank area is to identify bounding surfaces in an area of even lower accommodation than that of the BQ deposits.

The depositional environment of the Sunburst sand is similar to that of the Cut Bank sand (Hill, 1989). It is a fluvial sandstone that interfingers with lacustrine shales and limestones farther north near the Canadian border. The sandstones are primarily

channel-fill sands but are finer grained than those of the Cut Bank. They are very fine- to medium-grained and poorly sorted with an overall fining upward trend within the individual sand units.

2.6 Framework Composition and Texture

2.6.1 Composition

Lower Cut Bank sand is dark gray to black and is generally composed of approximately equal amounts of dark gray or black chert, and clear and translucent quartz grains, although in places, black chert predominates. Quartzite grains are also present.

Accessory minerals that have been identified by Blixt (1941) are pyrite, dolomite, biotite, zircon, tourmaline, garnet, and muscovite. Of these, pyrite, dolomite, and biotite are the most abundant.

Within individual layers, the grains are fairly well sorted, but grain-size gradation is well defined within sequence of layers, ranging from coarse at the base to fine sand at the top (Conybeare, 1976). Locally, the coarse-grained layers are conglomeratic, the maximum pebble size being 15 mm.

Texture of the lower Cut Bank varies from a pebble conglomerate or conglomeratic sandstone having pebbles up to 1/2 inch in diameter to fine-grained cherty quartzose sandstone. Interbedded with the black chert and quartz sand may be irregular lenses of chert-free sand or lenses of pure, cherty sand or cherty conglomerate. Generally, a persistent chert conglomerate a foot or less in thickness with a matrix of

fine, light gray sandstone mineralized with pyrite occurs at the base of the lower Cut Bank, erosionally overlying the Ellis shale.

Horkowitz (1987) described the Cut Bank sandstone framework composition as a three-component system composed of quartz, silicified carbonate clasts, and argillaceous chert clasts (Fig. 15). The quartz component is dominated by monocrystalline grains; polycrystalline quartz constitutes less than 1% of the quartz fraction. Quartz grains are dominantly equant in shape and slightly angular to subrounded. Abundance of quartz grains is negatively associated with grain size (Fig. 16a).

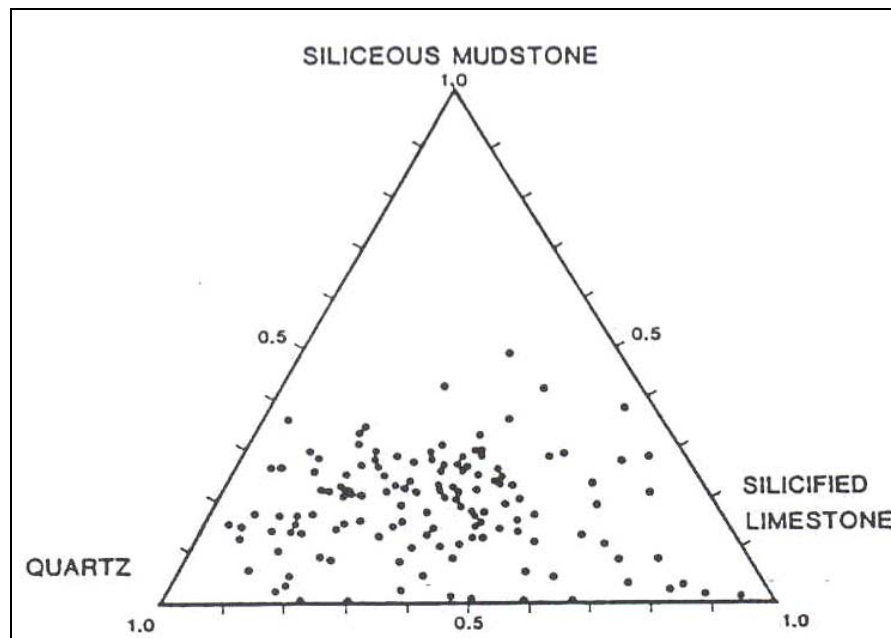


Figure 15. Cut Bank Field -Ternary plot of framework composition of Cut Bank sandstone. Sandstone framework composition is composed of quartz, silicified carbonate clasts, and argillaceous chert clasts (from Horkowitz, 1987).

Two main chert types are present, silicified carbonate clasts and argillaceous chert clasts (Horkowitz, 1987). Grains classified as silicified carbonate fragments exhibit fabric-selective intragranular porosity present in the form of isolated rhombic dolomolds, or molds of other dissolved intragranular material. The silicified carbonate clasts account for up to 70% of the sandstone and peak in abundance at a grain size of approximately 0.42 mm (Fig. 16b).

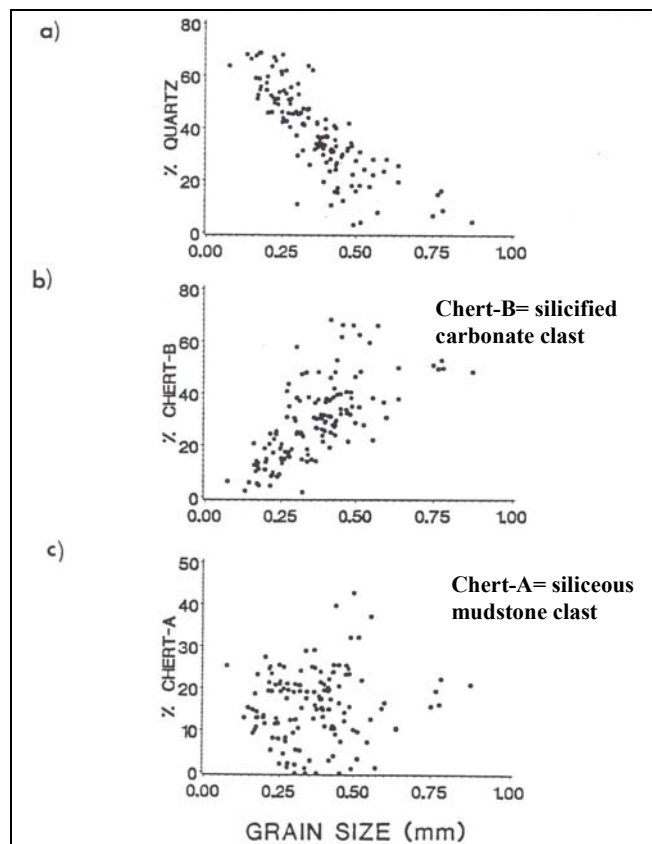


Figure 16. Cut Bank Field - Relationship between grain size and composition of Cut Bank sandstone: a) quartz content; b) silicified carbonate clast content (Chert-B); c) siliceous mudstone clast content (Chert-A) (from Horkowitz, 1987).

Grains classified as argillaceous clasts compose the third principal grain component in the Cut Bank sandstone. Argillaceous chert grains are typically equant to elongate in form. This grain type is predominately microporous with microporosity occurring uniformly throughout the fragments or in microlamellae within a fragment rather than as moldic pores as in the silicified carbonate clasts (Fig. 16c). This microporosity greatly reduces the effective porosity.

2.6.2 Sedimentary Structures

Medium-scale cross bedding is a dominant primary sedimentary structure, which occurs above massive bedding and below small-scale cross-bedding in the Cut Bank sandstone (Shelton, 1967). Other sedimentary structures, secondary structures include burrows, claystone chips (probably fragments of dried mud), and deformation probably caused by slumping of the unconsolidated sediment in a hydroplastic state. A shale bed locally present within the upper part of the Cut Bank (Conybeare, 1976).

Shelton (1967) noted that, within the sequence described above, average grain size decreases upward. The lower, well-developed sequence is characterized by medium- to coarse-grained sand, whereas the upper part of the sandstone is fine-grained. Maximum pebble size in the massive-bedded conglomerate is approximately 15 mm. The medium-scale, cross-bedded sandstone is well sorted; the other beds generally are moderately sorted. Bentonitic clay and silt are not uncommon as cementing materials and as such are significant modifiers of sorting, porosity, and permeability.

Horkowitz (1987) identified five sandstone lithofacies in the Cut Bank sandstone based on differences in external and internal geometry, physical structures present, patterns of grain size variation, and lateral and vertical facies associations. These are massive, lenticular sandstone; epsilon cross-bedded sandstone; horizontally-bedded sandstone; trough cross-bedded sandstone; and tabular cross-bedded sandstone. The mean grain size does not differ significantly between the five subfacies, each having a mean of 0.33 – 0.36 mm. The horizontally-bedded and epsilon cross-bedded sandstones have the greatest range in grain size. The massive, lenticular sandstone facies has the narrowest grain size range and the trough and tabular cross-bedded subfacies have a similar grain size range.

2.7 Hydrocarbon System

Weimer and Tillman (1982) concluded that oil and gas that were generated in the marine Ellis shale (Fig. 2) migrated into the Cut Bank sandstone, where they were trapped at the edge of the alluvial valley.

Dolson and Piombino (1994) described the Cut Bank Field as the largest valley fill trap in the Rocky Mountains. He suggested that the Lower Cretaceous Cut Bank sandstone produces from oil generated by the Mississippian/Devonian Bakken Shale (Fig. 2). Thermally mature Bakken oils in the Overthrust Belt footwall migrated vertically through the fractured Mississippian carbonates to regional seals in the Jurassic Ellis Group and then laterally updip at least 50 miles to Mississippian pools on the Sweetgrass Arch (Fig. 17).

The pre-Cretaceous unconformity, which underlies the Lower Cretaceous Cut Bank sandstone bevels across this Mississippian migration route downdip in Canada, diverting oils southward to the Cut Bank field accumulation. The pre-Cretaceous unconformity, which initially acted as a bypass zone for coarse gravels shed from western highlands, was folded and tilted toward the thrustbelt hingeline, causing deposition of the Cut Bank through Moulton sandstones. These alluvial plain and fan sandstones west of the field have sheet-like geometries and appear to have poor lateral seals. Cut Bank accumulation occurs where valley incisement of north-south trending paleodrainage system juxtaposes these sheet sandstones updip against Jurassic Rierdon and Sawtooth shales, forming regional valley wall trap.

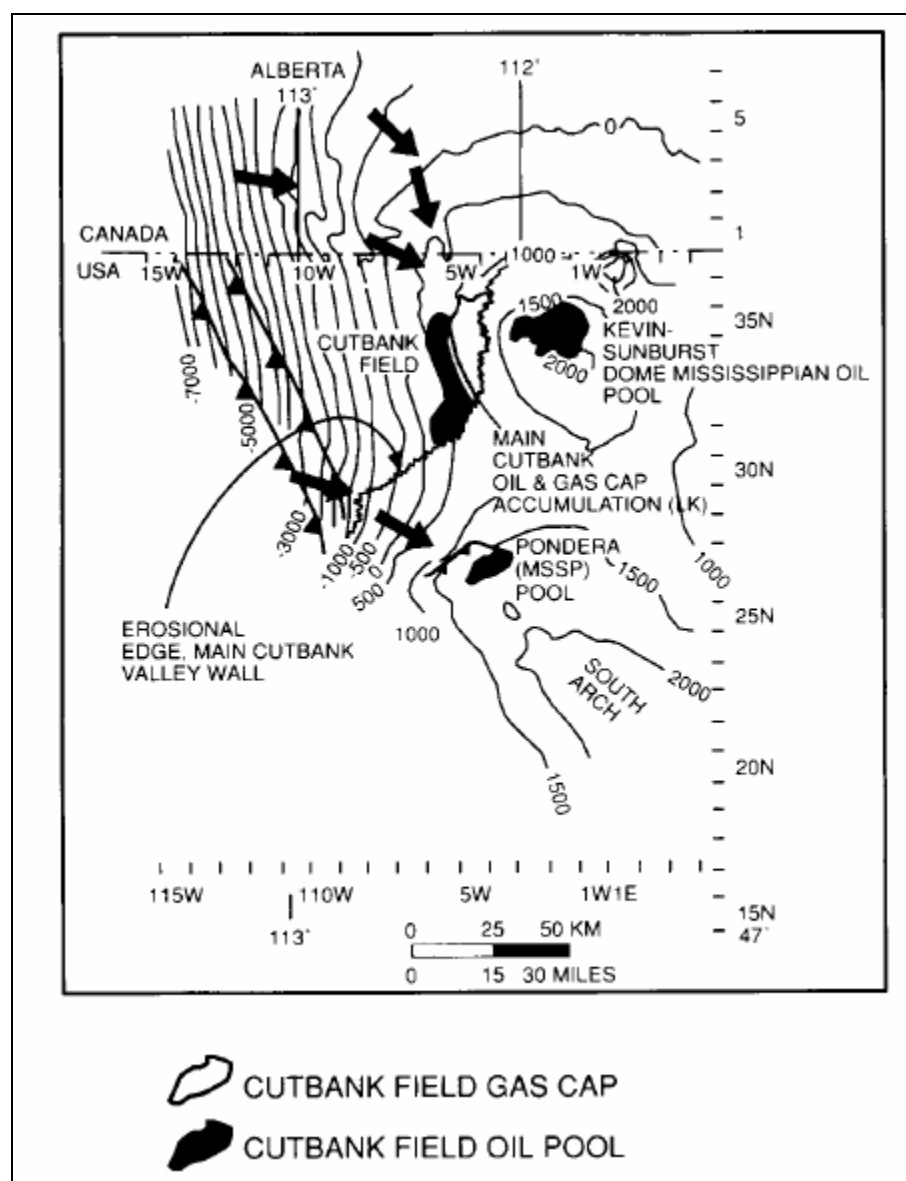


Figure 17. Migration routes of Bakken oil through Mississippian strata and lowermost Jurassic Sawtooth strata (arrows). Structure, top of Sun River Dolomite (in feet) (uppermost Madison Group) (Dolson and Piombno, 1994).

CHAPTER III

EVALUATION AND LIMITATION OF DATA

3.1 Database

The reservoir database includes a 3D seismic data set of an 8-mi² region and 275 wells, all located in the SCCBSU, NCCBSU, NWCBSU and TRIBAL units, Cut Bank field (Fig. 4). The geophysical log suite varies among wells; log suites available in the database are combinations of gamma ray, density porosity, neutron porosity and other curves, such as old gamma ray neutron, resistivity, and spontaneous potential (Fig. 18). In addition, core analysis results are available for 11 wells (Fig. 19). Production history data are available for 194 wells, not including injection wells and wells only with water production data. The current well spacing is 92 acres. Gross-sandstone thickness and net-reservoir thickness maps for this study were provided by Quicksilver Resources; the remainders of the maps were produced during this research.

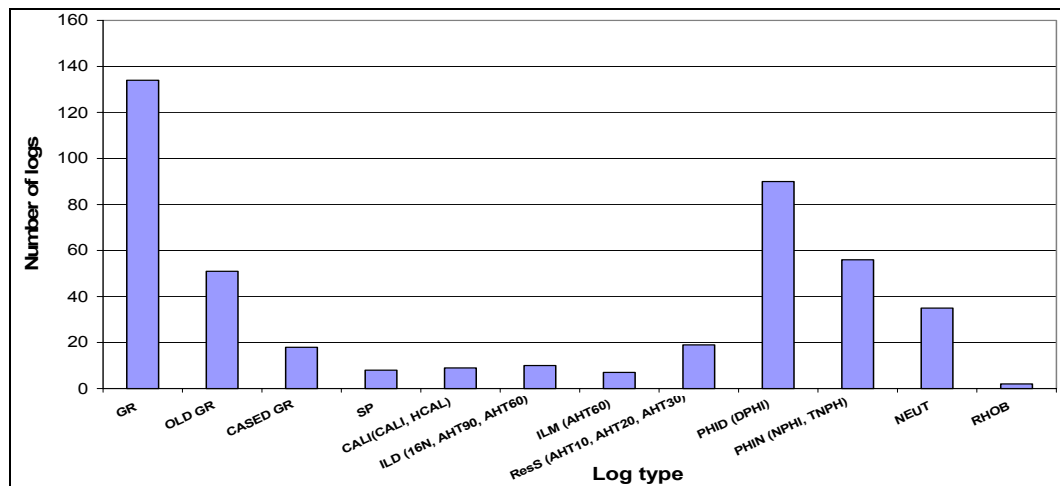


Figure 18. Plot of types of logs in the well logs database.

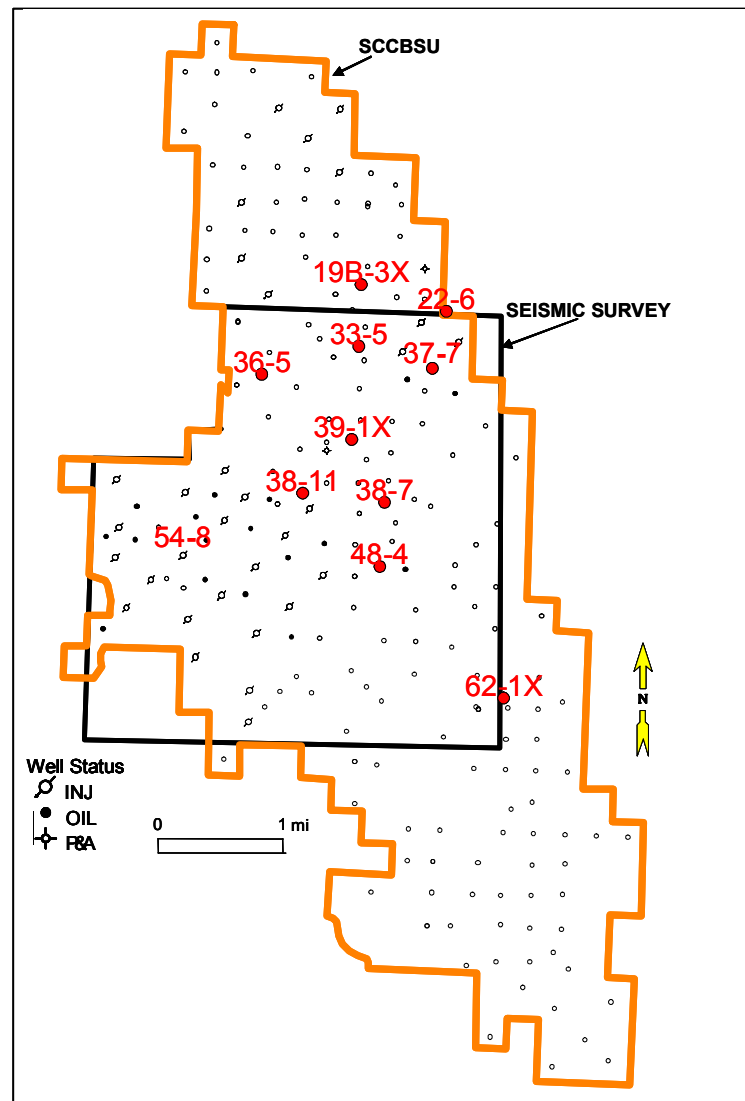


Figure 19. SCCBSU well base map with log data. Red are wells with core data. Well 54-8 has VSP data.

3.2 Assessing Data Quality

Modeling a complex oil field, with more than 60 years of production is a tremendous task that requires a multi-disciplinary organization and the effective management of a large amount of data (i.e., cores, logs, 3D seismic, production data, and previous

interpretations and geological models). Gathering and assessing quality of the necessary data are major and important steps in all reservoir characterization studies. Poor quality seismic and/or well log data can only result in poor reservoir characterization, and the data used in modeling should always be weighted according to its reliability. Well log information is generally considered “hard” or accurate data in geological modeling, because the measurements are made in the formation with a variety of tools that are directly related to the reservoir properties and, in most cases, have been calibrated using core analysis. However, problems can exist with the well log data. The logs were acquired over a number of years. Changes in logging tool response or processing parameters (like matrix density, clean sand, and shale baselines, etc.) can cause a bias in the petrophysical parameters which can seriously degrade the calibration between core, well and seismic data. In most cases the petrophysical properties were averaged to provide a single value of porosity (or other parameters) for the reservoir zone. This averaging, often performed with interpretive cutoff values applied, can greatly impact well log-to-seismic calibrations. Seismic data are considered “softer” or less reliable than well log information, because the measurements are made remotely and are only indirectly related to the reservoir properties (i.e., amplitude is proportional to reflectivity, which is proportional to the changes in acoustic impedance, which is proportional to density, etc.). The seismic data are limited in frequency (<100 Hz) and vertical resolution (10 ms or 100 ft). Deterministic models, generated at the scale of the seismic data, neglect small-scale geologic heterogeneity that may have a major impact on reservoir performance. Even high-quality seismic data may have localized problems

(noise, multiple contamination, acquisition footprints, poor stacking or migration velocities, etc.). In most cases the seismic attributes used in reservoir characterization are extracted from the 3D seismic volume along interpreted horizons. If the interpretation is not correct, the attributes are meaningless.

A review of Cut Bank data showed that a new model required revised interpretation of the stratigraphy. In many wells, lower Cut Bank, upper Cut Bank, and Sunburst contacts were inaccurately picked in previous studies, due to channel amalgamation. Although three Sunburst sands were mentioned in literature and reports, they were not identified on wells. Tinroof, Moulton and Lower Cretaceous Gorge picks were identified only on a few wells by earlier workers. For this study, it was necessary to normalize GR logs, evaluate maps and cross sections provided by Quicksilver Resources, estimate reservoir properties from well logs and seismic-to-well correlation, and evaluate the seismic interpretation of others.

I began correlating lower Cut Bank, upper Cut Bank, Sunburst, Tinroof, Moulton and Lower Cretaceous Gorge contacts/boundaries in well logs obtained from Quicksilver Resources and internet resources (Montana Oil and Gas Commission). In addition, I interpreted 2 shale beds above the study interval that were present almost on all the well logs. These shale beds were helpful in construction of stratigraphic well log cross sections and accurate interpretation of reservoir layering and sequence stratigraphic surfaces. Normalized gamma ray logs were used to ensure the consistency of the facies identification for all the wells. This normalization is highly recommended when such a classification is based on a non-homogenous set of wireline logs. Wireline log data are

subject to numerous potential errors due to the acquisition environment, assumptions made during acquisition, changes in logging tool response, and processing parameters).

3.3 Evaluation of Previous Geological Maps

QRI/BEG reports indicate that seismic average absolute amplitude was incorporated with well log data to construct the Quicksilver Resources/Bureau of Economic Geology (QRI/BEG) sand thickness map. By superposing the QRI/BEG net sand thickness map on the seismic average absolute amplitude map, I found that regions interpreted as higher average absolute amplitude correspond to higher estimated net sand thickness, except that of Well 49-14. At this well, the seismic amplitude is anomalously high and does not match expected thickness values (Fig. 20). Also, there is no correlation between the measured net sand thickness from the well logs (based on 60% GR and 10% porosity cutoffs) and the average absolute amplitude values (Fig. 21). Therefore, I concluded that there are limits on the accuracy of the QRI/BEG interpretation.

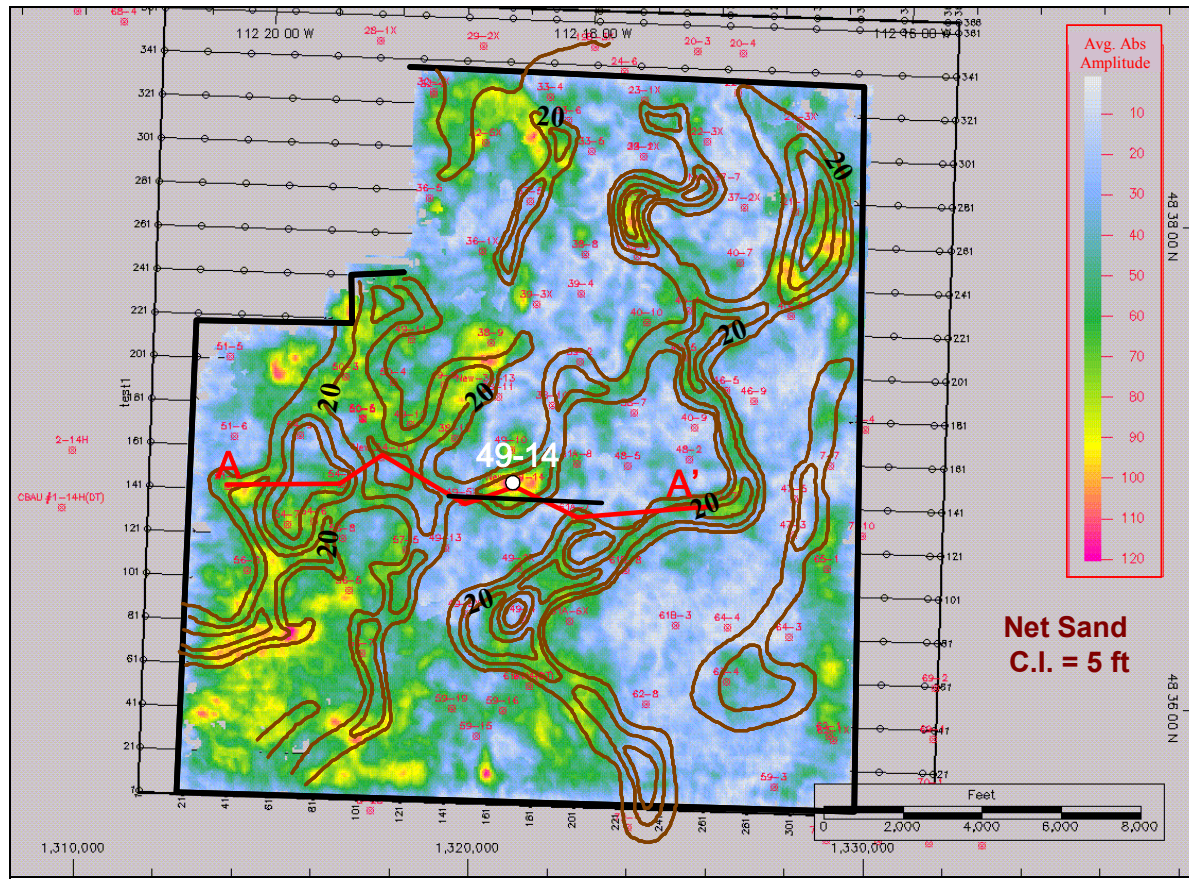


Figure 20. QRI/BEG net sand thickness (Quicksilver Resources, 2002) contours >15 ft superposed on the average absolute seismic amplitude map. Generally, higher average absolute amplitude corresponds to greater net sand thickness.

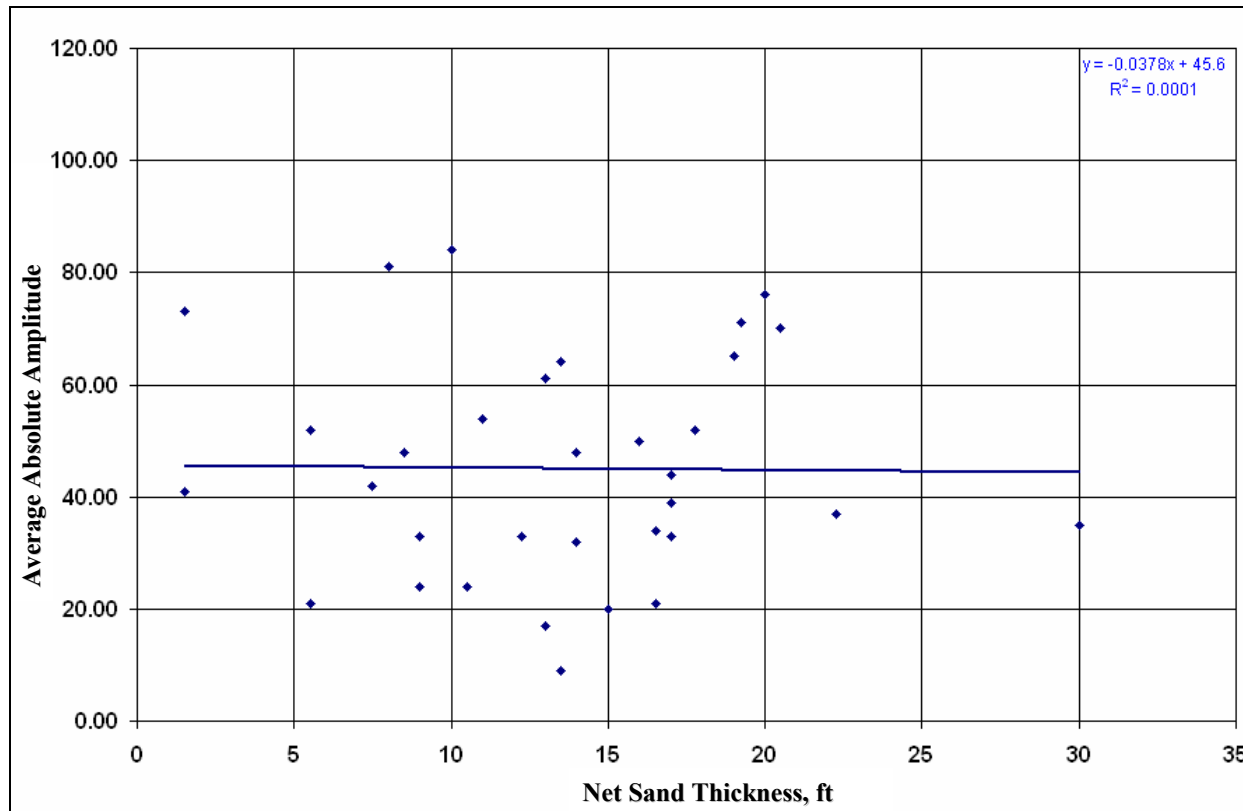


Figure 21. There is no correlation between net sand thicknesses from well logs (based on 60% GR and 10% porosity cutoff) and average absolute seismic amplitude.

3.4 Porosity Calculation

One aim of this chapter was to assess the usefulness of seismic data for predicting hydrocarbon production. Seismic-based porosity predictions are one way to incorporate the seismic data into a relevant reservoir model. Some data analysis is required, however, before seismic-determined porosities can be calculated. In particular, seismic attributes and well log porosities must be compared to demonstrate any relationships and to model the porosity distribution throughout the field. Normally, both seismic attributes and log properties are averaged for a stratigraphic interval. The objective is to have a pair of attributes and log properties values for each well that intersects the layer so that relationships between these data sets can be determined. Therefore, it is important to construct a representative model of reservoir porosity from well logs.

Core data were used to calibrate and refine the interpretation from well logs. The available core porosity data were cross-plotted with log-derived porosity on a well-by-well basis. Most of the wells in the Cut Bank field have a density porosity curve. Core data are available from 6 wells located in the northern part of seismic survey. Core data from a few other wells were not used for calibration because of the absence of density logs in these wells. Table 1 summarizes the results of correlating core and density porosity data for the wells that have both types of data. To reduce the degree of scatter, a running average was applied to the core porosities (smoothed with 3-point running average). Core porosity curves were depth shifted to match log depths using the gamma-ray curves.

Table 1. Summary of core porosity and density porosity calibration through cross-plotting.

Well #	Correlation Coef - R	Core data interval, ft	Relationship between core porosity and density porosity	Significance Levels of "F" (p-value)	Number of obs.
37-7	0.9581	2825-2855	Core_por=0.061+0.509*Dens_por	3.16694E-14	34
22-6	0.7960	2784-2805	Core_por=0.041+0.658*Dens_por	7.4136E-05	22
19B-3X	0.7782	2782-2808	Core_por=0.042+0.797*Dens_por	0.000120204	27
36-5	0.7485	2932-2957	Core_por=0.024+0.828*Dens_por	4.61557E-08	26
33-5	0.6877	2830-2855	Core_por=0.091+0.412*Dens_por	0.00181415	26
39-1X	0.3467	2923-2942	Core_por=0.068+0.426*Dens_por	0.006309857	20

While there is no direct relationship between correlation coefficient (R) and its significance level, the calculated p-values (or significance levels of "F" value) indicate that all curves fit their related data sets with a good significance level (not significantly different from zero) (Table 1). Well 37-7 has highest R value (Fig. 22) and very low significance levels of "F" value (very close to 0), indicating very low chances of the observed pattern of points having no linear relationship. When I applied the relationship between core porosity and density porosity from that well to other wells, it gave net pay average porosities of approximately 11 pu (porosity units). This value is 3 pu lower than field net pay average porosity value reported by Quicksilver Resources. In previous studies, net pay was defined based on a 10% porosity cutoff. Appropriateness of a 10% porosity cutoff was evaluated by cross plotting the available porosity and permeability data from 13 Cut Bank sand core reports from the Cut Bank field. There is a change in the relationship of the data below and above the 10% porosity line (Fig. 23). Porosity

values less than 10% correspond to very low permeability. From core reports the low values of porosity and permeability usually are in fine-grained sand.

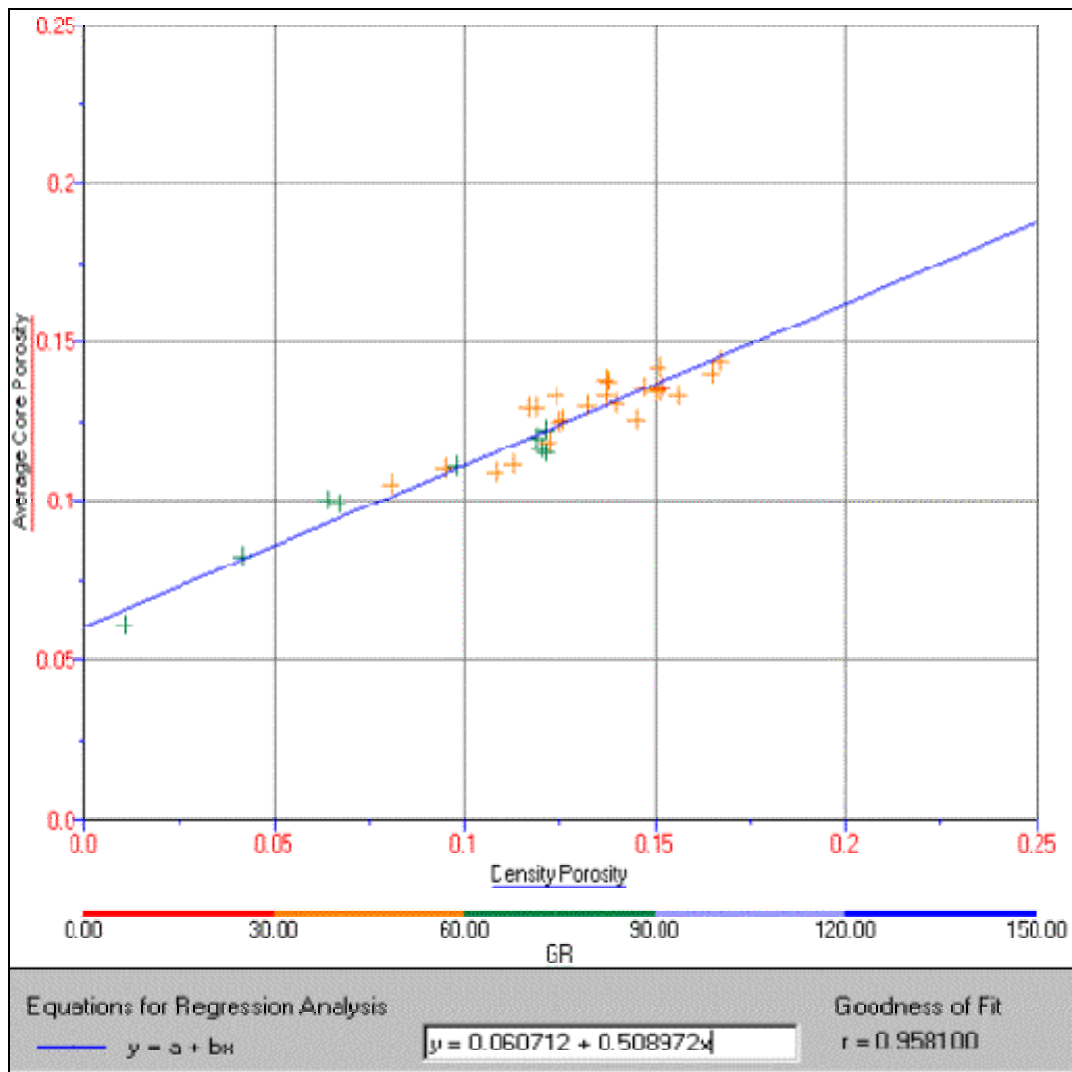


Figure 22. Well 37-7 - Core-well log porosity calibration for lower Cut Bank Sand.

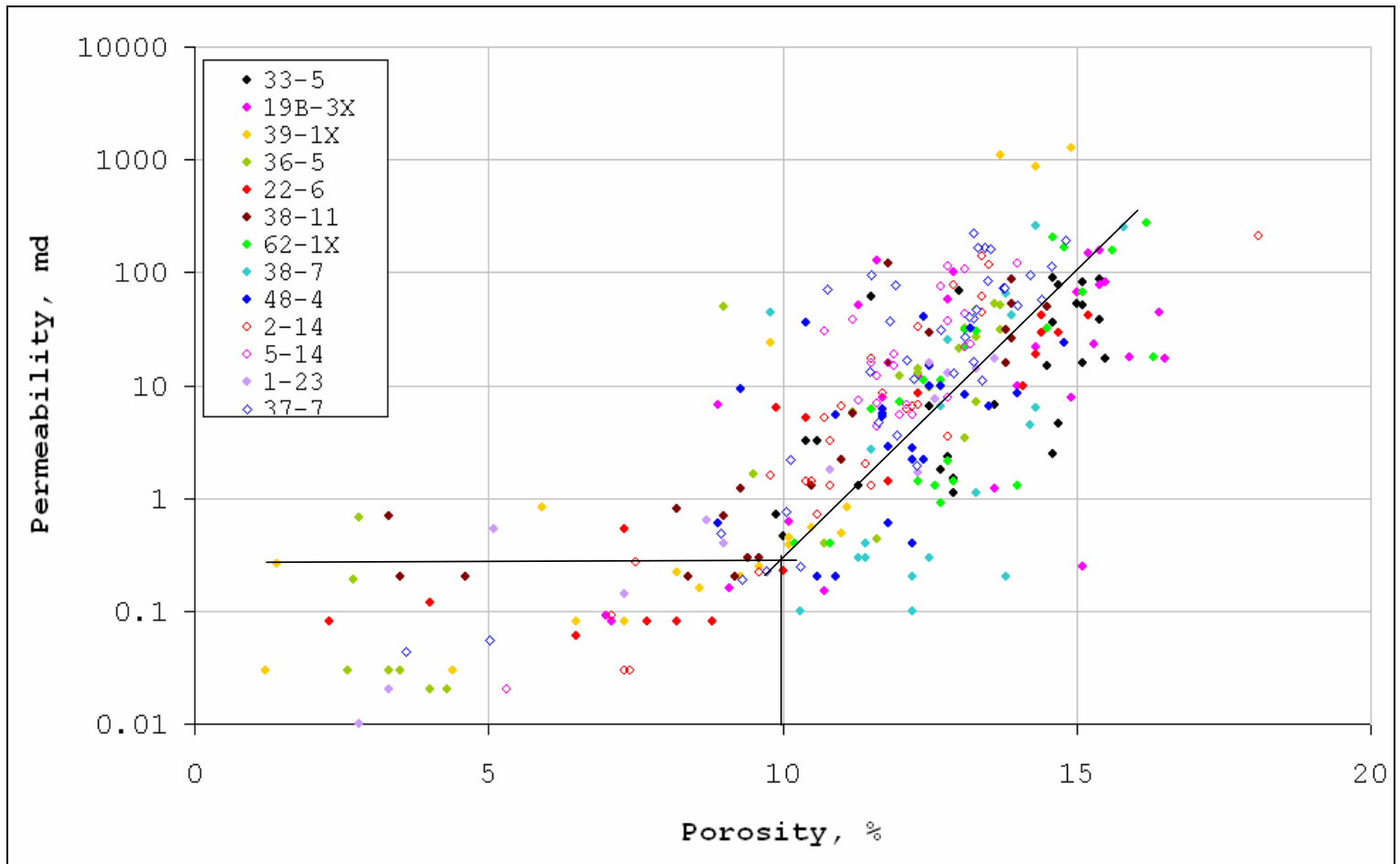


Figure 23. Core porosity-permeability crossplot. There is no relationship between permeability and porosity less than 10% porosity line (low porosity and permeability usually are in fine-grained sand). It appears there is a relationship above this line. The trend lines are hand drawn.

In an ideal case, there should be a one-to-one relationship between core porosity and density porosity. Data for wells 36-5 and 37-7 plot near the one-to-one line, indicating good correlation (Fig. 24). However, in Wells 33-5 and 39-1X, core porosity is consistently higher than density porosity. Based on core report summaries, cores from these two wells include abundant heavy minerals. This may also be the reason for poor agreement for wells 19B-3X, 36-1, and 22-6, where the log porosity underestimates the core-derived value. The conclusion is that the presence of heavy minerals causes the density log to be an unreliable porosity predictor.

Because the density log does not appear to give reliable porosity estimates, I examined porosity in wells that also had a neutron log. Relationship between neutron and core porosity from only one well that has both data available is very poor. Also, neutron vs density porosity plot gave very low R^2 value. The combination of density and neutron logs gives porosity estimates that are less sensitive to lithologic variations than the density porosity alone. There are 21 wells in the SCCBSU area that include both density and neutron porosity logs. The neutron-density average porosity (PHIA) value is close to the field-wide average (14%) reported in literature and reports (Fig. 25). Therefore, I decided to use PHIA values for the log porosity-to-seismic porosity calibration.

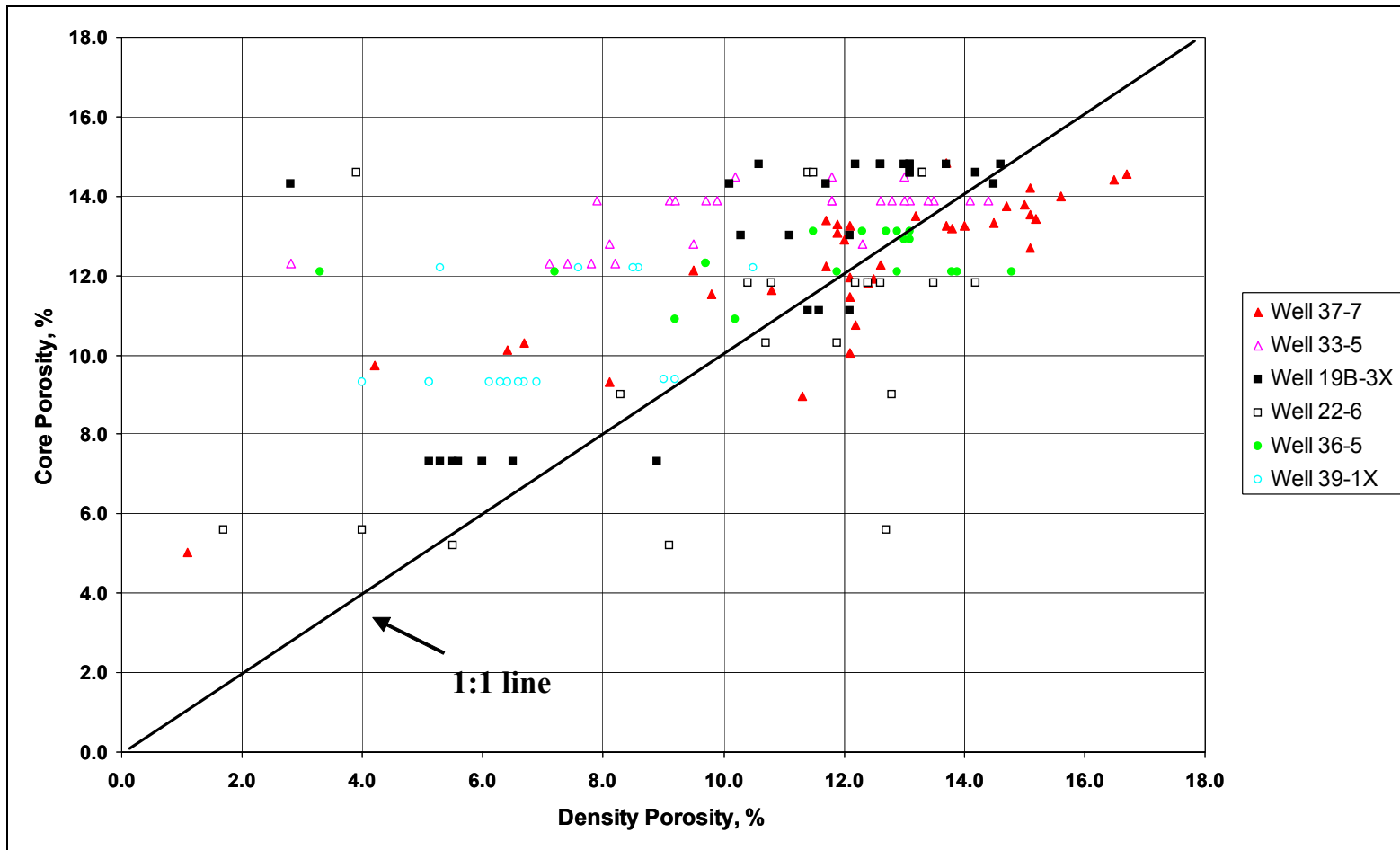


Figure 24. Core vs. density porosity comparison for all cored wells in the Cut Bank Sand.

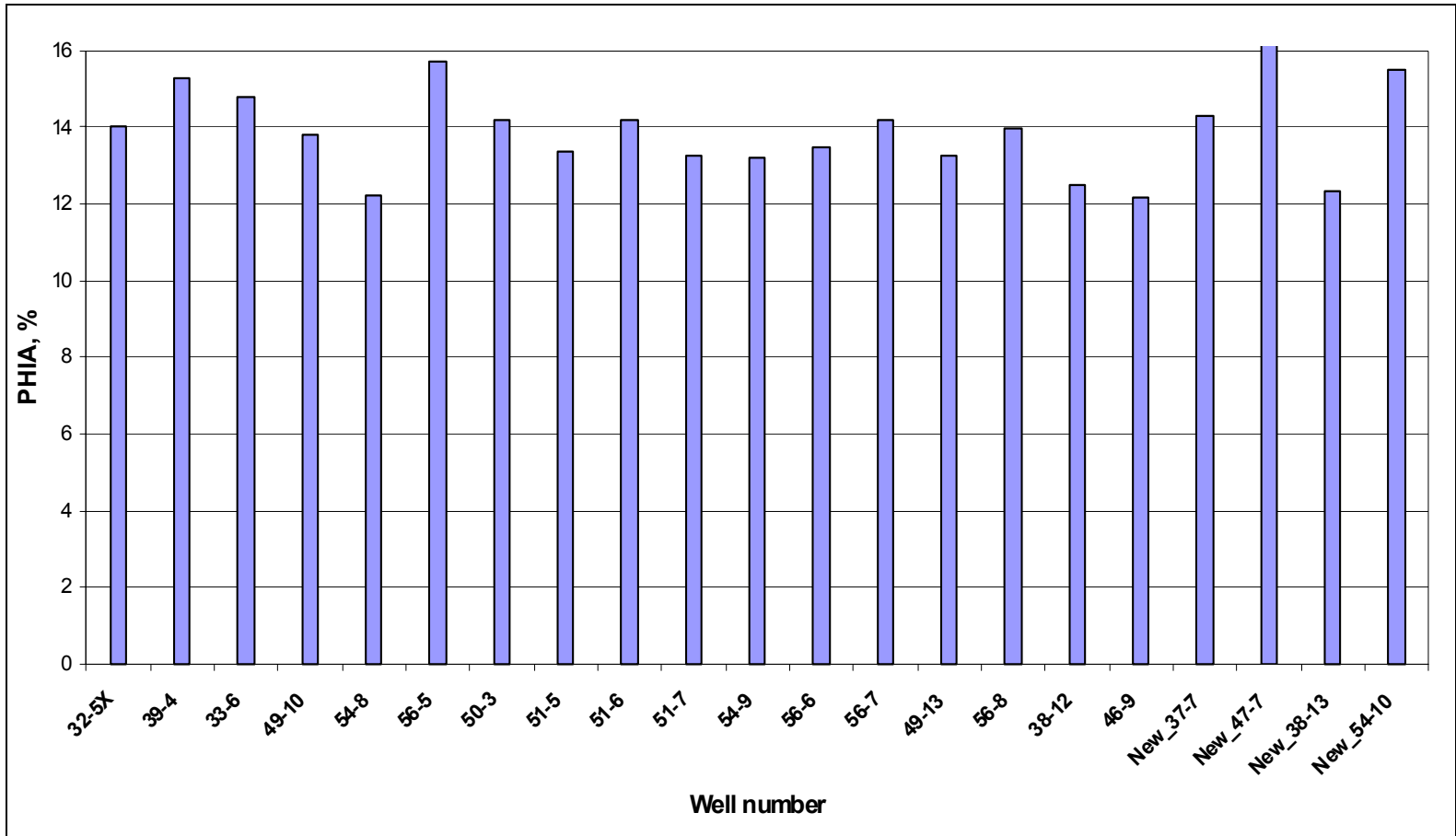


Figure 25. Neutron-density average porosity values for net pay in the lower Cut Bank Sand. Net pay is based on a 10% porosity cutoff

3.5 Integration of Seismic and Well Log Data

Using the VSP calibration data, DeAngelo and Hardage (2001) interpreted the base of Cut Bank or top of Ellis group at the zero crossing (cross-over from positive to negative amplitude) at 520 ms in the 3D seismic volume and named it lower stratal surface (Fig. 26). The zero crossing from negative to positive amplitude above this was interpreted as the top of reservoir and was named upper stratal surface. The mid-stratal surface is a line between upper and lower stratal surfaces and divides upper and lower reservoir intervals. Tinroof corresponds to strong positive amplitude just above the upper stratal surface.

At this point, it is important to discuss the resolution of the seismic data at the reservoir interval, i.e. at the interval between Tinroof and Ellis group. Average seismic velocity in the reservoir interval below Tinroof is 11,300 ft/sec based on VSP data. As shown in Figure 26, the resolution (amplitude length) in this interval is no more than 10 ms, which corresponds to 113 ft (11,300 ft/sec x 0.001 sec) thickness. The average gross thickness of lower Cut Bank is about 35 ft. As stated earlier in this chapter, the fact that reservoir thickness is far less than seismic resolution, indicates that small-scale geologic heterogeneity that may have a major impact on reservoir performance may be neglected.

The critical step in seismic-guided log-property mapping is having accurate time-to-depth relationships. I estimated velocities from density logs using the Gardner equation ($\rho=cV^\alpha$, where $\alpha=0.21$ and $c=0.35$) (Gardner et al., 1974). The Gardner

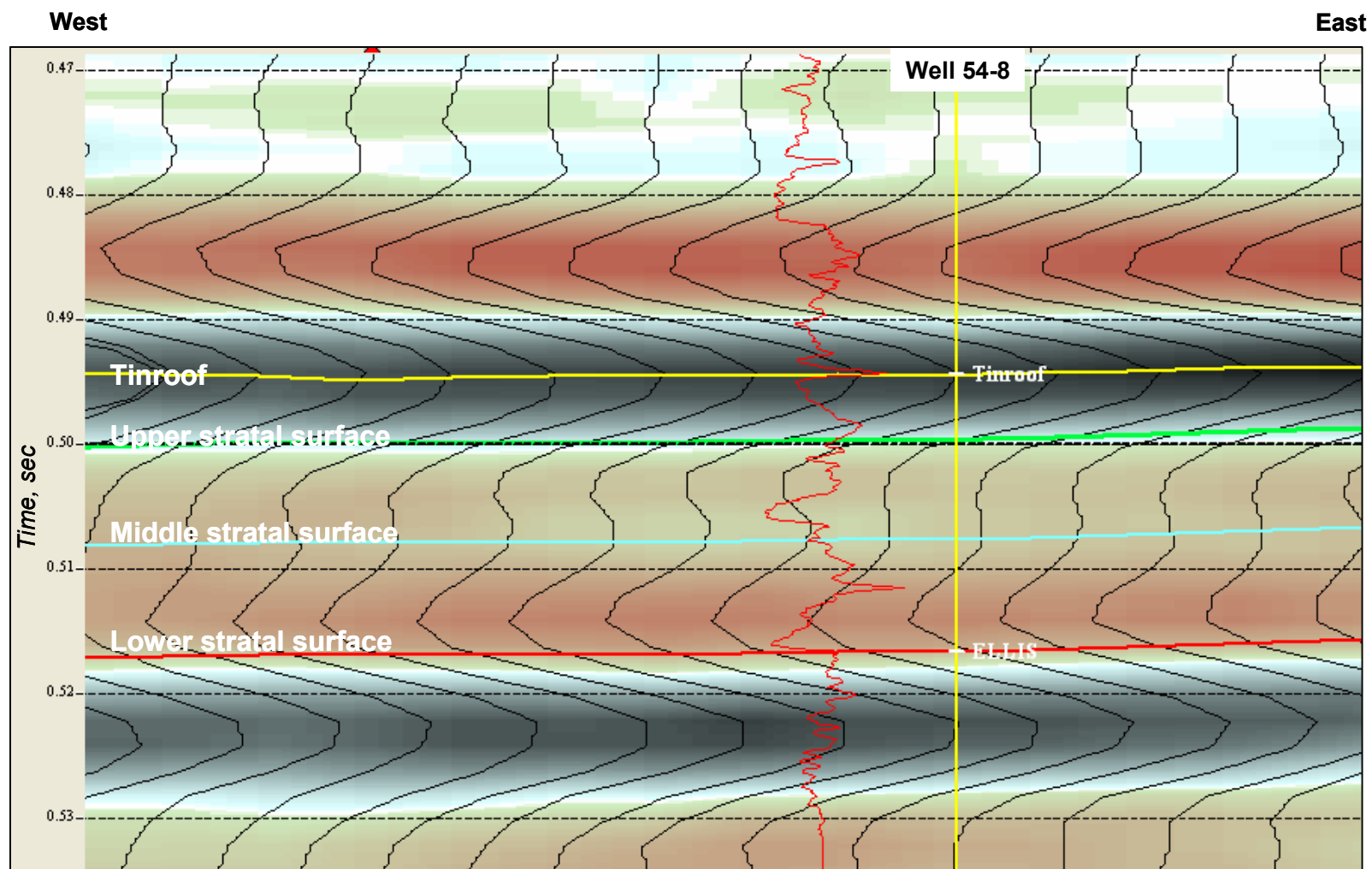


Figure 26. Seismic inline 145 displaying upper, middle, and lower bounding stratal surfaces the resolution of seismic data in the interval between Tinroof shale and Ellis group at the VSP well. Red curve is GR log.

equation parameters (α and c) were estimated by combining data from 4 wells that have density logs and either sonic log or a borehole seismic report available.

Seismic velocity estimates determined from VSP (vertical seismic profile) data are available for one well (Well 54-8) in the study area, and this allows a check of depth-time relationships determined from log data alone. The two approaches compared favorably in the southwest area, but in the northeast part of the seismic survey area, the VSP data produced a significantly different depth-time relationship. Specifically, the difference between the estimated two-way travel time at the relevant Cut Bank formation was approximately 25 msec. Thus, to tie seismic and well data, I used VSP (Well 54-8) data for the south and southwest parts of the seismic survey area. Sonic data derived from the density (Well 37-7) were used for the northeast area.

Seismic and well log data in the Cut Bank field were integrated to determine which, if any, seismic attributes can be used to map reservoir properties. The variations observed in seismic attributes, such as amplitude, should be a function of variations in reservoir parameters such as porosity. Seismic attributes were compared with well log porosities to model the porosity distribution throughout the field.

I checked whole series of attributes to assess relations between seismic attributes and reservoir properties. To avoid spurious (by chance) correlation (Kalkomey, 1997), I focused on amplitude attributes, because, in many cases, the amplitude of a reflection corresponds directly to the porosity (meaning that there is physical relationship between rock physical properties, such as porosity and seismic amplitude). The assumption is that amplitude (both negative and positive) is proportional to reflectivity. By plotting the

average Cut Bank sandstone porosity at each well against the seismic amplitude at that well, the nature and strength of the relation was investigated. I used average neutron-density porosity (PHIA) values for 21 wells.

The three amplitude attributes extracted from the lower Cut Bank sandstone interval of the 3D seismic volume were maximum amplitude, mean amplitude, and root-mean-squared (rms) amplitude. The correlation between porosity and both mean amplitude and rms amplitude are poor. On the other hand, the maximum amplitude varies inversely with porosity of the Cut Bank reservoir (Fig. 27). The regression had a value of 0.51 when fitting the maximum amplitude to the average porosity of net pay (PHIA > 10%). Two points, wells 49-10 and 39-4 (Figs. 27 and 28), were excluded in obtaining this relationship.

The maximum amplitude at the Well 49-10, located at the center of the seismic survey area, is anomalously high compared to the average log porosity (PHIA). Moreover, this well is near Well 49-14, where the seismic amplitude is anomalously high and does not match expected thickness values. This high value may result from an inconsistent interpretation of the base of the lower Cut Bank (Ellis top) in this area. This horizon is at the zero crossing above positive amplitudes (peaks) throughout all of the seismic survey (Fig. 29), with the exception of the problem area of Well 49-10 (Fig. 30). Another cause may be the location of this well adjacent to the western edge of the Lower Cretaceous Gorge. Well 39-4 is also located near the western edge of the Lower Cretaceous Gorge. In this well the maximum amplitude value again under-predicts the porosity. Here, also, another explanation may be an inconsistency in the interpretation

and stratigraphic ties of the lower Cut Bank interval in well log and seismic data (Fig. 31).

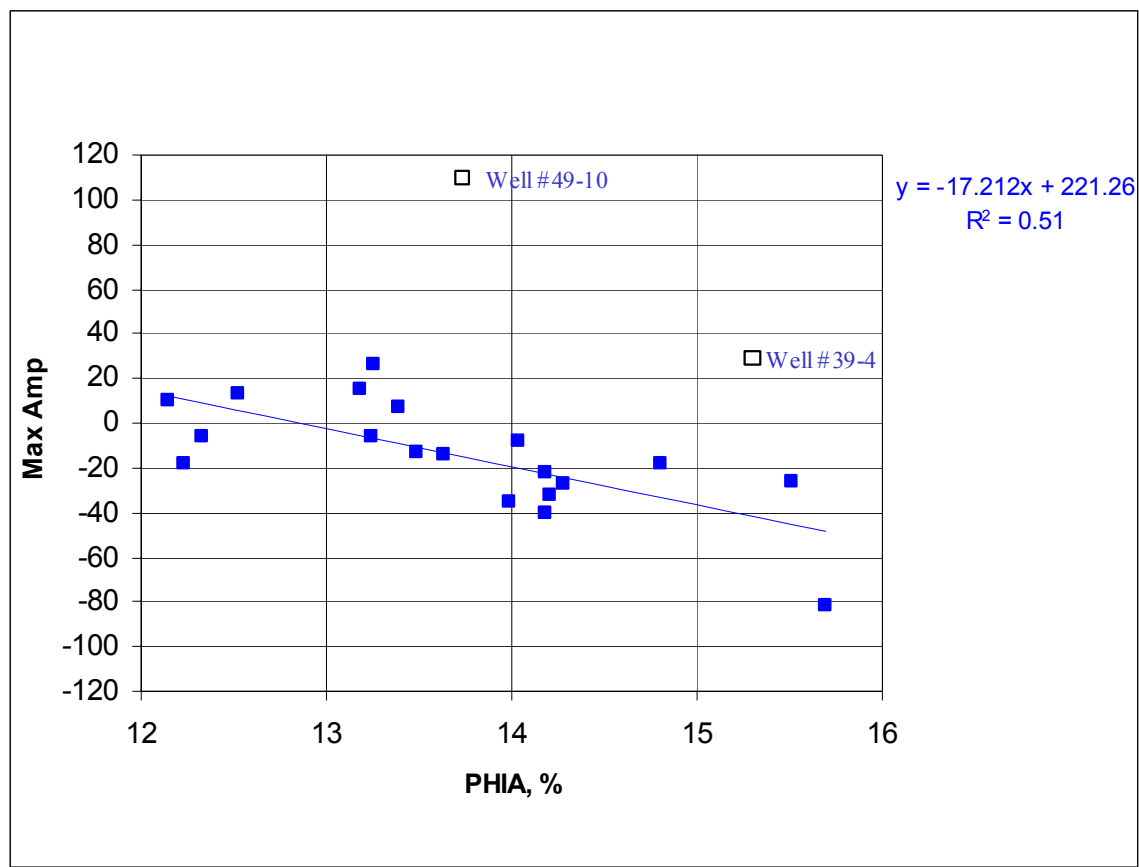


Figure 27. Relation between the log neutron-density average porosity and 3-D seismic amplitude at the well ties. Each point represent a well with a given single character name. The empty squares are the excluded wells. Significance F = 0.000706847 or 0.0707%.

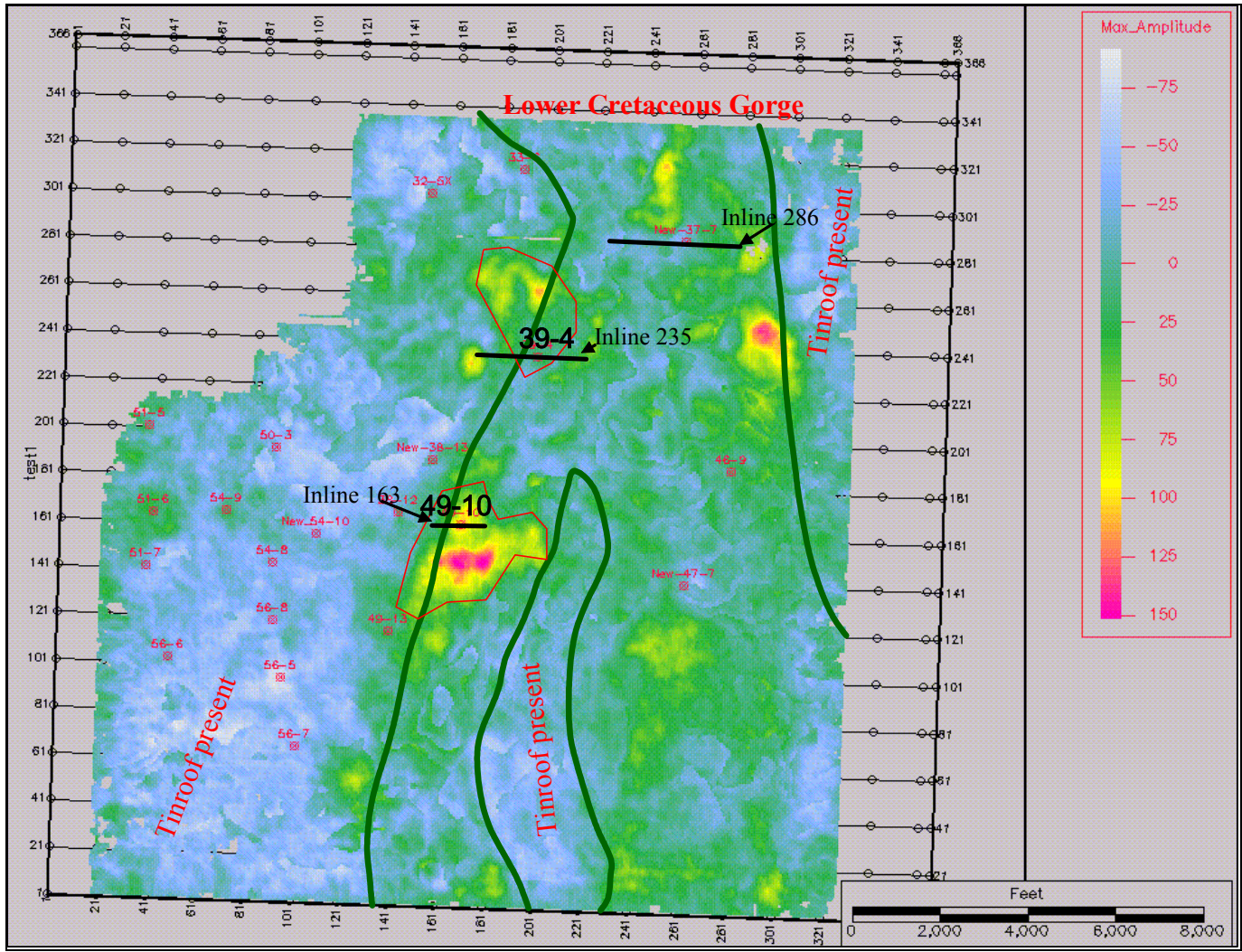


Figure 28. Maximum amplitude of lower Cut Bank horizon. Red is highest amplitude and blue is lowest. Red polygons around wells 49-10 and 39-4 are areas of mismatch

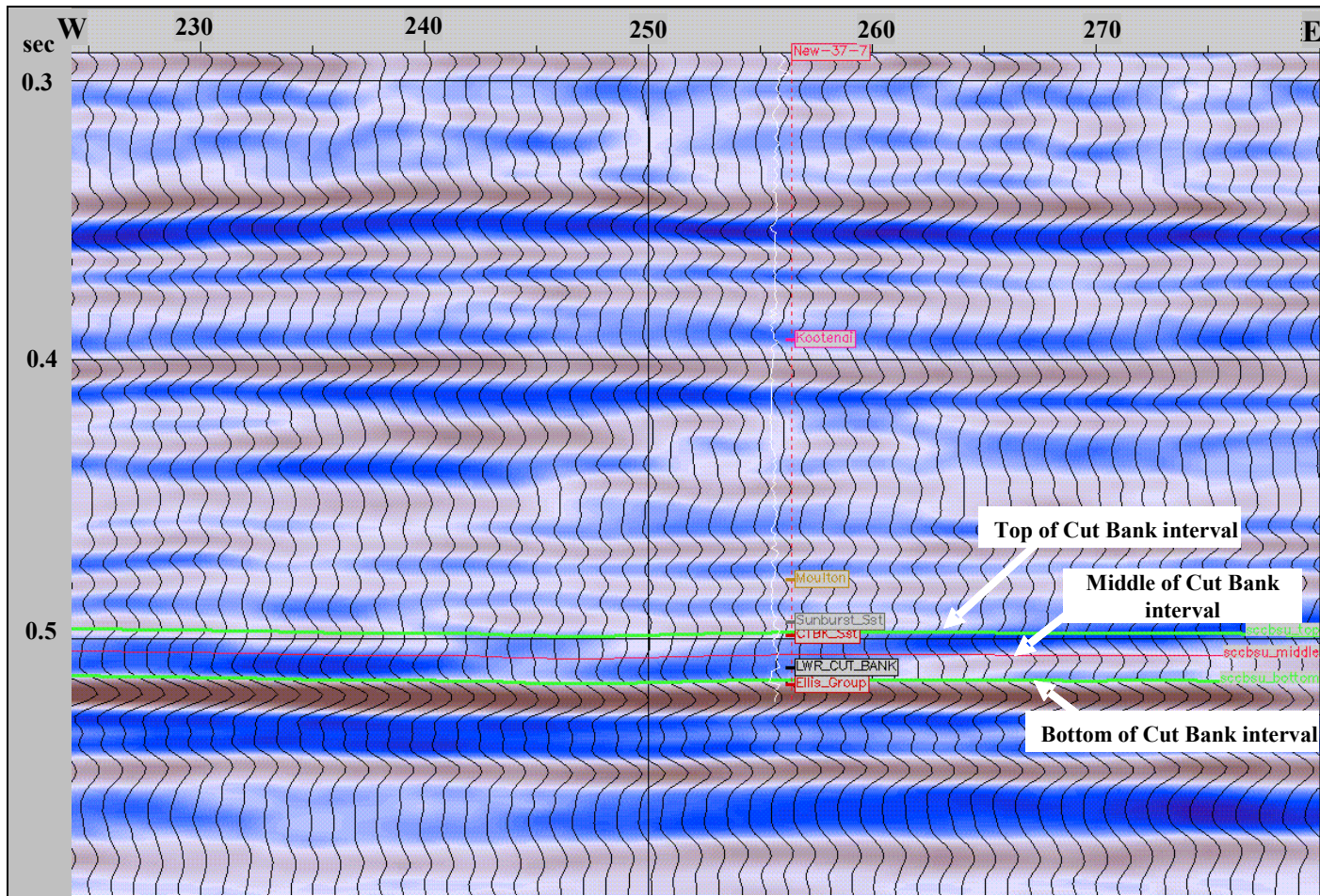


Figure 29. Seismic inline 286 displaying upper, middle , and lower bounding stratal surfaces. Notice the bottom of lower Cut Bank interval, or top of Ellis, is at the zero crossing above the positive amplitudes (Location on Figure 28).

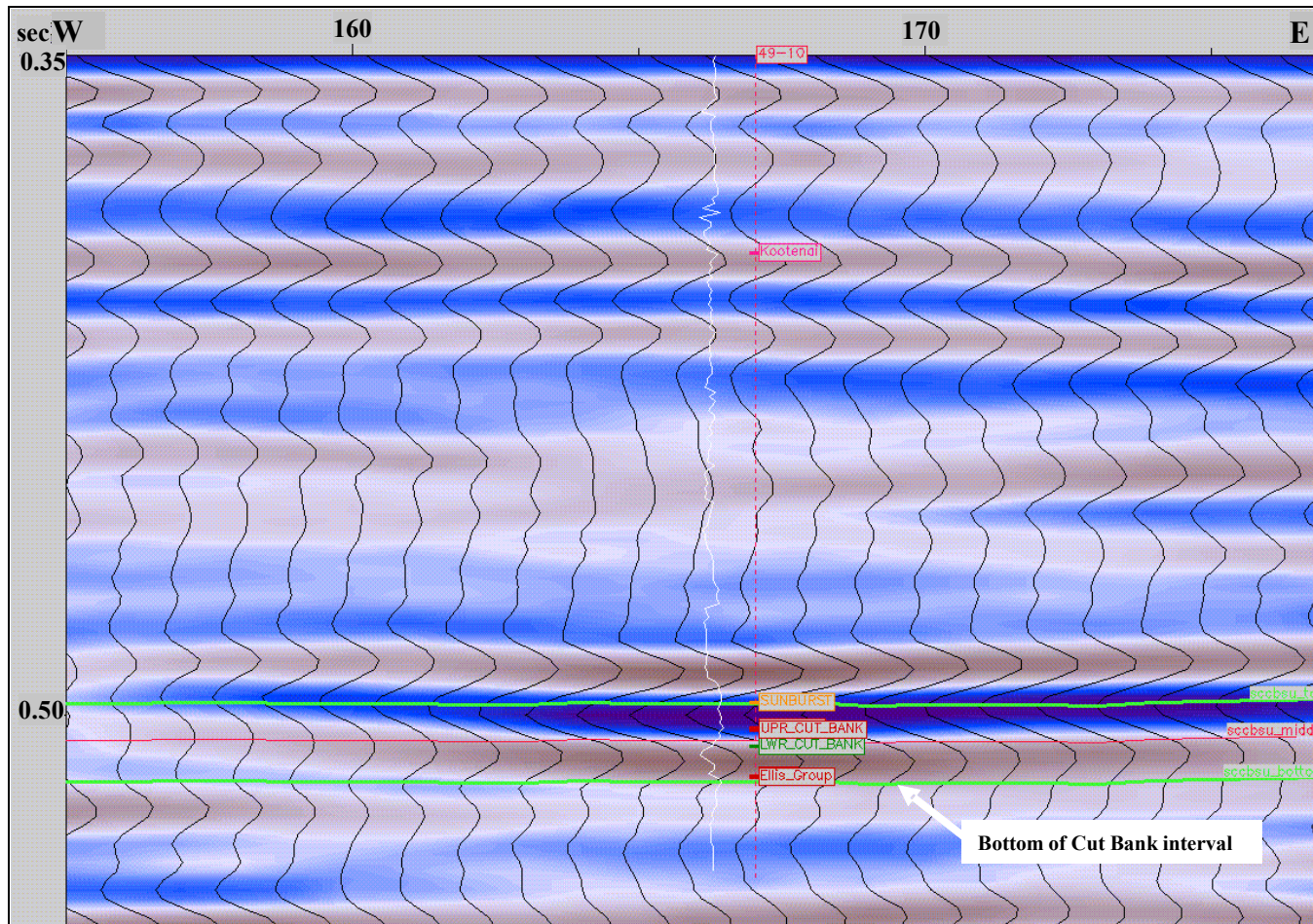


Figure 30. Seismic inline 163 displaying upper, middle, and lower bounding stratal surfaces. Maximum amplitude at Well 49-10 is anomalously high compared to the average log porosity value. One reason for that may be inconsistent interpretation of the bottom of the lower Cut Bank strata in this area. This surface is at the zero crossing above the positive amplitudes all over the seismic survey (see Figure 29) except in the problem area (Location on Figure 28).

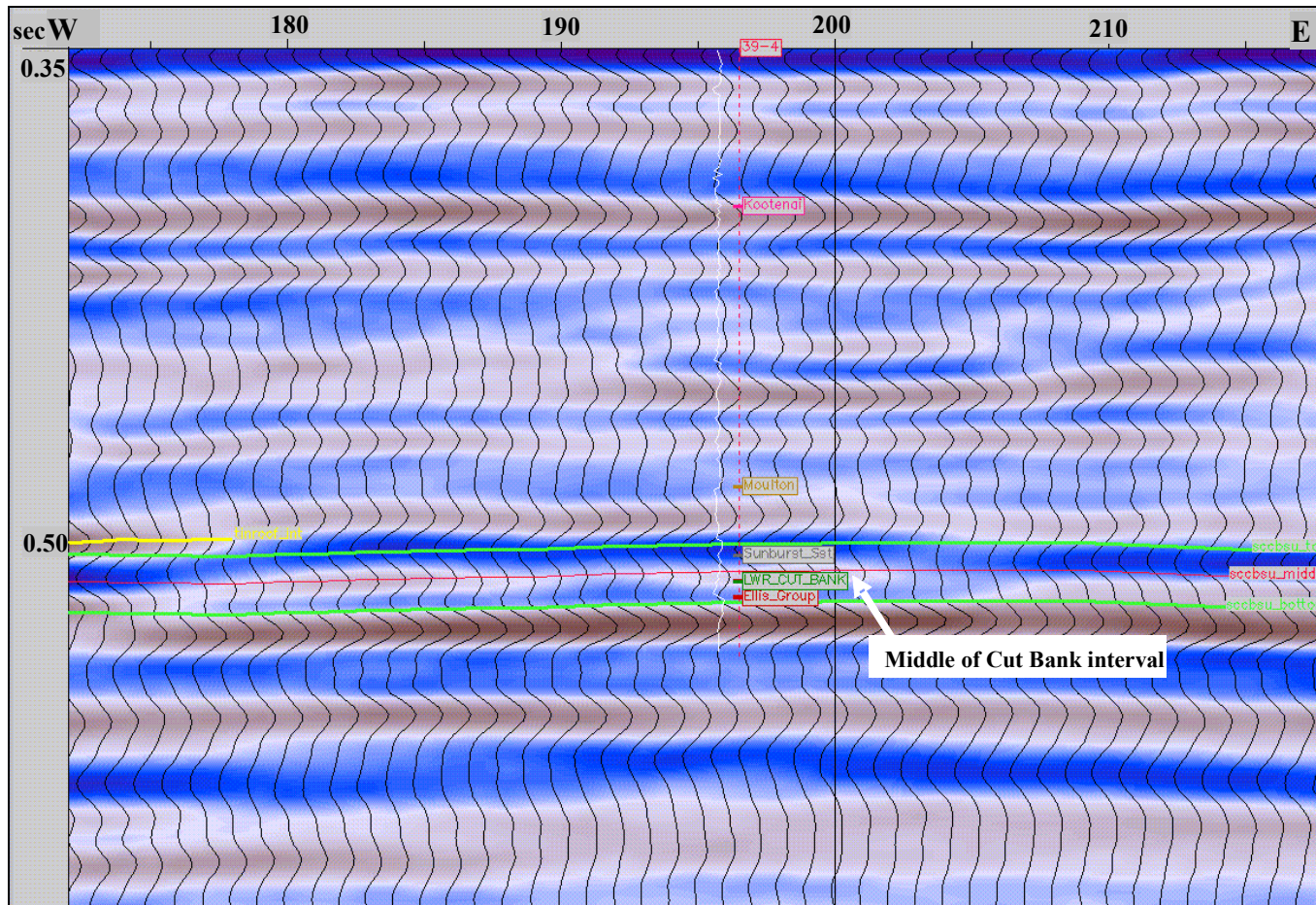


Figure 31. Seismic inline 235 displaying upper, middle, and lower bounding stratal surfaces. In Well 39-4 the maximum amplitude value under-predicts the porosity. One of the reason may be inconsistency of interpretation of lower Cut Bank interval in well log and seismic interpretation. Middle of Cut Bank interval in seismic does not correspond to the top of lower Cut Bank interval (Location on Figure 28).

On the basis of the relation between PHIA and maximum amplitude, it is clear that seismic amplitudes provided additional information about the variation of the lower Cut Bank reservoir thickness, and average porosity in the interwell space. However, at some wells relations did not follow the main regression trend, demonstrating the uncertainty associated with indirect methods of thickness determination and reservoir mapping. Closer examination of the interpreted horizons in the vicinity of these wells indicated that the seismic data were misspiked due to a crossing channel system. At this point, the ideal solution would have been to correct the seismic interpretation and repeat the analysis. Unfortunately, the seismic response in the area of the crossing channels was complicated due to interference between events, and the event that could not be interpreted with confidence.

Thus, characterization of Cut Bank reservoir and recognizing potential compartmentalization in SCCBSU area using seismic data continues to be challenging due to inconsistent seismic imaging of the target formation. Therefore, I decided to model this complex reservoir by combination of stratigraphic models and probabilistic simulations using well log and core data. Application of high-resolution sequence stratigraphy at the reservoir scale provides the correlation scheme of the reservoir and enables one to predict the reservoir geometry and extension within a deterministic framework. Furthermore, these conceptual models are able to predict the reservoir extension and architecture up to a certain level: estimation of the channel amalgamation, and then gross reservoir quality can be predicted with such an approach.

However, in many cases, at reservoir scale, accuracy of such models often remains insufficient to predict realistically the distribution of internal heterogeneities within reservoir units. Furthermore, fluid- flow modeling requires a representation in terms of petrophysical properties. Stochastic approaches simulate the distribution of either small-scale sedimentary bodies or the internal reservoir heterogeneity and provide equiprobable realizations of the heterogeneity distribution.

CHAPTER IV

FACIES ANALYSIS

4.1 Lithofacies Interpretation

A thorough understanding of the sedimentology is required to realize high-resolution stratigraphic correlations (Wescott, 1993; Robinson and McCabe, 1997) and when building a reservoir model to guide decisions concerning the proper modeling technique (object or pixel-based) (Henriquez et al., 1990; Hirst et al., 1993). Therefore, I evaluated depositional systems of reservoir rock in Cut Bank field using well logs, cores and outcrop description. Fluvial depositional systems are composed of four basic building blocks - channels, splays, levees and floodplain sedimentary facies. Original porosity and permeability vary greatly among these facies. Moreover, the reductions of porosity and permeability during burial and diagenesis are strongly facies controlled.

Well-log analysis is used to define electrofacies associated with sedimentary facies deduced from core analysis, and to infer electrofacies associations and depositional environments directly from well logs. For this purpose, well logs must be calibrated with cores.

Although core data were extremely limited in Cut Bank field, they were critical to analysis of depositional systems and determination of reservoir properties. A key approach of this study was to develop facies models that integrated the core and wireline log data. In addition, it was necessary to review the conceptual and analog depositional models to provide the optimum interpretation of sedimentary facies and sand body distribution. Thus, the sedimentological interpretation in this study is based on core

descriptions from 6 wells, my description of four cores (wells 38-11, 36-5, 33-5 and 39-1X) at Quicksilver Resources core repository in Casper, Wyoming, and two core descriptions (wells 37-7 and 22-6) obtained from QRI , log data and the available literature.

I used gamma ray log (GR) character to produce a log-pattern (electrofacies) facies map of the more continuous Lower Cut Bank Sandstone member. Cut Bank Sandstone log patterns are blocky in the mid-channel deposits and upward fining or serrated at the channel margins. In the interchannel, floodplains areas, the sand thickness decreases markedly, and the log patterns are serrated or sometimes upward-fining.

Overlaying the GR logs on a gross sand thickness map allows assessment of the reservoir architecture - geometry, size, vertical contacts, bedding characteristics, and thickness (Fig. 32). Also, this technique can be used to map porosity logs to evaluate vertical porosity distributions.

4.2 Lithofacies Descriptions from Cores

In the summer of 2004, I described 128 ft of core from 4 wells stored at a Quicksilver Resources core repository in Casper, Wyoming. Two of these cores had missing intervals. In addition, the company provided core photos from well 37-7, one of the most recently drilled wells in SCCBSU, and routine core analysis reports from 6 wells that includes above wells. Thus, core description in this study included the available cores for description and reports provided by Quicksilver Resources. The cores and core reports are primarily from the lower Cut Bank and secondarily from the upper Cut Bank

interval. In the cores I recognized and interpreted seven types of sedimentary lithofacies. The main characteristics of these lithofacies are summarized in Table 2.

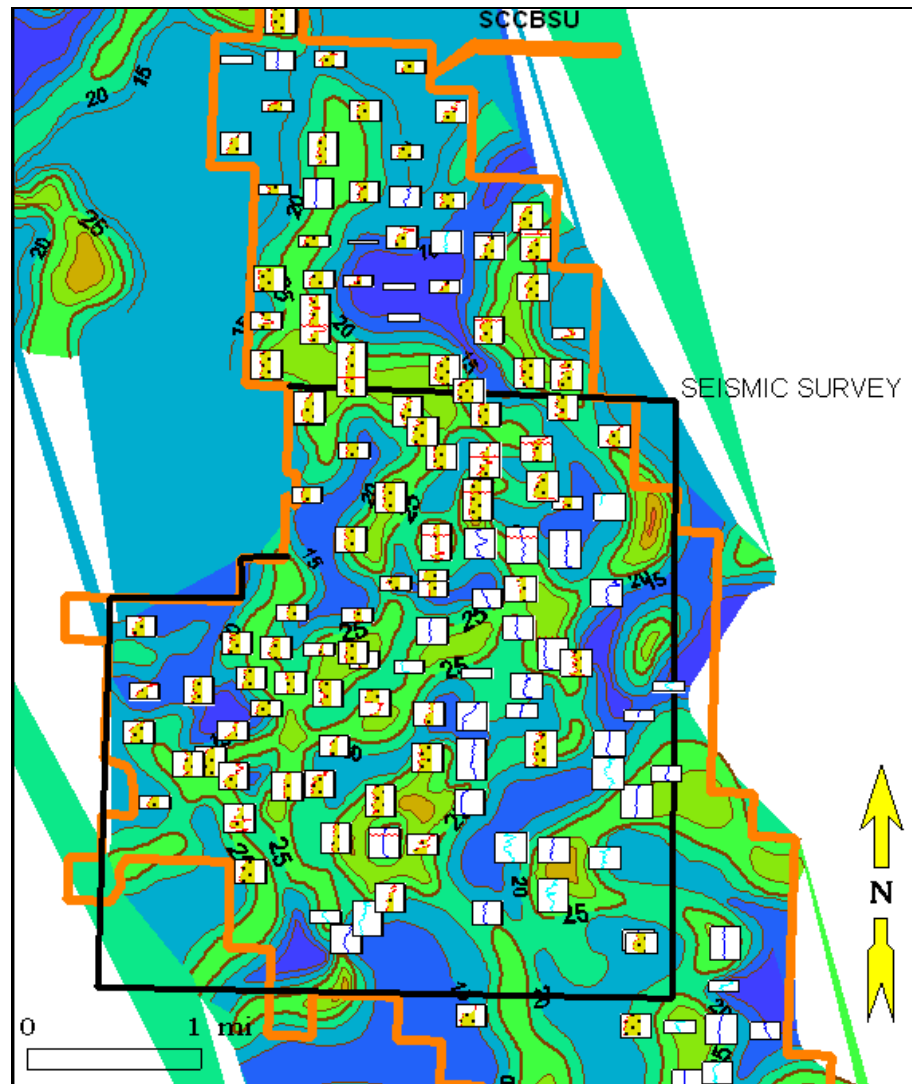


Figure 32. Log-pattern (electrofacies) facies overlain on Quicksilver Resources gross thickness map of lower Cut Bank sand (Quicksilver Resources, 2002). Red curve is GR log increasing from 0 to 150 API from left to right, light blue is cased GR, dark blue is old GR logs. Log patterns are blocky in the mid-channel deposits and upward fining or serrated at the channel margins. Thickness decreases markedly, and the log patterns are serrated or sometimes upward-fining in interchannels.

Table 2. Main Cut Bank Sandstone lithofacies characteristics from core data from 6 wells, my description of four cores (wells 38-11, 36-5, 33-5 and 39-1X) , and two core descriptions (wells 37-7 and 22-6) obtained from QRI.

Lithofacies	Description	Occurrence	Depositional Process and Interpretation
1. Coarse-grained pebbly sandstone	Coarse-grained sandstone with conglomeratic fragments (conglomerate fragments are 0.1-1.0 cm in size), dark chert and light colored quartz fragments; light and dark colored pebbly inclusions; massive or faint planar bedding	Observed at the base of fining-upward channel sequences overlying basal erosional contact of Ellis shale	High energy tractive currents, bed-load charge of alluvial channels
2. Mud-supported conglomerates and breccias	Poorly sorted, mud-supported polygenic conglomerates and breccias with dominance of angular dark chert. Dark gray colored shaly matrix derived from the floodplain shales	1 to 4 in thick beds	Unchannelized debris-flow deposits, distal alluvial fan setting
3. Clean, coarse- to medium-grained sandstone	Coarse- to medium-grained, upward fining, clean sandstone; crossbedded; moderately well sorted	Overlie lithofacies 1, forming upward fining sequences	High energy, unidirectional, tractive currents
4. Clean, medium- to fine-grained sandstone	Medium- to fine-grained sandstone with hematite grains, trough cross-bedded or massive	Overlie facies 3, forming and sometimes ending the fining upward sequence	Low energy tractive currents
5. Fine-grained sandstone or siltstone	Fine-grained, massive or current ripple-laminated sandstones. Occasional fine bioturbation	Overlie facies 4, ending the fining upward sequences	Low energy tractive currents, overbank alluvial deposits, levees and crevasse splays
6. Silty mudstones	Olive-gray to reddish mudstones with floating quartz grains	Units alternating with the channel fills	Floodplain or mud-flat deposits
7. Shale olive-gray and reddish	Olive-gray to reddish mudstones, finely laminated	Up to 20 ft thick beds	Ephemeral lake deposits

The log signature of each lithofacies was also calibrated on the core description (Figs. 33 and 34). Not all seven facies were present in cores from one well.

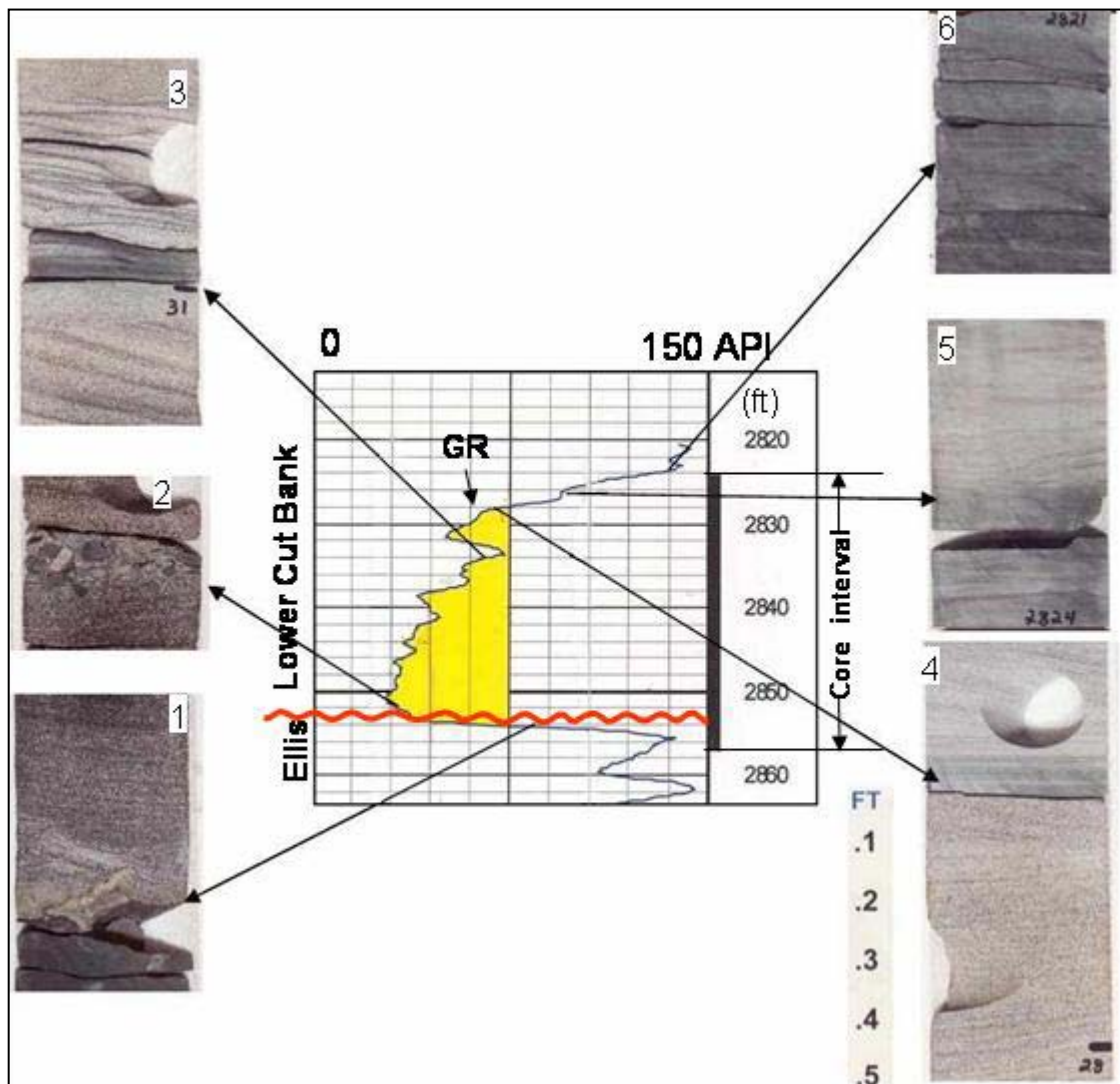


Figure 33. Calibration of the well log signature of lithofacies to the core, Well 37-7. Six of the seven lithofacies identified in cores were found in cores and calibrated to log data in this well. For lithofacies 7 see Figure 34. Numbers in white boxes on each core photograph correspond to lithofacies number in Table 2.

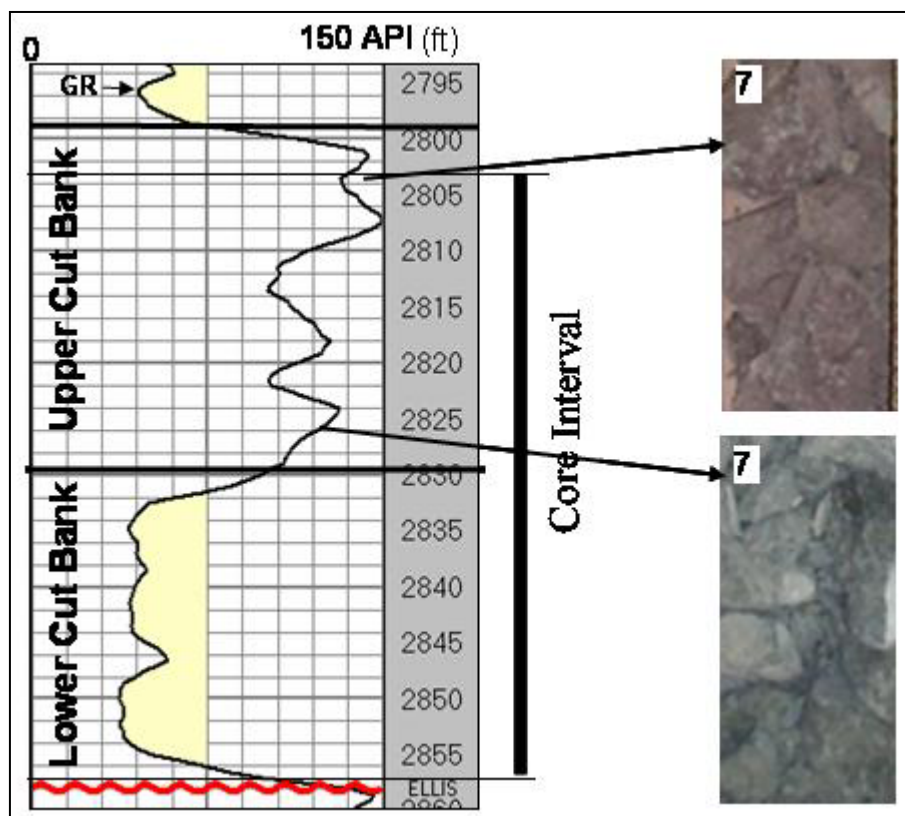


Figure 34. Calibration of the well logGR signature of lithofacies 7 to the core, Well 33-5.

Lithofacies 1: Coarse-Grained Pebbly Sandstones

This facies occurs at the base of upward fining channel sequences overlying the basal erosional contact with the Ellis Group shale. This facies was deposited as high energy, tractive currents, the bed-load charge of fluvial channels. In the cherty unit at the bottom of Cut Bank sandstone, chert clasts sometimes constitute more than 60% of all pebbles. The clasts are eroded from the proximal Rocky Mountain area to the southwest, and their sub-angular morphology suggests a short transport distance.

Lithofacies 2: Mud-Supported Conglomerates and Breccias

The muddy matrix of these breccias suggests deposition by debris flow. This facies is most common at the base of the series where it is interbedded with medium- to fine-grained tractive currents sands. This facies inferred to result from unchannelized gravity flows in an alluvial-fan setting.

Lithofacies 3: Clean Medium- to Coarse-Grained Sandstones with Trough Cross-Bedding

Lithofacies 3 was deposited by high-energy unidirectional tractive currents, as suggested by the abundance of trough cross-bedding. Individual channels commonly are isolated in floodplain shales and are remarkably thin (4-7 ft). Several stacked channel sands may be amalgamated in units up to 25 ft thick. Correlation of individual channel sequences is difficult between wells, which commonly are 2,000 ft apart.

Lithofacies 4: Clean, Fine- to Medium-Grained Sandstones

These trough cross-bedded or massive, medium- to fine-grained sandstone with hematite grains overlie facies 3, forming and sometimes ending the upward fining sequence. This facies is interpreted as a deposits of low-energy tractive currents.

Lithofacies 5: Massive, Fine-Grained Sandstone or Siltstone

These fine-grained, massive or current ripple-laminated sandstones overlie facies 4, ending the fining upward sequences. This facies corresponds to overbank alluvial deposits associated with low-energy tractive currents ending the channel infill or, occasionally, to sheet-flood or crevasse-splay deposits in a floodplain setting.

Lithofacies 6: Silty Mudstones

These olive-gray to reddish mudstones with floating quartz grains alternate with the channel fills suggesting the facies was deposited in a flood-plain or a mud-flat setting.

Lithofacies 7: Laminated Mudstones.

These are finely laminated olive-gray to reddish mudstones from upper Cut Bank interval. At this interval most wells intersect one or more channel and/or crevasse-splay sandstones, such that unbroken mudstone intervals are typically few feet thick. In isolated locations, however, much thicker mudstone successions are encountered; in some instances, up to 30 ft thick (Fig. 34). These anomalously thick mudstones represent areas that were never occupied by a fluvial channel. I infer these mudstones result from the subaqueous sedimentation of the mud that were deposited in shallow, ephemeral lakes. Similar Cut Bank mudstones were described by Hopkins (1993) at an outcrop in Great Falls area.

4.3 Depositional Model

The main characteristics of the lower Cut Bank sandstone from available core data are summarized as follows.

- Sandstones and conglomerates were dominantly deposited by high-energy unidirectional flows.
- Channel-fill deposits are very common; they commonly interfinger with gravity-flow deposits.
- Lateral continuity of individual channel-fill sands is poor;
- Organic matter is rarely preserved.

These criteria are typical of alluvial-fan depositional systems (Nilsen, 1982; Blair and McPherson, 1994) formed in semiarid conditions. The predominance of channels vs. debris-flow deposits may indicate that the lower Cut Bank Sandstone was located in the distal part of an alluvial-fan system. The axis of the alluvial fan was WSW–ENE oriented with the terrigenous sediments being introduced from the west-southwest. The channel-fill deposits are characterized by sandy and sometimes gravelly at the base of bedload-dominated deposits and could be attributed to braided channels. Regionally, the pattern of channels extends for more than 80 km into Canada, in the Lower Cretaceous Basal Quartz of Southern Alberta where the basal sandbodies were created by coarse-grained meandering rivers in a setting with slow net aggradation and extensive cannibalization of overbank deposits ((Zaitlin et al., 2002 and Lukie et al. 2002).

Characterization of the upper Cut Bank and Sunburst interval is difficult because of the lack of core data. Well-log information was used to characterize the main sedimentary facies of upper Cut Bank and Sunburst zones. Based on log data, the basal sands of lower Cut Bank are gradationally overlain by a mudstone-dominated deposit that contains isolated, fluvial-channel and crevasse-splay sandstones of upper Cut Bank interval. Channel sandstones and crevasse splays typically constitute around 50% of the interval.

In the Cut Bank area, the Sunburst zone is about 45 ft thick, with sandstone beds ranging from almost zero to the entire thickness of the zone. Based on description by Hayes (1990), the Sunburst zone comprises interbedded, varicoloured mudstones, siltstones and sandstones of continental origin. The Sunburst sandstones are fine to

medium grained, composed primarily of quartz with minor amounts of chert grains and rock fragments, and are cemented by silica and clay.

The Sunburst zone of the Cut Bank area represents relatively low-energy fluvial and floodplain deposits lying more or less conformably on the higher-energy, braided stream Cut Bank sandstones. The Sunburst sandstone is comparable in stratigraphic position and genesis to Lower Mannville continental sandstone bodies throughout southern Alberta and northern Montana (Hayes, 1986).

I infer that an analog to Cut Bank field is the distal part of a Middle Triassic alluvial fan system at Chaunoy field in the Paris basin, France. Figure 35 is reconstruction of the depositional environments in Chaunoy field by Lemouzy et al. (1995). The Chaunoy Sandstones (a Carnian–Norian lithostratigraphic formation) at Chaunoy field composed of small ribbon channel deposits, interbedded with flood-plain environments.

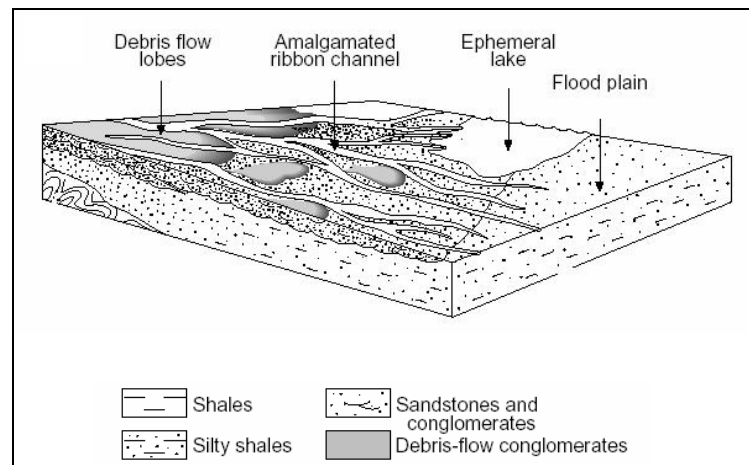


Figure 35. Analog field-reconstruction of the depositional environments in Chaunoy field (from Lemouzy et al., 1995).

4.4 Channel Geometry

Valley size and geometry are important for the reservoir description because they strongly influence channel-fill sandstone reservoir architecture and connectivity. The values of these parameters are difficult to estimate.

Fluvial channel-fill sand bodies are commonly discontinuous. Therefore, linear interpolation of reservoir characteristics between wells provides unrealistic models of reservoir extent and fluid distribution. Meandering and braided rivers produce reservoir sand bodies of different dimensions and heterogeneity. Commonly used methods for estimating the geometry of channels are (1) well-to-well correlation, (2) empirical equations relating maximum channel depth, channel width, and channel-belt width, and (3) amplitude analysis of 3D seismic horizon slices. Correlation of specific channel-fill sandstone bodies using wireline-logs is the most common method for estimating channel-fill widths and orientations. The spatial resolution of this technique can be no better than the average well spacing; therefore, if well spacing is 1,000 ft, sandstone bodies less than 1,000 ft wide cannot be resolved. In SCCBSU area average distance between two logged wells is no less than 1,000 ft.

Geological equations for the prediction of channel fill width are not robust. Meandering and braided channel systems coexisted during deposition of the Cut Bank, as can be seen on well log cross sections from the north and central part of SCCBSU area (Figs.12 and 36). Meandering channels were common in the northern area of the field (lack of channel stacking) (Fig. 36), whereas braided channels were more common

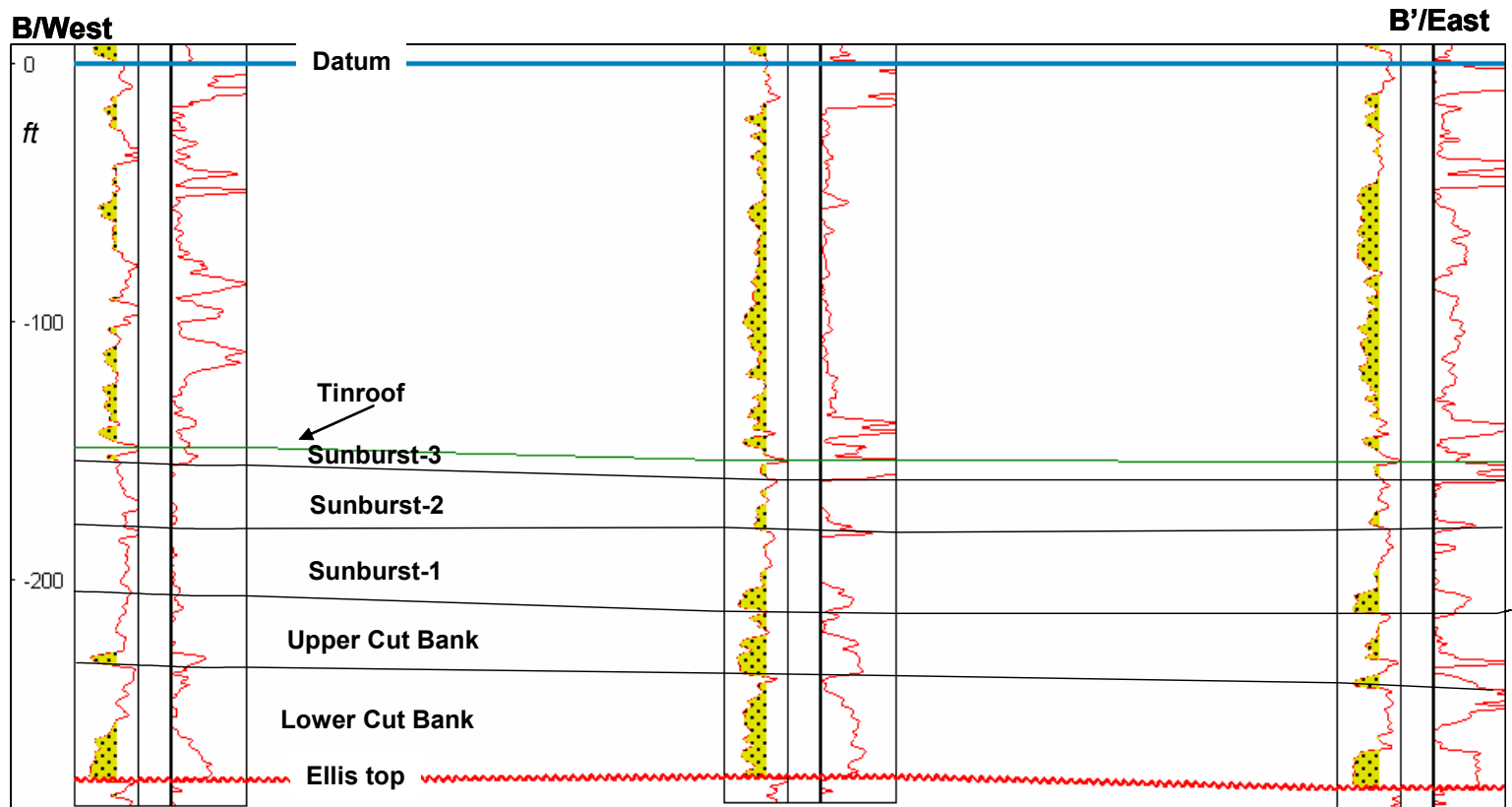


Figure 36. West to east well log stratigraphic cross section B-B' from the north of SCCBSU area (See figure 11 for location). Vertical Exaggeration=10.6667.

in the central and southern portion of the field (vertical and lateral stacking of channels) (Fig. 12). The lack of multiple fining-upward cycles within the roughly 70 ft-thick lenticular sandstones of upper Cut Bank and Sunburst member indicates that the sandstone bodies are not stacked braided river channel deposits but instead are point bars or remnants of point bars in a meandering river system.

Individual channel meandering streams typically have a thickness-to-width ratio of 1:25 to 1:100, based on different references and empirical equations (Lorenz et al. 1985; Fielding and Crane, 1987; Davies et al., 1992). Relatively thin channel-fill sands are due to the extensive lateral migration that most high sinuosity streams undergo. If no lateral migration occurs because of stable banks, then multi-cycle relatively narrow sand bodies can form, similar to those formed by anastomosing river systems (Nanson, 1980). Because of their overall high sinuosity, meandering streams sediments contain crossbed foresets with a wide range of paleocurrent orientations (Miall 1996).

Braided streams have thickness to width ratios of 1:100 to 1:500 (Fielding and Crane, 1987; Davies et al., 1992). This is because of the great width and largely unconfined nature of braided streams relative to their depth, despite the multi-cycle nature of their deposits. Because the individual channels in a braided stream have relatively low sinuosity (Miall 1996), plots of palaeocurrent directions from foreset beds will show a lower degree of variation than for sand bodies deposited by meandering or anastomosing streams.

Cut Bank channel sandstones are usually multi story with complex stacking patterns. Insufficient outcrop and core data made it difficult to distinguish single story

sandstone body dimensions. To acquire accurate thickness and width information of single stories I attempted to define the frequency distribution of sand thicknesses that was measured on wireline logs using a 100 API gamma ray cutoff by building histograms (Fig. 37). Thickness of lower Cut Bank sand varied from 1.5 to 40 ft and mean thickness was 19 ft. Thickness range 5-20 ft has the highest frequency.

The GR log pattern in 5-20 ft thickness interval is mostly blocky (Fig. 38a). The sandbodies above 20 ft thick are multistory, with complex stacking pattern. However, in some cases 1, 2 or even 3 thin shale interlayers are observed, showing vertical stacking of several channels discretely (Fig. 38b).

Thus, I used 5 to 20 ft for single channel thickness to reconstruct width of individual channels. There are several published empirical equations that predict the width of channel belts if channel depth or sandstone body thickness is known. I used empirical equation by Bridge and Mackey (1993) that relate channel thickness to channel width in braided fluvial systems:

$$w = 58.88d^{1.82};$$

where w is channel width and d is channel depth. The individual channel width of lower Cut Bank interval varied from 1,100 ft to 13,000 ft. Average distance between logged wells in SCCBSU is approximately 2,500 ft.

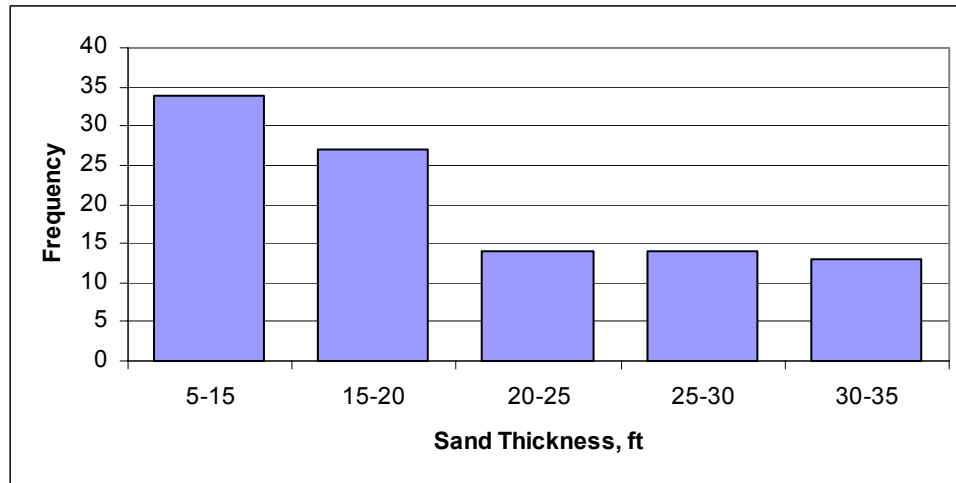


Figure 37. Frequency distribution of lower Cut Bank sandbody thickness to define the single story channel thickness.

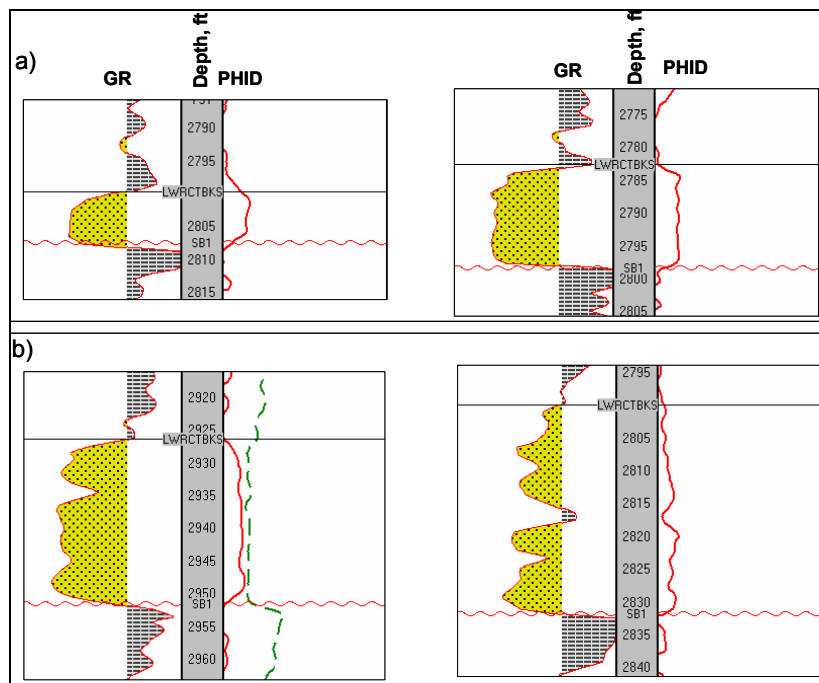


Figure 38. Log patterns of lower Cut Bank sandstone bodies: a) the GR log pattern in 5-20 ft thickness interval is mostly blocky; b) the sandbodies above 20 ft thick are multistorey, with complex stacking pattern. In some cases thin shale interlayers are observed, clearly showing vertical stacking of several channels.

Amplitude analysis of 3-D seismic horizon slices (Weber, 1993; Hardage et al., 1994, 1996; Burnett, 1996) is the only method capable of directly yielding the width of channel belts and imaging the channel pattern (sinuosity, channel splitting) of subsurface sandstone bodies. This is also the only method that can be used to predict the spatial distribution of channel-belt thickness and lithofacies. These are major advances; however, the integrity of 3-D analyses depends on the resolution of the seismic data relative to the thickness of the sandstone bodies imaged. In general, sandstone-body thickness must be greater than approximately 30 ft.

Thus, in SCCBSU area, none of the techniques gives reliable channel geometry because: (1) well spacing is greater than sand body dimensions, (2) empirical equations relating maximum channel depth and channel width, have a lot of scatter; and (3) resolution of the seismic data is low relative to the thickness of the sandstone bodies.

CHAPTER V

SEQUENCE STRATIGRAPHY

5.1 Sequence Stratigraphy Model

Deterministic models based on sequence stratigraphic analysis can identify sequence boundary and systems tract geometries, thus delineating the large-scale heterogeneity. Prediction of facies distributions within each sequence becomes possible because specific depositional patterns are expected to have occurred in varying positions within the sequence. This predictable character within the sequences produces the framework needed for application of geostatistical modeling. Miscorrelation across the bounding surfaces (sequence boundary and flooding surface) in both model development and simulation is avoided using this approach.

Sequence stratigraphy concepts derive historically from seismic stratigraphy (Vail et al., 1977). High-resolution sequence stratigraphy is based on identification of the smallest stratigraphic units [parasequences (Van Wagoner et al., 1990) or genetic stratigraphic sequences (Busch, 1971)] in sedimentological studies. These smallest stratigraphic units reflect relative sea-level variations in marine environments or base-level variations in continental deposits. While they are clearly recognizable in nearshore marine strata, they are much more difficult to recognize and correlate in continental settings. The major underlying believe in non-marine sequence stratigraphy is that allogenic processes, particularly cyclic base-level fluctuation, exert an important control on fluvial architecture (Shanley and McCabe, 1991). However, is it possible to realize high-resolution correlations within alluvial systems?

In this study, I analyzed the possibility of high-resolution sequence stratigraphic correlations in low-accommodation alluvial systems in the Cut Bank and Sunburst members of Kootenai Formation in South Central Cut Bank Unit of Cut Bank field and attempt to build stratigraphic framework of the study interval based on base-level variation. Base-level is a theoretical surface below which sediments accumulate and above which erosion takes place (Wheeler and Murray, 1957, and Schumm, 1993). The response to a change in base-level determines stratigraphic architecture at the scale of stratigraphic cycles (Galloway and Williams, 1991). Base-level variation cycles are controlled by variations in accommodation space (A) and sediment supply (S). A base-level fall is the result of a decrease in accommodation space and/or an increase in sediment supply (decreased A/S ratio). Base-level fall leads to the development of a regional erosion surface with incised valleys (Van Wagoner et al., 1990). Subsequent base-level rise (increased A/S ratio) allows deposition that initially is confined within the valleys, followed by nonconfined deposition on alluvial plains. Confinement of river channels within the valleys and deposition under relatively low rates of base-level rise typically preserve amalgamated fluvial channel facies within the valleys (Fig. 39) (Shanley and McCabe, 1991). These sandstone-rich fluvial deposits commonly are the best reservoir units within fluvial formations. Nonconfined deposition on alluvial plains usually occurs during periods of relatively high rates of base-level rise, producing isolated channel-belt sandstones encased in overbank mudstones.

Sequence stratigraphic methods to accurately predict facies distributions is based on following specific steps:

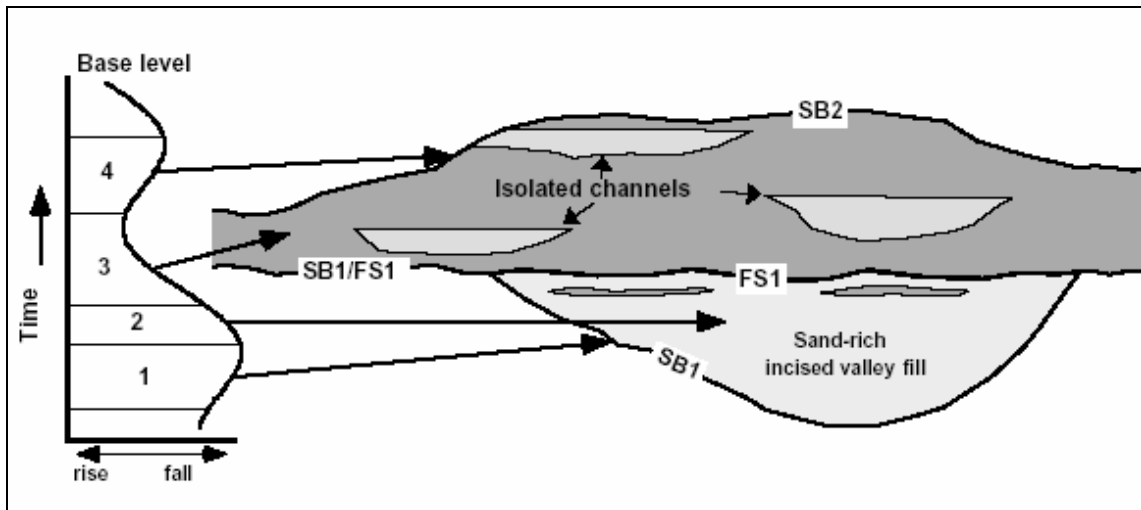


Figure 39. Conceptual framework for bounding surface development driven by cyclic base-level fluctuation. (1) Base-level fall leads to the development of a regional erosion surface with incised valleys, sequence boundary 1 (SB1). (2) Low rates of base-level rise/aggradation and confinement of rivers within the valley produce a sand-rich valley fill that can be capped by a significant base-level rise or flooding surface 1 (FS1). (3) Higher rates of base-level rise/aggradation and a wide, nonconfined alluvial plain leads to the preservation of isolated channels within mudstone-rich overbank deposits. (4) Renewed base-level fall causes the development of the next regional erosion surface (SB2), and so on (from MacDonald et al (1998) after Shanley and McCabe (1991)).

1. identify chronostratigraphic surfaces;
2. determine the correlatable thin shale units, and their relative stratigraphic positions; and
3. identify the bounding hiatal surfaces that separate genetic units.

The important challenge in this study is to identify and map (1) the base-level fall surfaces (sequence boundaries) and (2) the base-level rise surfaces (flooding surfaces).

My approach is to use well log correlations that show a relationship between base-level variations and channel amalgamation. In low-accommodation settings, style of depositional fill changes stratigraphically and spatially. Individual sequences can be differentiated by their texture and composition (different fill patterns). For the Cut Bank

field within the study interval (Cut Bank and Sunburst members), sedimentary environment variations are observed in most of the wells: vertical transitions from amalgamated channels to floodplain and to channel systems. I identified base-level fall and base-level rise based on following observations from well log cross sections:

Base-level fall (Fig. 40), corresponds to:

- periods of low facies preservation;
- many amalgamated facies characteristic of lag deposits; and
- erosion periods with no preservation of lag or paleosol.

Base-level rise (Fig. 40), corresponds to:

- high facies preservation;
- well-developed channel facies;
- channel-floodplain, ranging from 5 to 20 ft thick; and
- grain size become finer.

There is an upward decrease in channel amalgamation from the basal sandbody into the overlying mudstone-dominated deposits suggesting there is a progressive increase in accommodation during deposition of the successions. I interpret the succession as an unconformity-bounded sequence, in which the basal amalgamated sandbody is equivalent to the "lowstand" (low accommodation) systems tract of the fluvial sequence models of Shanley and McCabe (1991), while the upper mudstone-dominated deposits represent the "highstand" (high accommodation) systems tract (Fig. 41).

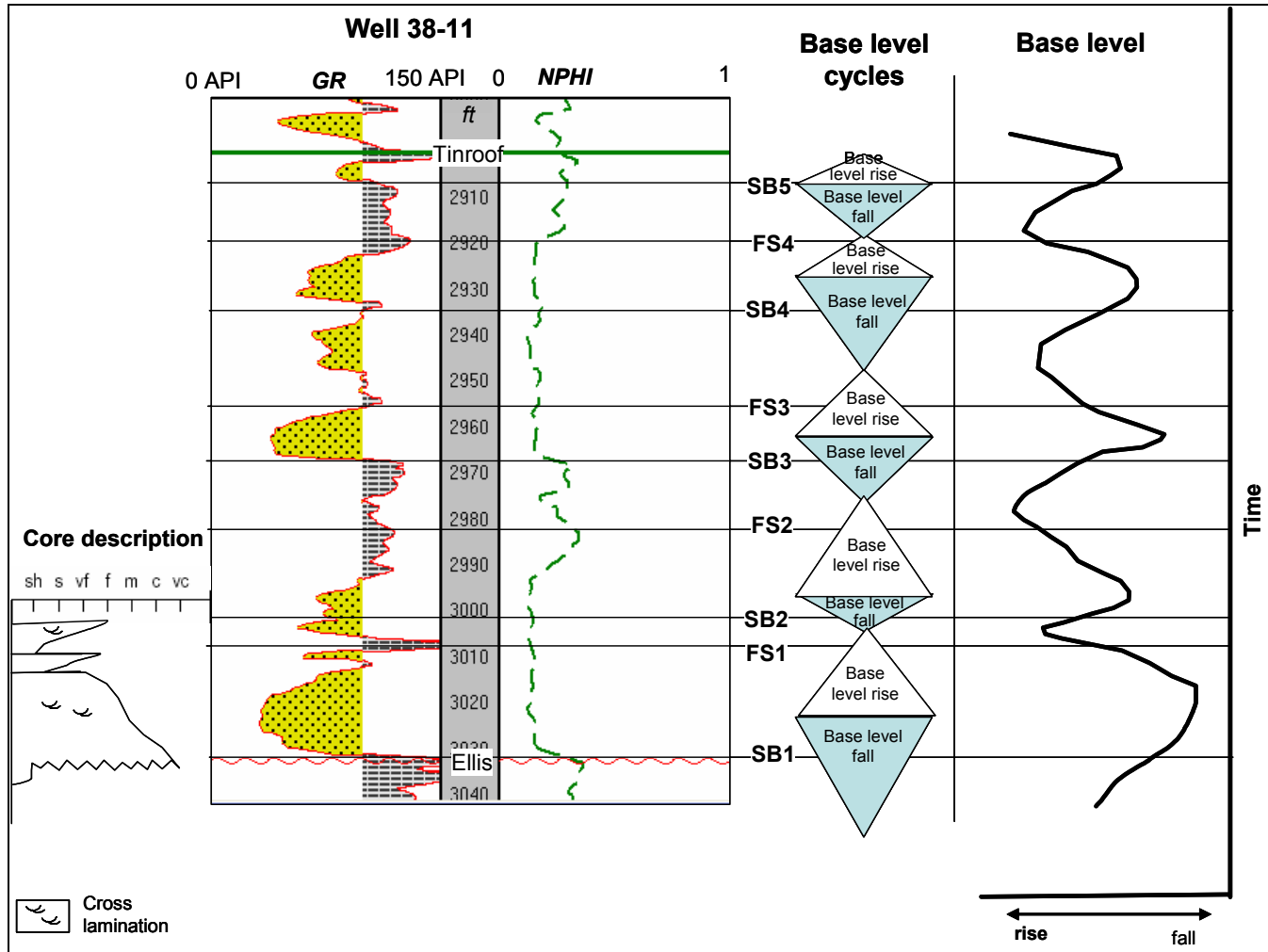


Figure 40. Core description, well log profile and sequence interpretation of Well 38-11.

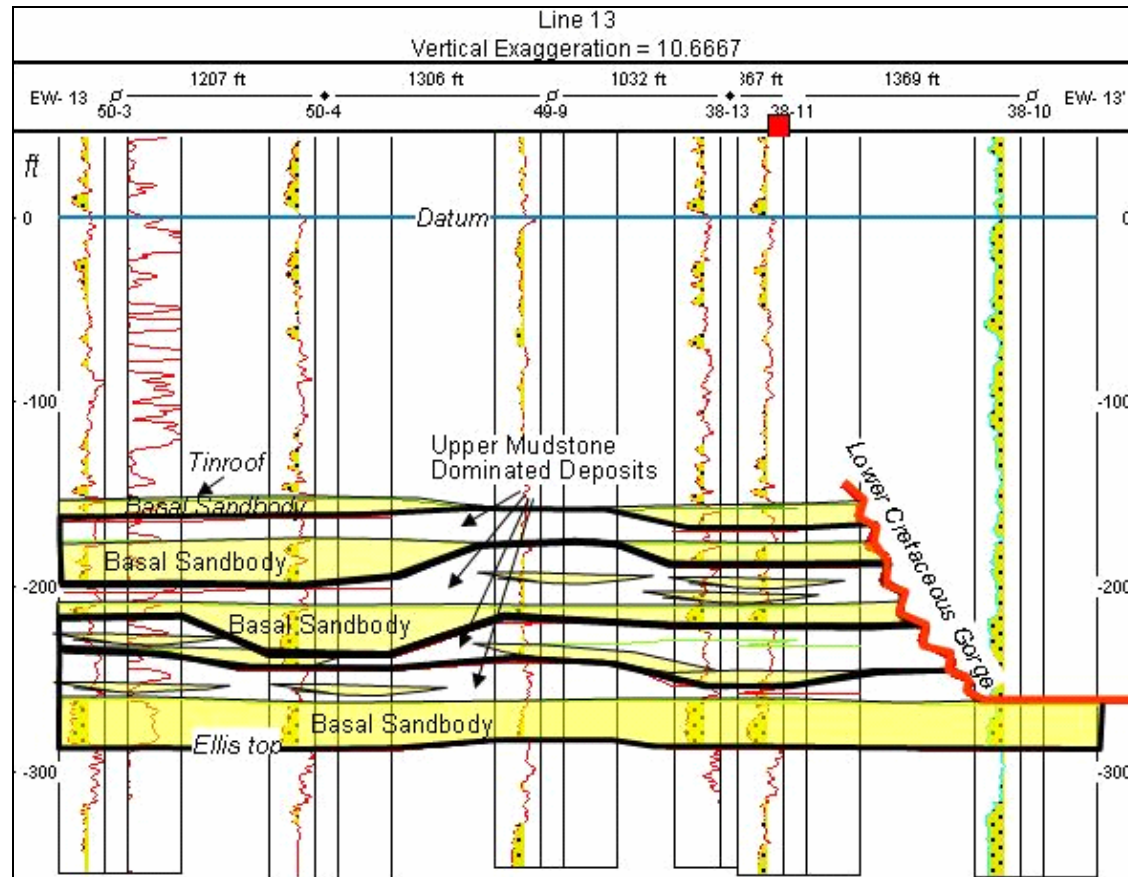


Figure 41. Stratigraphic cross section along line 13 (location on Fig. 42) showing the two-part subdivision of sequences. A sheet-like sandbody comprises the base of the succession, whereas the upper part consists of overbank mud.

Bases of most channel sandstones are assumed to reflect base-level fall and incision events. The erosion surface, “sequence boundary”, generated by base-level fall within fluvial formations typically is composed of two types of geomorphological elements: incised areas formed by downcutting rivers and streams; and relatively flat areas where stream downcutting is insignificant. The incised areas are the valley systems, and relatively flat areas are interfluves. Sequence boundaries are immediately overlain by laterally amalgamated fluvial sheets and deposits that have high percentages of interconnected, coarser-grained, channel-fill sandstone. The sandstone-rich valley fill deposits of “lowstand” systems tract are bounded by a sequence boundary at the base and a flooding surface at the top, and are termed “valley fills” (VF). Numerous erosion surfaces are present in this sandbody, separating truncated and amalgamated, fining-upward channel deposits. The sediments fine upward overall through the composite sandbody, from coarse and medium sandstone in lower channels, to fine sandstone in higher ones. The sediments within each channel deposit also fine upward. These sandstone-rich valley fill deposits are gradationally overlain by a mudstone-dominated deposits of “highstand” systems tract. However, channel-fill sandstones and crevasse splays are also present, but typically constitute less than 50% of the interval. The channel-fill sandstones average approximately 10 ft; amalgamation is rare. These shale-rich inter-reservoir barriers are bounded by a flooding surface at the base and a sequence boundary at the top, and are termed “highstands” (HS).

“Flooding surface” denotes any significant time-related surface developed in response to rising base-level, irrespective of whether the base-level rise has led to a genuine transgression. Flooding surfaces are relatively flat.

5.2 Sequence Stratigraphic Surfaces

I interpreted five sequence boundaries and four flooding surfaces within the 120-ft thick interval from Tinroof shale to Ellis top. Correlations were made well-by-well along 18 west-to-east correlation lines that cover all the wells with log data (Fig. 42). Depending on their geographic location relative to Lower Cretaceous Gorge, the upper one, two, three or even four cycles may be missing. The results are summarized on a single cross section along east to west correlation line 13 (Fig. 43).

Sequence Boundaries. I infer sequence boundaries at the base of thick, correlatable channel sandstones interpreted as valley fills (surface SB1-SB5, Fig. 44). All valley fills are recognized in most of the wells. Identifying the exact location of the interfluvial parts of the sequence boundaries is more difficult. In presence of core, the interfluvial parts could be identified at mature paleosol horizons. However, no paleosol were identified in any of the available cores. Therefore, because of the scarcity of core, the interfluvial parts generally were picked at a stratigraphic level approximately equivalent to the top of the valley fill in adjacent wells. At this point, it is worth mentioning that core data are available mostly from valley fill of Sequence 1, except well 33-5 (Fig. 45).

Flooding Surfaces. Identifying significant base-level rise surfaces in the study interval is difficult; for practical purposes the surfaces were picked at stratigraphic levels

equivalent to the top of the confined valley fill (surface FS1-FS4, Fig. 43). This surface is important, because it separates the mudstone-rich facies from the sandstone-rich facies (Fig. 44). Correlation of the top of the valley fill is very important for the reservoir subdivision, and in contrast to the sequence boundaries that can have very complex geometries, flooding surfaces were assumed to be relatively flat and should be present in adjacent wells at equivalent stratigraphic levels, except where removed by subsequent erosion.

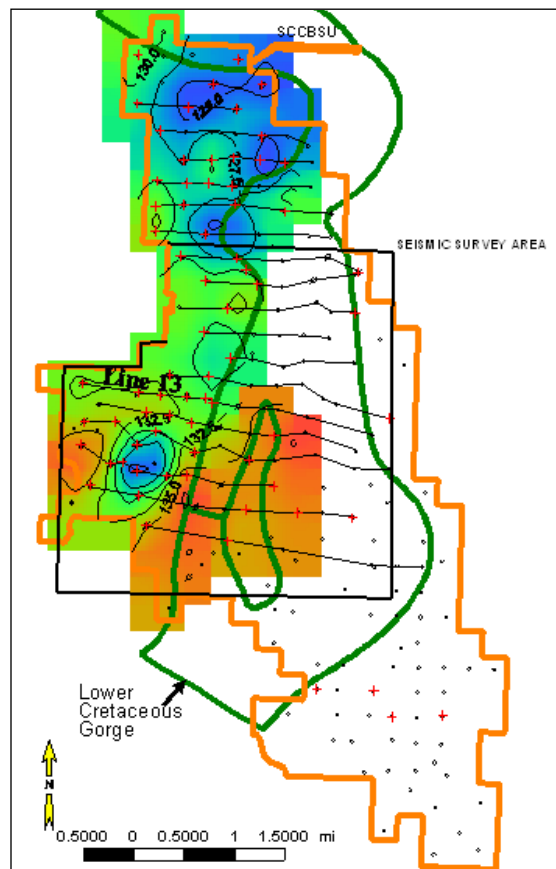


Figure 42. Locations of the cross sections lines (there are 18 lines, line numbers increase from north to south) overlain on thickness map from Tinroof to Ellis.

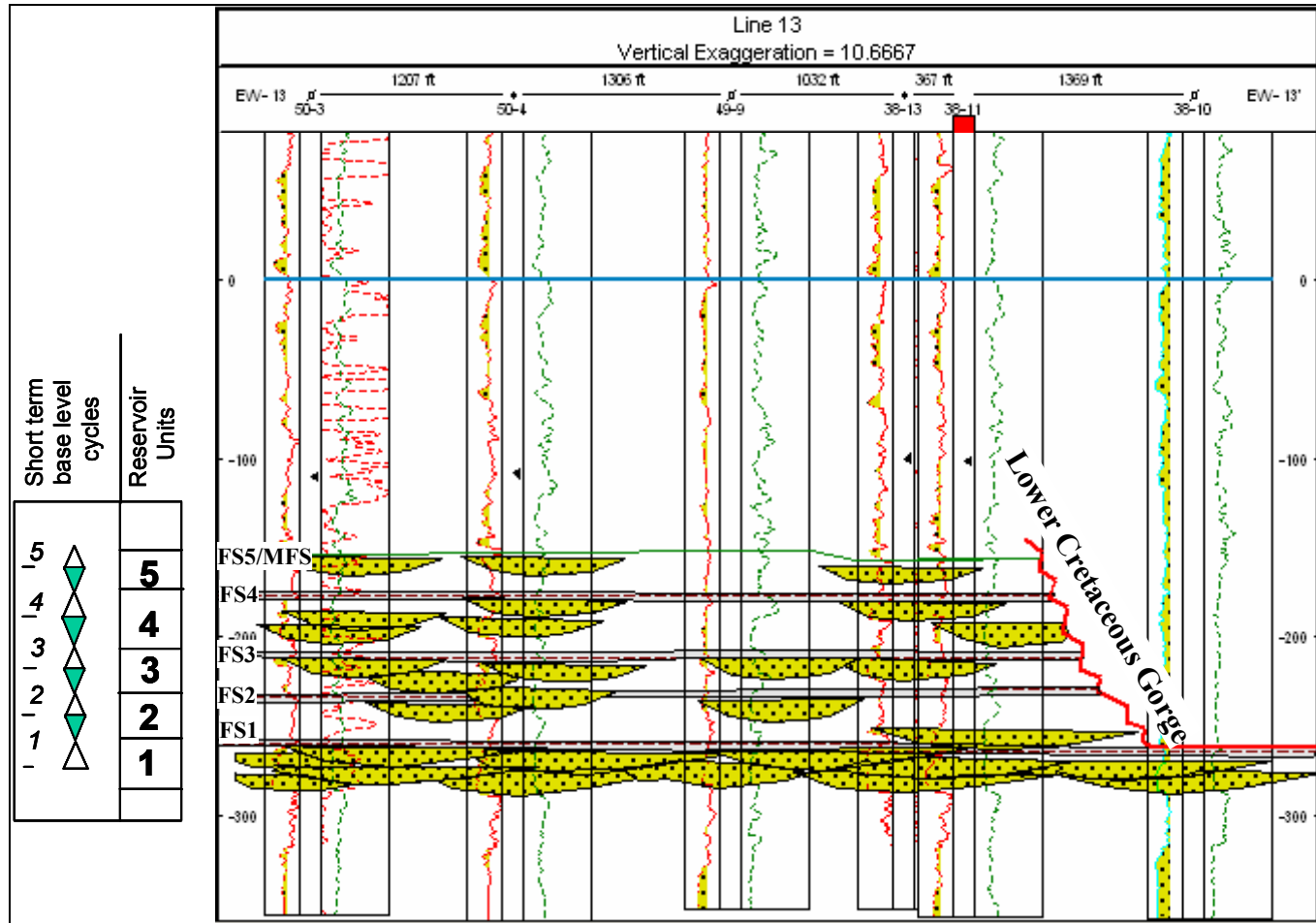


Figure 43. Synthetic reconstruction of the reservoir geometry in SCCBSU with short term base-level cycle interpretation. FS1-FS5 are flooding surfaces. Red square at the top of the well shows there are core data for that well. Green correlation line is Tinroof shale that correspond to FS5 or maximum flooding surface (MFS). Correlation is illustrated by GR (on the left) and porosity logs (on the right red density porosity, green neutron porosity).

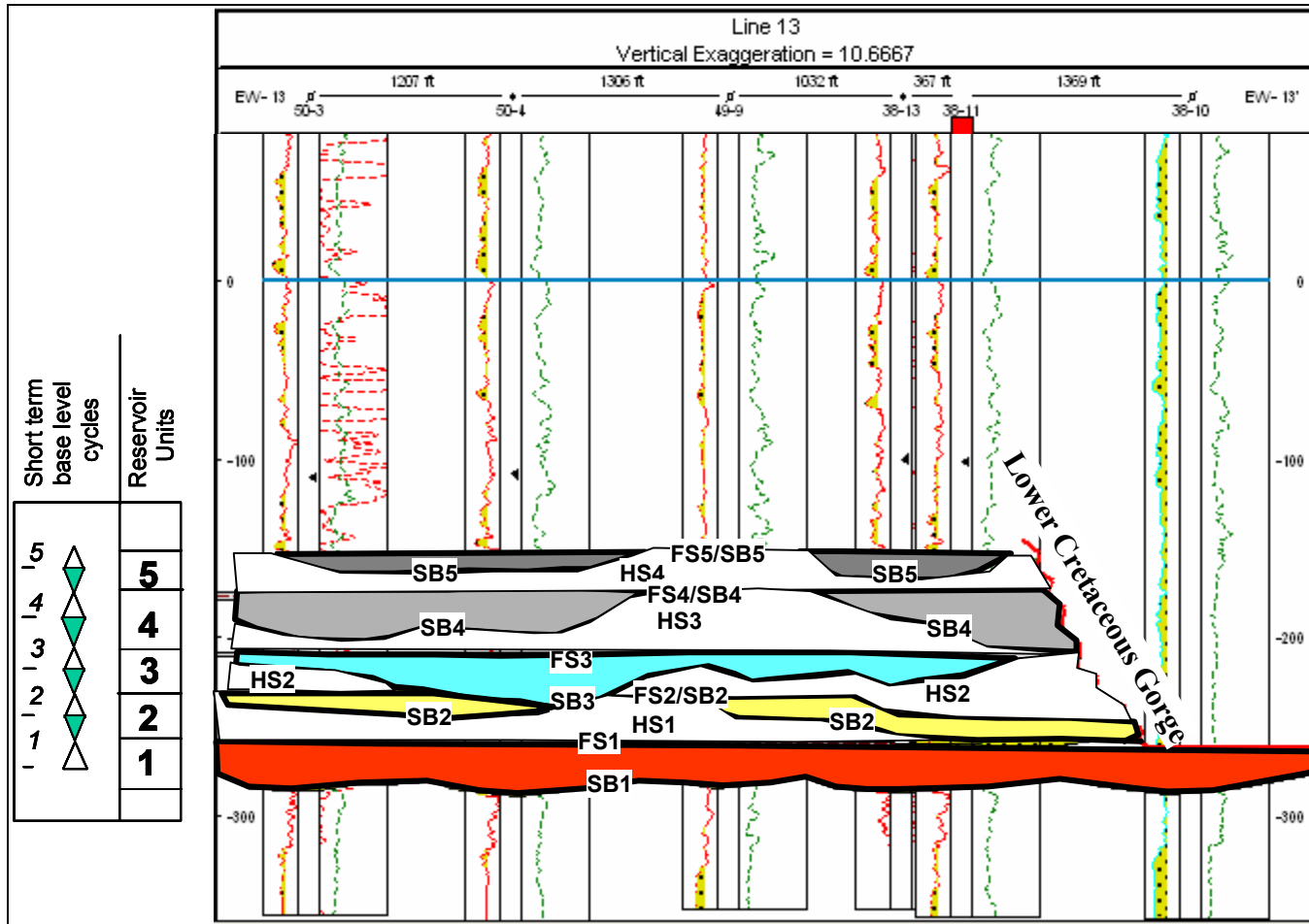


Figure 44. Sequence stratigraphic correlation/interpretation along Line 13. Five sequence boundaries and four flooding surfaces were identified between Tinroof and Ellis Group. Color filled part of each sequence corresponds to “VF” (valley fill), and white is “HS” (highstand). Valley fills are amalgamated, continuous channel fills, therefore have best reservoir quality and connectivity. Highstands consist of channel fills isolated within flood plain shales.

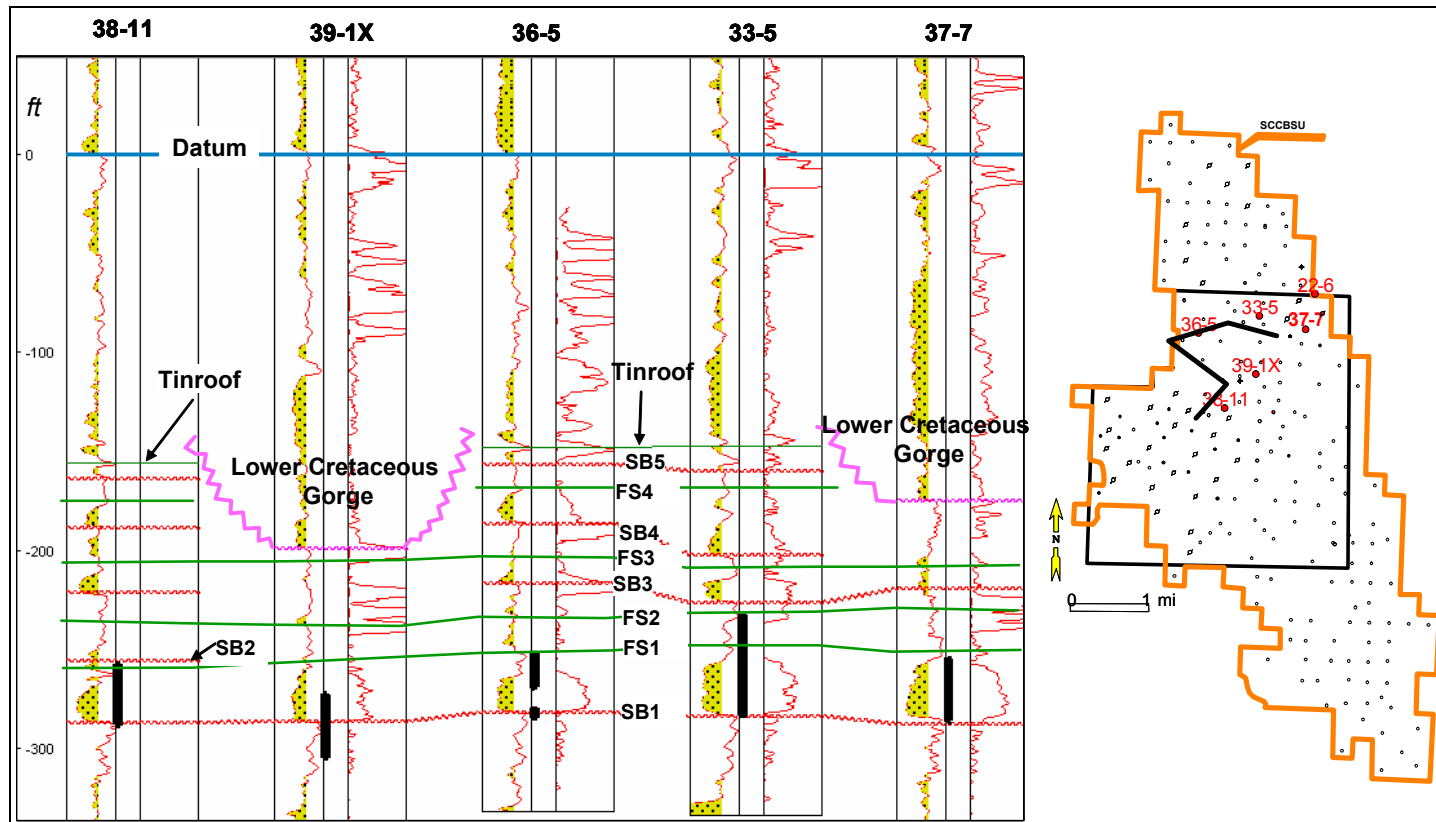


Figure 45. Cross section showing interpretation of sequence stratigraphic surfaces and cored interval (thick black vertical lines). There is no horizontal scale because the section was constructed using equal distance between wells, just to show all cored wells on the same cross section. Map on the right shows the location of cross section. Available core data is mostly from valley fill of Sequence 1 (VF1), except well 33-5.

5.3 Sequence Stratigraphic Interpretation

Sequence 1: Lower Cut Bank

SB1, which corresponds to the Ellis top, is present in most of the SCCBSU wells, and it is directly overlain by amalgamated channel sandstones of lower Cut Bank (Figs. 43 and 44). This amalgamated belt of braided stream channels forms a heterogeneous but laterally continuous sand sheet that formed when a low accommodation favored channel stacking. The coarse sediment of the laterally continuous basal sand sheet are the most proximal deposits of the alluvial fan system. This belt of stacked channels is relatively thick (35 ft) in the south part of SCCBSU and is thinner (20 ft) with less channel amalgamation at the north (Fig. 46).

Flooding surface FS1 was present in most of the SCCBSU wells and directly overlies the amalgamated channels. In some wells it was eroded by the overlying SB2. FS1 is overlain by the shale-rich inter-reservoir barriers of HS1 (highstand). As stated above, highstands are bounded by a flooding surface at the base and a sequence boundary at the top. Within the highstand, channels are isolated in floodplain shaly sediments. Overbank deposits, such as crevasse splays or sheet flood sands, were preserved in the floodplain. Channels in the highstand sequence record the flood-plain aggradation and a lack of stacking of the channels as accommodation increased.

The isopach distribution of the lowstand or valley fill of each sequence is assumed to approximate the geometry of the valley floor. The valley fill of Sequence 1 is relatively uniform in thickness at south (Fig.46; average 32 ft), largely because of the absence of significant large-scale relief on the valley floor.

However, when examined in more detail, there are a number of abrupt changes in the nature of the valley at the central and north part of SCCBSU. Accompanying these changes, the average, total thickness of valley fill tends to be less in central (27 ft) and north part (25 ft) than to the south and the thinnest basal sandstone (20 ft) occurs in northern end of SCCBSU.

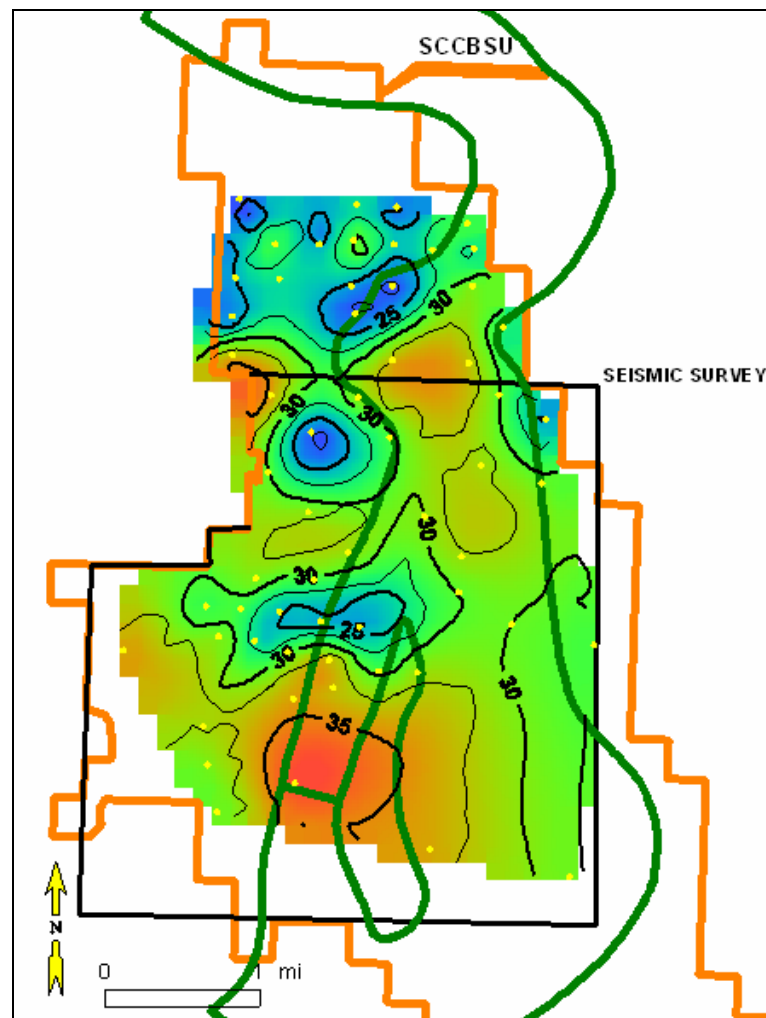


Figure 46. Isopach map of valley fill of Sequence 1 (VF1, gross thickness from FS1 to SB1). Points indicate location of wells used to draw the map. Contour interval is 2.5 ft.

Net-to-gross ratio distribution of valley fill of Sequence 1 reflects the northeast trending channel directions (Fig. 47). Average is about 0.6, and higher values occur in the central part of SCCBSU due to vertical stacking of several channel-fill sands. As stated in the previous chapter, in north part stacking is not as common, and because of the fining upward nature of channel sands, the net-to-gross ratio is lower.

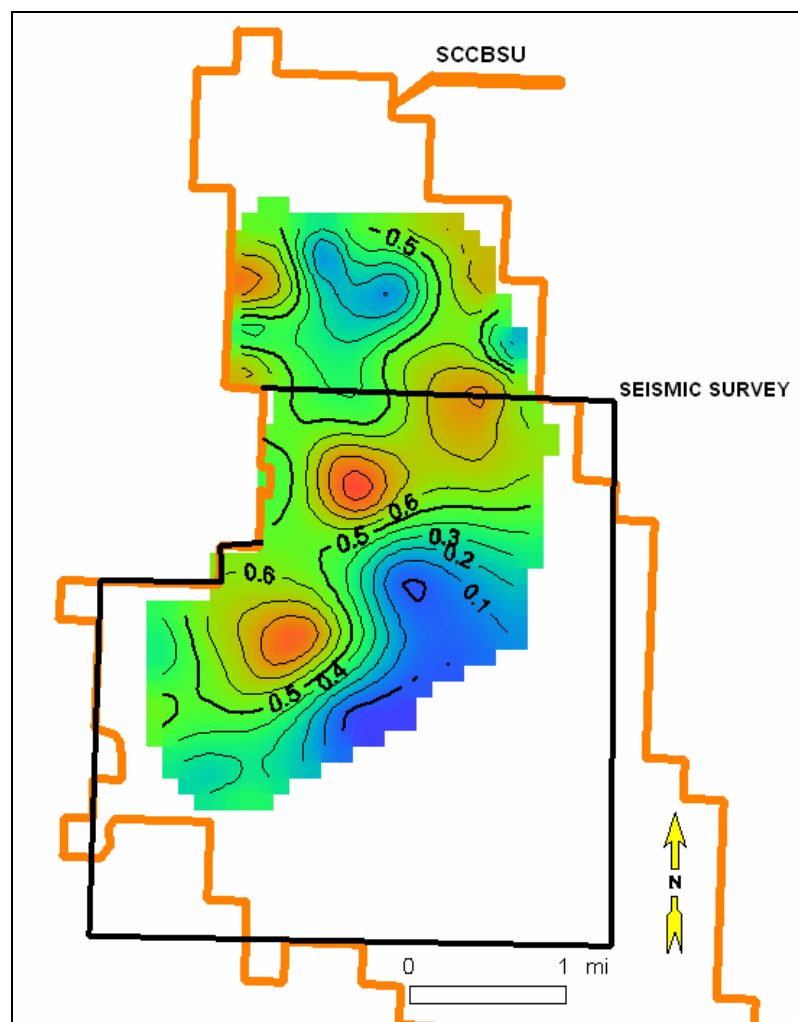


Figure 47. Net-to-gross ratio map of the valley fill of Sequence 1 (FV1, gross thickness from FS1 to SB1) (lower Cut Bank). Contour interval is 0.1.

Sequence 2: Upper Cut Bank

SB2 corresponds to base of upper Cut Bank sand and is overlain by channel sandstones with less amalgamation in comparison to channels of Sequence 1, owing to greater accommodation. These channels, with mostly upward fining log pattern, have a meandering geometry and correspond to a more distal alluvial depositional setting. In places, SB2 is incised into the channels of Sequence 1, favoring a vertical connection between the reservoirs sands of the 2 sequences.

Flooding surface FS2 occurs in most of the SCCBSU wells and overlies the channel-fill sandstones. It was eroded and removed by overlying SB3 in many wells. It is overlain by the shale-rich HS2.

Average thickness of the valley fill of Sequence 2 is 15 ft (Fig.48). At some of the southern wells it is cut by Lower Cretaceous Gorge. Therefore, in gorge area general northeast channel trend is not observed.

Net-to-gross ratio distribution of valley fill of Sequence 2 also reflects the northeast trending channel directions (Fig. 49). The high net-to-gross ratio values are in north part of the SCCBSU and it is almost zero toward the south, proving the statement from previous studies that upper Cut Bank produces only in north part of SCCBSU.

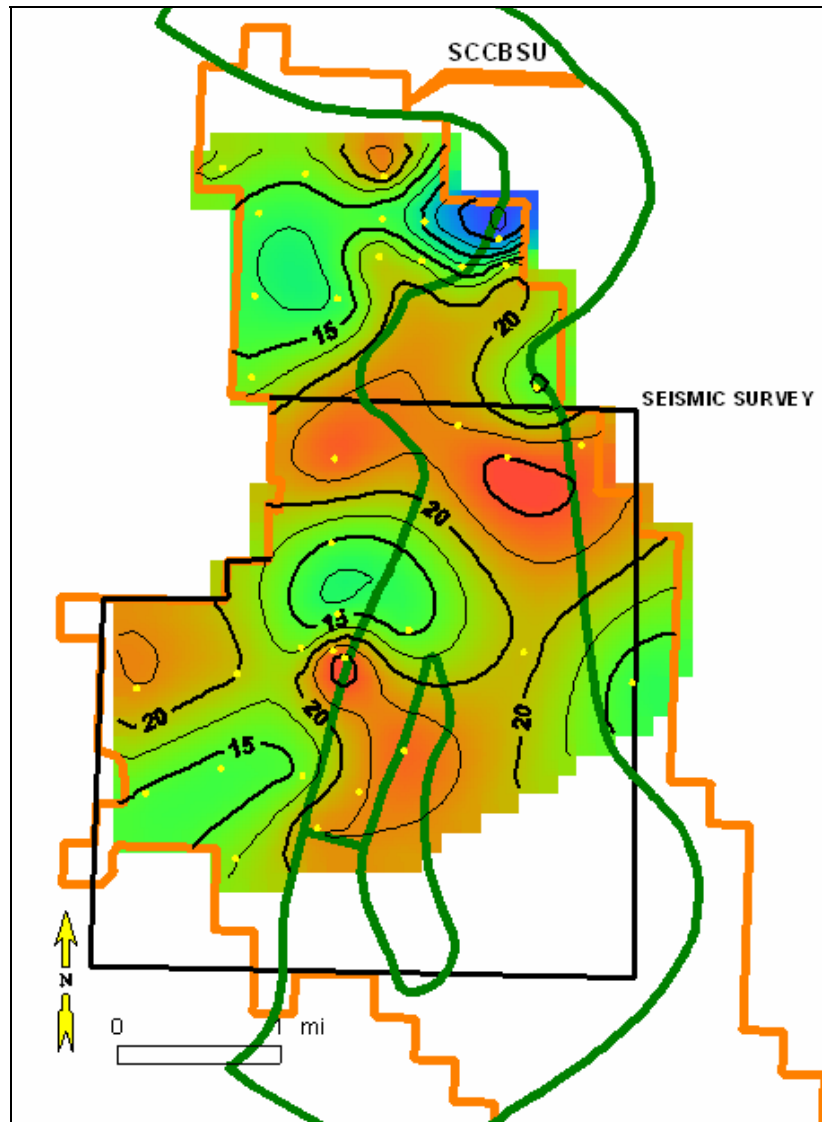


Figure 48. Isopach map of valley fill of Sequence 2 (VF2, gross thickness from FS2 to SB2). Points indicate location of wells used to draw the map. Contour interval is 2.5 ft.

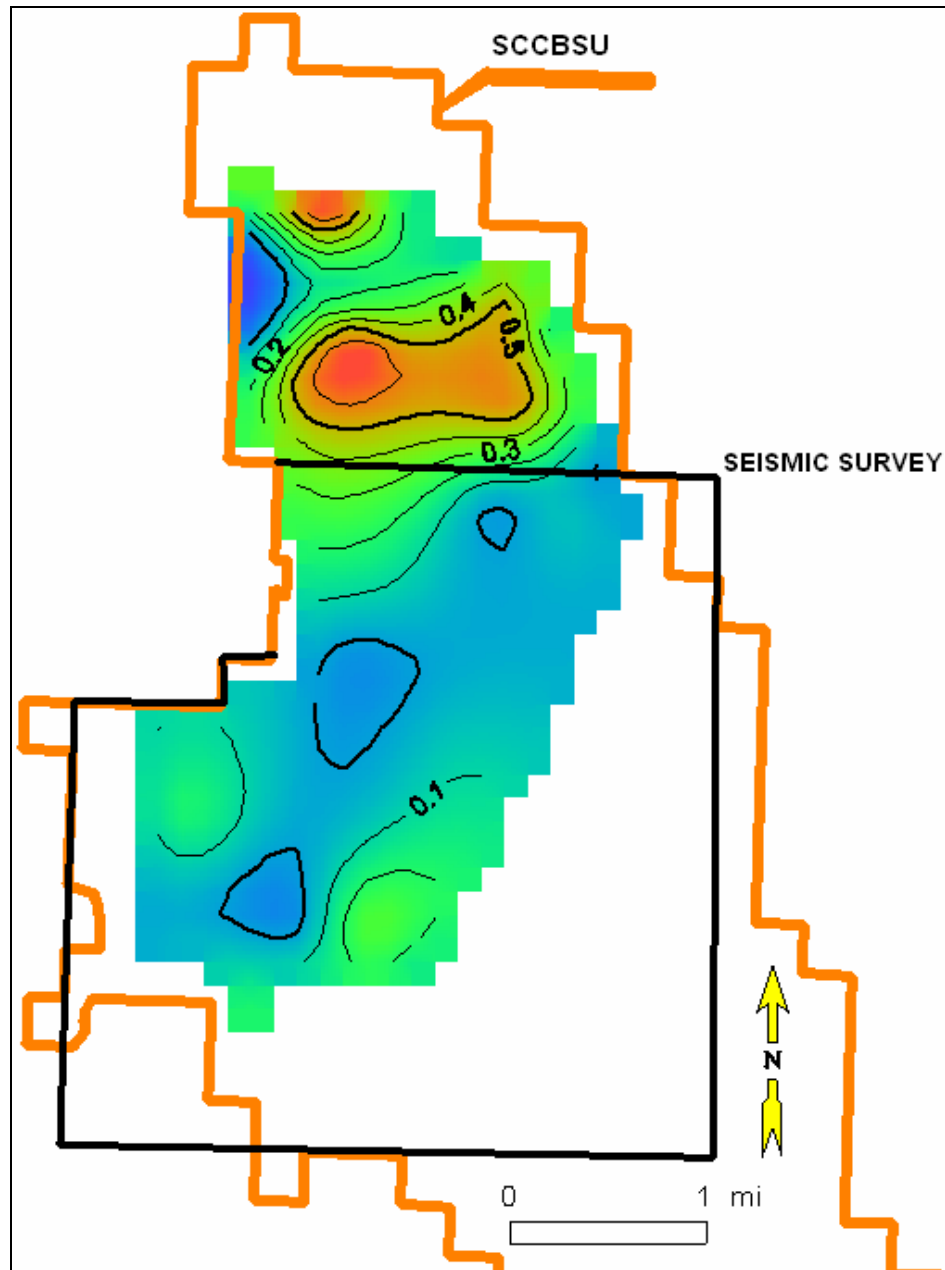


Figure 49. Net-to-gross ratio map of valley fill of Sequence 2 (VF2, gross thickness from FS2 to SB2) (upper Cut Bank). Contour interval is 0.1.

Sequence 3: Sunburst 1

SB3 corresponds to base of Sunburst 1 sands and is overlain by amalgamated channel-fill sandstones. Compared to underlying Sequence 2 sands, more amalgamation is present in Sequence 3, showing lower accommodation; however, amalgamation is not as pronounced as in Sequence 1. Sequence 3 channels are meander deposits and this sequence corresponds to a more distal alluvial depositional setting than does Sequence 1. At places, SB3 incises into the channels of Sequence 2, favoring vertical connection between the reservoirs sands of Sequences 2 and 3, and in some wells even Sequence 1.

Flooding surface FS3 is present above Sequence 3 in most of the SCCBSU wells. It is overlain by the shale rich HS3 and has been eroded by overlying SB4 in a few wells.

Average thickness of the valley fill of Sequence 3 is about 18 ft (Fig. 50). It is cut by Lower Cretaceous Gorge in central and north central part of the SCCBSU. There are some abrupt changes in thickness.

Net-to-gross thickness ratio distribution of valley fill of Sequence 3 averages about 0.3 (Fig. 51). This lower value is because of the fining upward nature of the channel sands, and because the amalgamation or vertical stacking is not as high compared to Sequence 1. However, compared to Sequence 2 it has higher average net-to-gross ratio values.

Sequence 4: Sunburst 2

SB4 corresponds to base of Sunburst 2 sands and is overlain by less amalgamation of channel sandstones than is present in Sequence 3, showing higher accommodation.

These channels have more of meandering nature and correspond to more distal alluvial fan depositional setting. SB4 incise into the channels of Sequence 3 in a few wells.

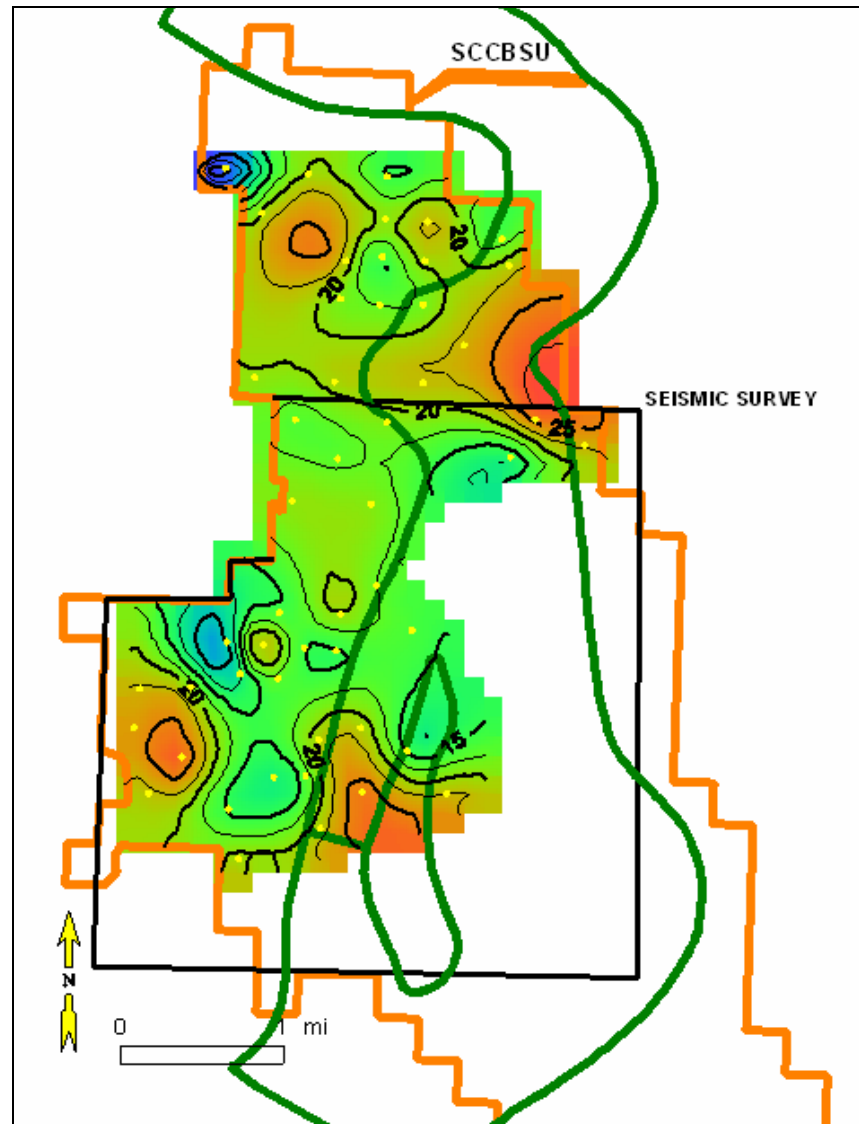


Figure 50. Isopach map of valley fill of Sequence 3 (VF3, gross thickness from FS3 to SB3). Points indicate location of wells used to draw the map. Contour interval is 2.5 ft.

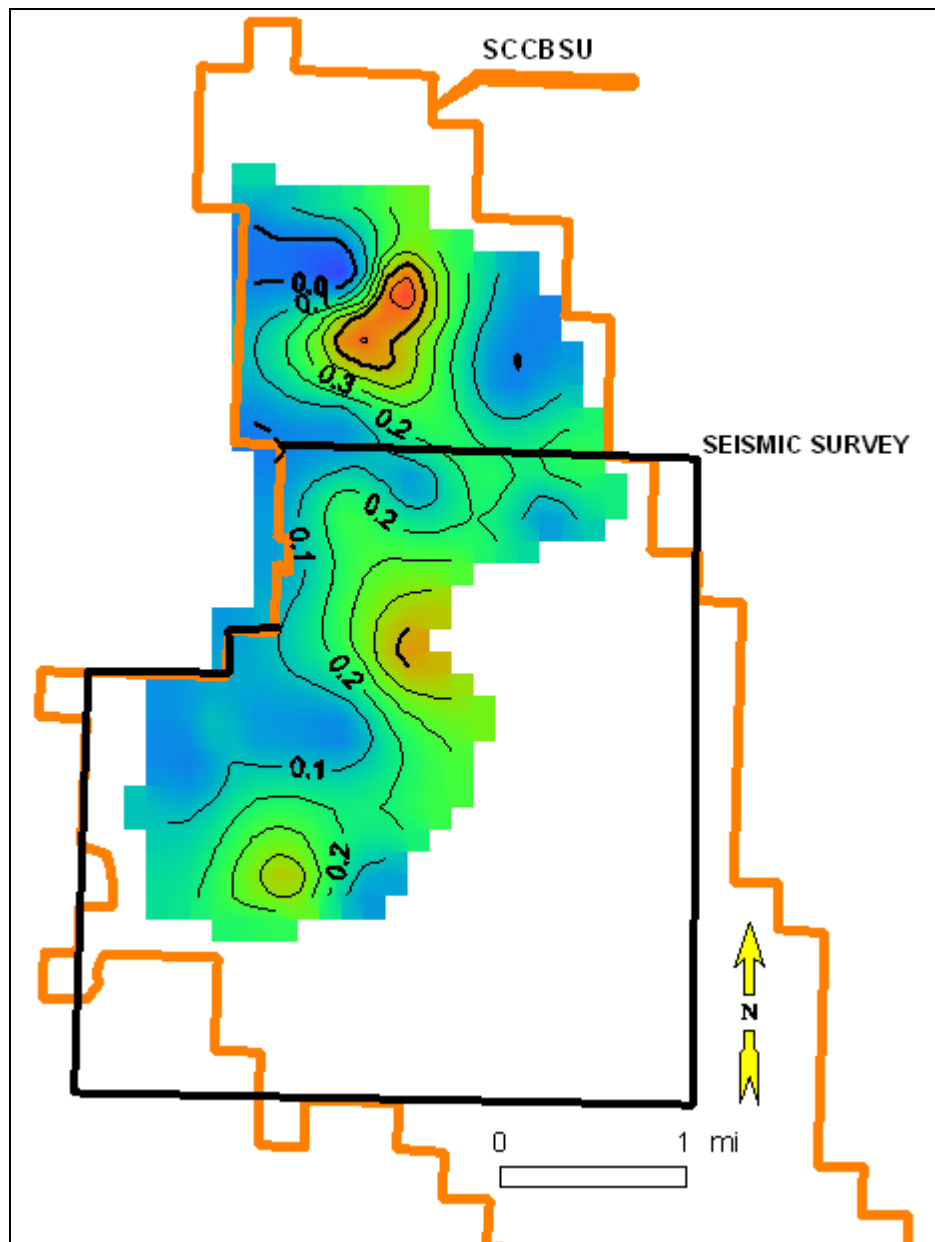


Figure 51. Net-to-gross ratio map of valley fill of Sequence 3 (VF3, gross thickness from FS3 to SB3) (Sunburst 1). Contour interval is 0.1.

Flooding surface FS4 is present in most of the SCCBSU wells and overlies the Sequence 4 channels. This flooding surface is overlain by the shale-rich HS4.

Average thickness of the valley fill of Sequence 4 is 18 ft (Fig. 52). It is absent in Lower Cretaceous Gorge area. There are some abrupt changes in thickness.

Average net-to-gross ratio value of Sequence 4 is very low, about 0.15. This indicates that Sunburst 2 sands have lower reservoir quality compared to Sunburst 1 sands.

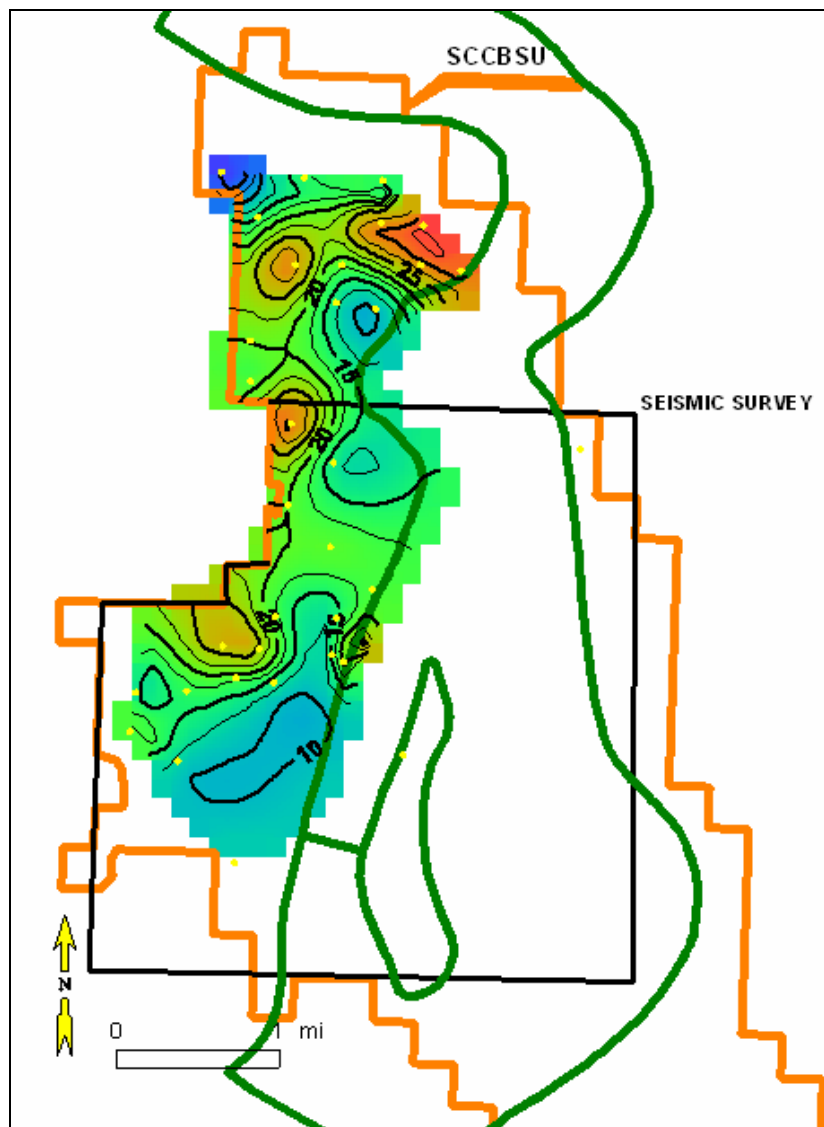


Figure 52. Isopach map of valley fill of Sequence 4 (VF4, gross thickness from FS4 to SB4). Yellow dots indicate location of wells used to draw the map. Contour interval is 2.5 ft.

Sequence 5: Sunburst 3

SB5 corresponds to base of Sunburst 3 sands and is overlain by isolated channel sandstones. Sunburst 3 sands usually are upward fining with thickness less than 7 ft and have more of meandering nature and correspond to more distal part of alluvial depositional setting.

Sands of the Sequence 5 are overlain by the Tinroof shale, which corresponds to a maximum flooding surface.

The valley fill of Sequence 5 is average 10 ft in thickness. (Fig. 53). It is absent in Lower Cretaceous Gorge area.

Average net-to-gross value in Sequence 5 is nearly 0, indicating very low reservoir quality of the Sunburst 3 interval. Thus, from 3 Sunburst sand intervals the lowest (Sunburst 1) sand has the highest reservoir quality.

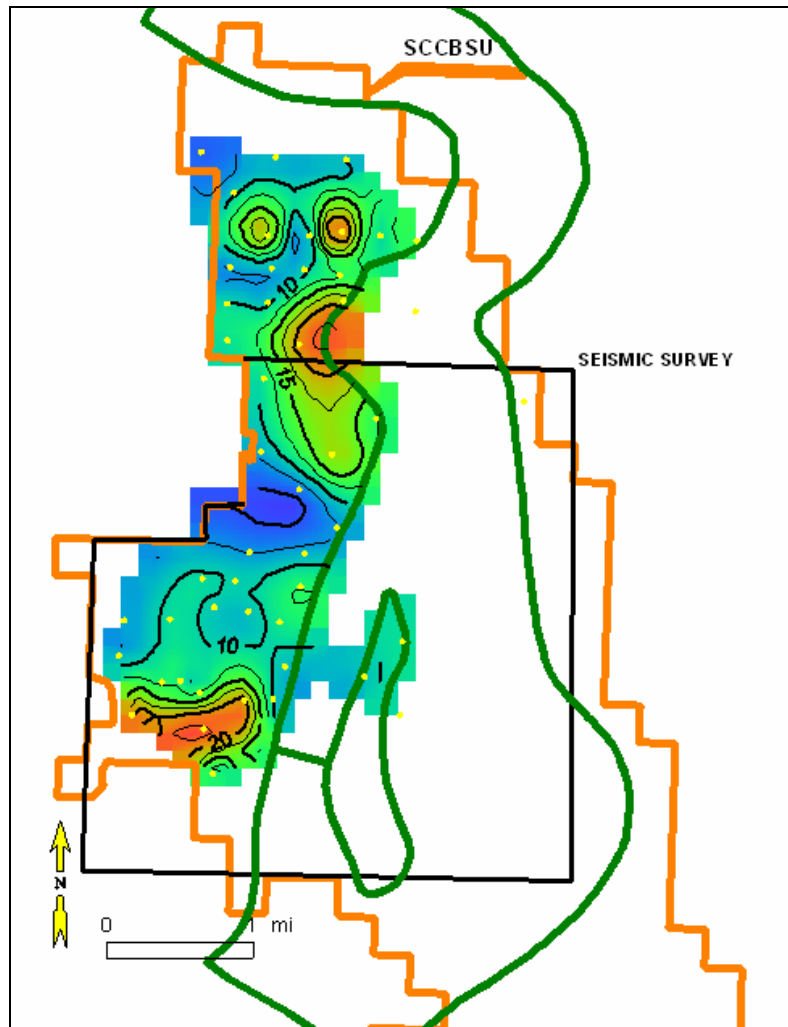


Figure 53. Isopach map of valley fill of Sequence 5 (VF5, gross thickness from Tinroof to SB5). Points indicate location of wells used to draw the map. Contour interval is 2.5 ft.

5.4 Stacking Pattern

Base-level variations of alluvial systems strongly influence the facies distribution and the channel geometry. Base-level variations are dependent on the accommodation/sediment supply ratio. This ratio controls the space available for the sediment in the alluvial plain, and therefore, it influences the channel types, their

stacking, and their amalgamation patterns (Posamentier et al., 1988; Van Wagoner et al., 1988, 1990; Shanley and McCabe, 1991). At Cut Bank field, between the Tinroof and top of the Ellis Group, five genetic sequences induced by base-level variations were identified. Each sequence is approximately 20 ft thick and can be correlated across the field (Figs. 43 and 44). A typical sequence, deposited during a complete base-level cycle, from base to top includes the following components.

- An amalgamated channel belt favored by minimum accommodation and forming a very heterogeneous but laterally continuous sand sheet. No evidence of deep incision is recorded at the base of the cycle. Reservoirs are laterally extensive vertically and laterally amalgamated channel-fill sand deposits with a complex internal architecture.
- Above the amalgamated channel-fill sand deposits, channel-fill sands isolated in floodplain shaly sediments record floodplain aggradation and less stacking of the channels as accommodation increased. Channel avulsion was more common, and overbank deposits, such as sheet floods or crevasse splay deposits, were preserved in the floodplain. Reservoirs have poor vertical and lateral interconnections.

Of particular interest is the expression of the different cycles in a vertical profile to interpret the long-term evolution of the base-level variations (Figs. 43 and 44). The basal contact of the Cut Bank member (Sequence 1) clearly records an important base-level drop within the basin, with sediment bypass and a sudden increase of the sediment supply. The coarse sediments of the laterally continuous basal sand sheet form the most

proximal deposits of an alluvial fan system. A longterm base-level rise then occurred, emphasizing the transgressive character of the subsequent 4 cycles. Their relative thicknesses and extent are very comparable. Channel-fill sands are also fine-grained and mineralogically mature. This evolution indicates an overall increase of the accommodation space.

Tinroof shale records a maximum flooding above the Cut Bank and Sunburst sandstones.

5.5 Description of the Conceptual Low Accommodation Alluvial System Sequence Stratigraphic Model

Assessment of Cut Bank field showed that it is possible to identify systems tracts in low-accommodation alluvial systems on the basis of sequential position, facies associations and systematic changes in architectural style and sediment body geometries. Multiple cycles (sequences) may be found over a short vertical range of stratigraphy, separated by unconformities (sequence boundaries). Average sequence thickness in Shanley and McCabe's (1991) non-marine conceptual sequence stratigraphic model is no less than 100 m (300 ft). I extended this concept to much lower alluvial accommodation setting where average sequence thickness is no more than 40 ft (Fig. 54).

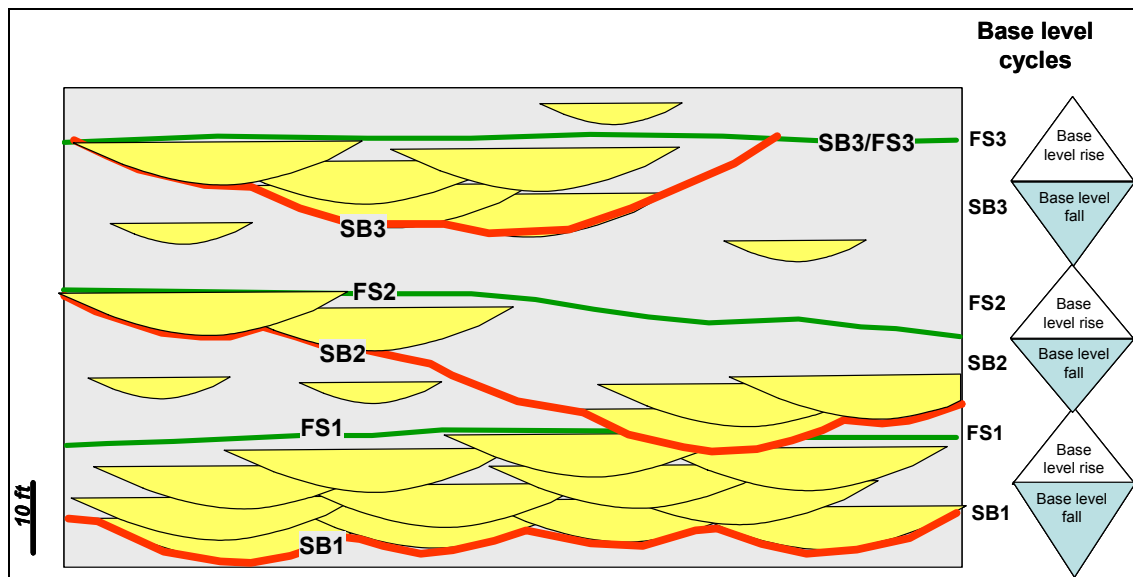


Figure 54. Stratigraphy developed in low accommodation alluvial setting. Deposits of lowstand or valley fill are dominated by both vertically and laterally amalgamated units. Base-level fall leads to closely spaced unconformities which corresponds to base of these amalgamated units, sequence boundaries (SB1, SB2, SB3). Low rates of base-level rise produce a sand-rich valley fill that is capped by a significant base-level rise or flooding surface 1 (FS1). Higher rates of base-level rise leads to the preservation of isolated channels within mudstone-rich overbank deposits. Renewed base-level fall causes the development of the next erosion surface (SB2, SB3), and so on.

Base-level fall (decreasing accommodation to sediment supply ratios) promotes the preservation of lowstand systems tract deposits, as these are preferentially deposited in stratigraphically low positions such as the base of incised valleys. Low A/S results in the erosive migrating base of channel systems returning close to their earlier stratigraphic level, producing a succession that contains numerous erosion surfaces and preferential preservation of the lowermost part of fluvial successions as amalgamated channel deposits. Channel lags and cross-bedded basal channel fills are the dominant form of sediment preserved. The geometry of the preserved sediments is that of a fluvial sheet sand.

Base-level rise (increasing accommodation to sediment supply ratios) results in a greater vertical distance between successive lateral migration paths of channel bases. This in turn allows for the greater preservation of higher stratigraphic elements in the fluvial system such as channel fills and in particular, levee and floodplain deposits. Within the highstand sequence set, amalgamation is at a minimum and channel-fill deposits tend to stack discretely with the maximum amount of fine-grained sediments between them. Increasing preservation of intervening floodplain facies make the channel-fill sand bodies less interconnected and more ribbon-like in geometry.

Highstand systems tracts were more exposed and subject to removal by subsequent cycles of erosion. Incision associated with sequence boundaries commonly removed part of “highstand” and sometimes even “lowstand” of the underlying sequences.

5.6 Reservoir Geometry and Compartmentalization

High-resolution stratigraphic correlation permits accurate representation of reservoir compartmentalization in a spatial and temporal framework. In alluvial systems the boundaries of the main reservoir layers coincide with stratigraphic boundaries of genetic sequences. Channel-fill sandstones, and in some cases crevasse complexes, are the reservoir units; overbank and floodplain mudstones are seals and fluidflow barriers. The size and geometry of reservoirs are mainly defined by the degree of amalgamation and connectivity of fluvial channel sandstones.

Channel-fill sandstones in Cut Bank field range transitionally from amalgamated, multilateral, multi-storied, areally continuous sheet sandstones to isolated sandstone bodies embedded in floodplain mudstones (Fig. 43). Transitional changes in channelbelt sandstone morphology, geometry, facies components and successions, and diversity of facies tracts are stratigraphically sensitive, and these are related to changes in the accommodation to sediment supply ratio (A/S) conditions through time.

Channel sandstones deposited in low A/S conditions are amalgamated and areally continuous. The finer sand and muddy sediments composing the upper parts of channel bars and most floodplain sediment are not preserved. The resulting reservoir sandstone is homogeneous, porosity is good and reduced clay content enhances permeability. Higher A/S conditions result in a lower degree of amalgamation and increased preservation of floodplain sediment. Channel sandstones tend to be single storied, isolated bodies embedded in flood plain deposits. The geomorphic elements composing the individual channels are more fully preserved and more mud is preserved. Porosity and permeability profiles decrease strongly upward in individual sand bodies. Where several channel sandstones are interconnected, major changes in rock properties and internal permeability barriers may exist between channel sandstone elements. The increased proportion of fine sand and mud reduces permeability and connectivity.

Thus, stacking-pattern analysis provided clues for correlation of the main reservoir units and of the main vertical permeability barriers across the field. The resolution of the correlation, however, is insufficient to ensure the correlation of individual channels, or to quantitatively estimate the distribution of the heterogeneity

within the sand sheets. To address the issues of reservoir connectivity, I built a geological model populated with reservoir parameters and used geostatistical studies to provide equiprobable representations of the geological heterogeneity of the main reservoir units.

CHAPTER VI

GEOSTATISTICAL MODELING

6.1 Reservoir Geostatistical Model

The sequence stratigraphy provides a framework within which geostatistical modeling can aid in simulating the internal small-scale facies distributions, as well as the porosity distributions. Stratigraphically-based geostatistical simulation has several advantages over nonstratigraphic approaches. First, the sequence boundaries are marked by unconformities. Therefore, facies that exist on one side of the unconformity do not correlate with facies across the unconformity. Second, facies distributions can be predicted based on position within a sequence, thus allowing quantitative use of the sequence stratigraphic conceptual model.

Geostatistical techniques designed to provide missing data can be classified in two ways: by the allowable variation of the property at a given point; and by the way data are organized. There are two classes of property variation, continuous and discrete. Continuous models are suited to properties such as permeability, porosity, residual saturation and seismic velocity that can take any value. Discrete models are suited to geologic properties, like lithology, that can be represented by one of a few possibilities.

Data organization has developed along two paths, depending on how the models are built. One is grid based, in which all properties are represented as numbers in a grid, which is then used for fluid-flow simulation. The second is object based, in which reservoir features such as shales or sands are generated in space, and a grid is then superimposed on them.

In this study I decided on grid-based approach, considering the fact that meandering and braided rivers produce reservoir sand bodies of different dimensions and heterogeneity. In Cut Bank field, techniques for estimating the geometry of channels suffers from major drawbacks: (1) well spacing is greater than sand body dimensions; (2) empirical equations relating maximum channel depth and channel width have a lot of scatter; and (3) resolution of the seismic data is low relative to the thickness of the sandstone bodies.

Populating the geological model with reservoir parameters using geostatistics requires 2 main steps. First, stochastic simulation of lithotypes is computed from the well data. This provides a representation of the reservoir geology in a high-resolution grid; the consistency of the simulation can be directly estimated from a geological viewpoint. This step is crucial because it ensures a reasonable representation of the reservoir architecture and facies distribution. Second, the lithotype simulation is then transformed into a petrophysical grid by assigning a petrophysical distribution law to each of the simulated lithofacies. Landmark Geographix software was used to construct the 3D earth-model with dimensions of cells governed to adequately control the detail of the structural surfaces (x and y increments of 180 ft).

Earthdecision GOCAD software was used to construct the 3D cell model. The cell size was controlled by the desire to use a similar grid increment as the GeoGraphix grids but to still allow rapid visual movement of the model on the workstation. Dimensions of the model are presented in Table 3. The vertical thickness of the model

Table 3. Dimensions of the geostatistical GOCAD model.

Axis	Number Cells	Size
X	100	180 ft
Y	142	180 ft
Z	36	~ 3 ft
Total	582,200	~97,200 ft ²

was constrained by the top and base structure surfaces, which define the interval between combined Tinroof and Lower Cretaceous surface at the top and the Ellis Group at the bottom. A 9-layer model was generated, in which the layers from bottom to top were: VF1, HS1, VF2, HS2, VF3, HS3, VF4, HS4 and VF5 (Fig. 55) (VF-valley fill, HS-highstand; numbers correspond to sequence number; see previous chapter for explanation of these layers). The 3D cell model is referred to as a stratigraphic grid, (Sgrid), and is displayed in Figure 56.

Data requirements for the geostatistical population of the model were:

- neutron-density average porosity log (PHIA);
- computed lithofacies (sand: $GR < 60$ API, shaly sand: $60 < GR < 90$ and shale: $GR > 90$);
- variogram data for the reservoir parameters; and
- sequence stratigraphic surfaces (GeoGraphix grids).

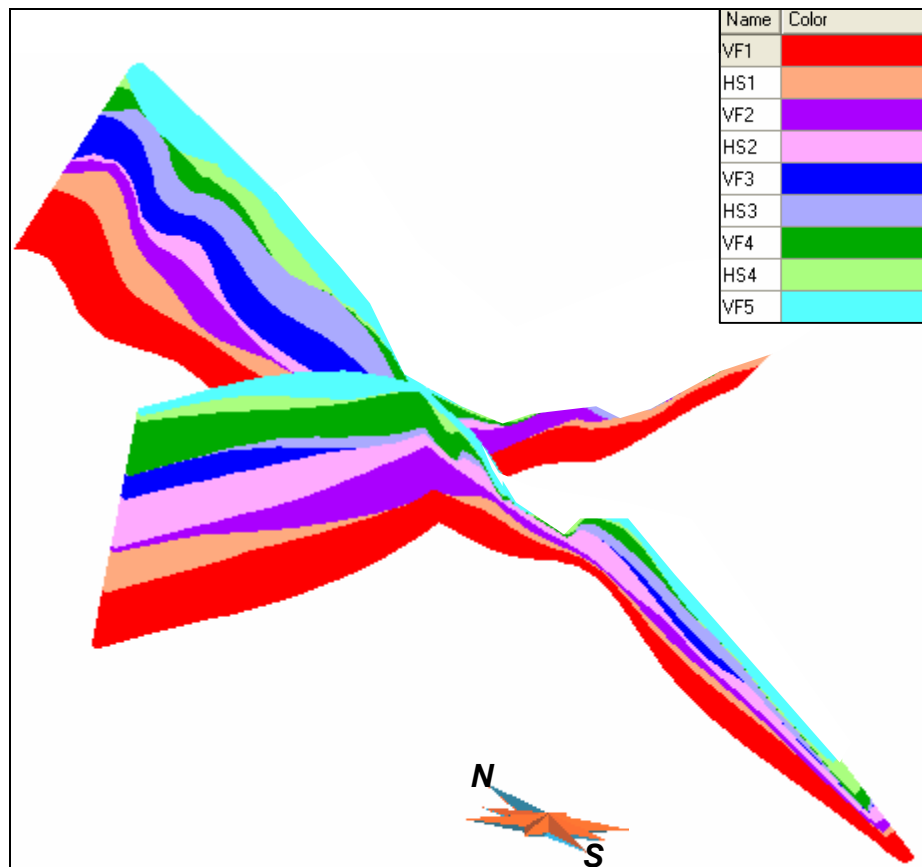


Figure 55. North-south and west-east cross section showing sequence stratigraphic correlation in the interval between Ellis top at the bottom and combined Tinroof and Lower Cretaceous surface at the top. VF-valley fill, HS-highstand.

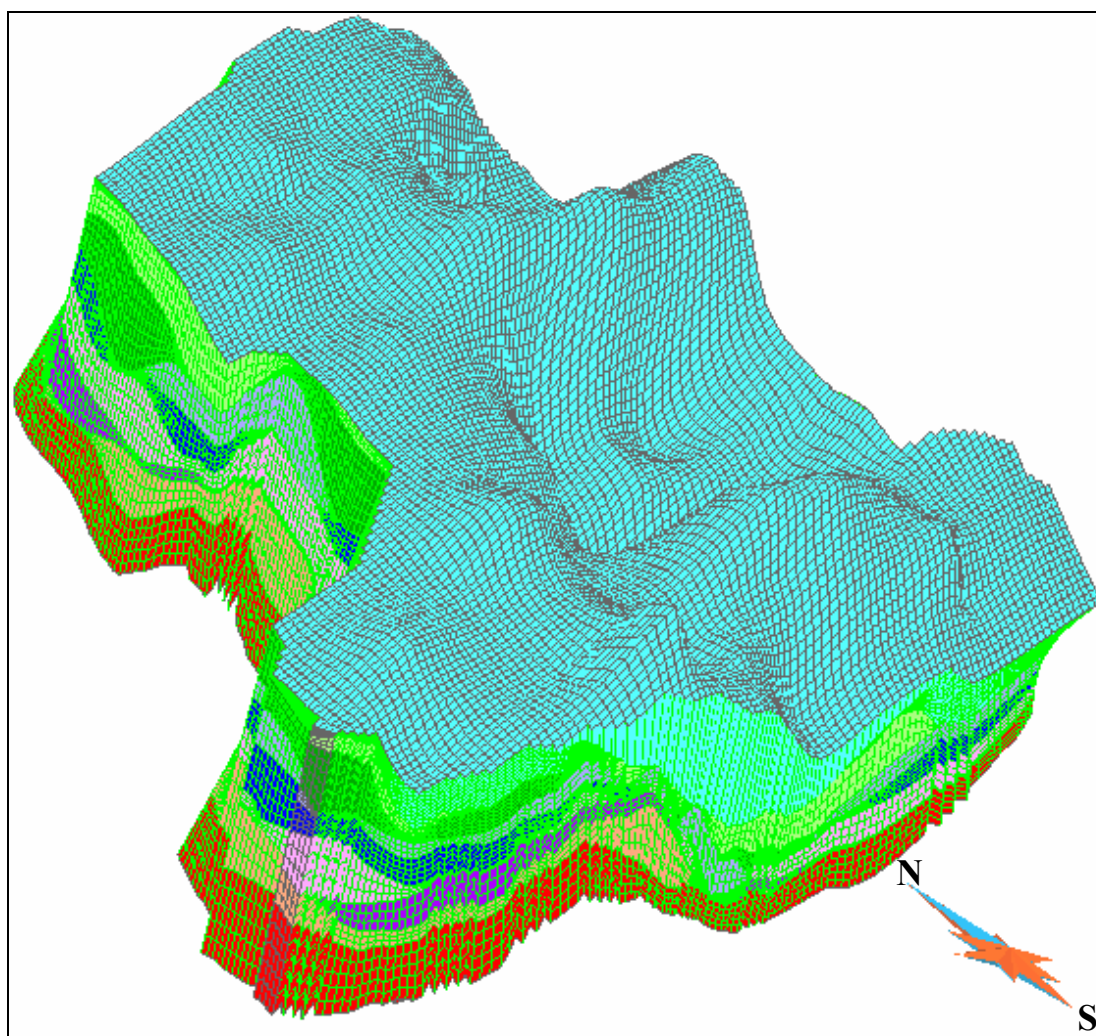


Figure 56. 3D Sgrid model bounded by combined Tinroof and Lower Cretaceous Gorge base surface at the top and Ellis at the bottom.

Each cell within the Sgrid can be assigned properties; the following 2 reservoir properties were modeled: facies (reservoir sand quality) and porosity. Simulation was first performed with a geological variable to make geological quality control easier. Ideally, the most relevant variable should have been the lithofacies defined in the core sedimentological analysis, but in practice, not every well has been cored. The database

must then be compiled from well-log data, and because log signatures are not unique, this requires a grouping the lithofacies into a few lithotypes. A lithotype must be relevant from both a sedimentological and a petrophysical viewpoint. Determining the lithotype allows qualitative control of the simulation. Each lithotype was characterized by a specific porosity distribution. At Cut Bank field, the seven previously described lithofacies were regrouped as 3 lithotypes discernible by log signatures; channel-fill sands correspond to lithotypes 1 and 2. Sands with GR values less than 60 API, sandy shales with GR values between 60 and 90 API and passing upward to flood plain shales with GR values greater than 90 API (lithotype 0).

Many geostatistical methods are available when modeling. The method chosen may be influenced by the data format and the geological environment. In this case, stochastic simulations were performed using a method based on truncated Gaussian random functions (Matheron et al., 1987). The method allows simulation in a three-dimensional space of facies sequences and easy conditioning of the simulation to the reservoir data.

Lithofacies were modeled within each major stratigraphic unit. The model was populated by assigning cells with one of 3 numbers (the lithotypes divisions described above). Figure 57 shows north-south and west-east cross section of the facies realization, and Figure 58 is a 3-D view of the facies in valley fill of Sequence 1 (VF1) (Lower Cut Bank).

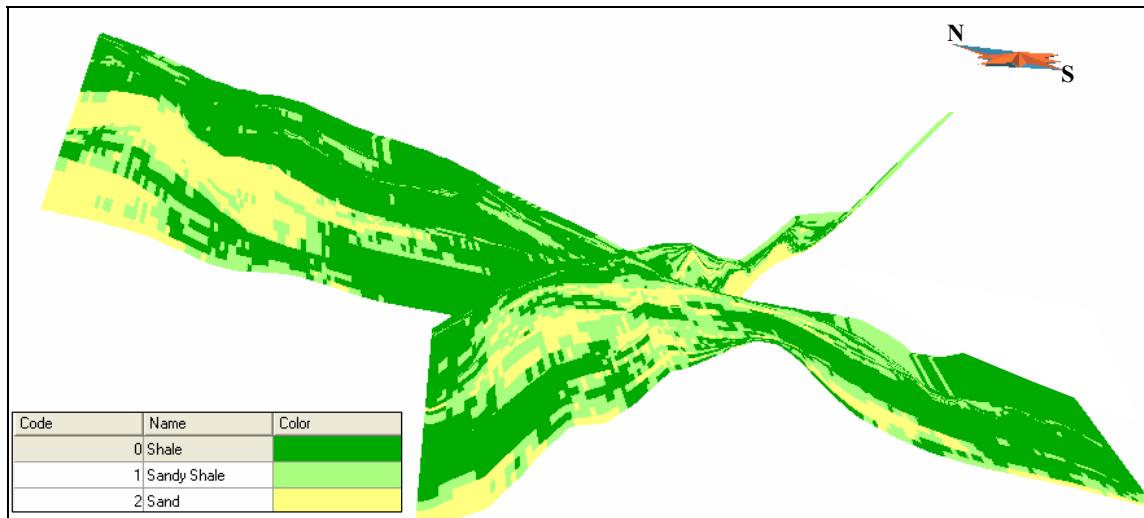


Figure 57. North-south and west-east cross sections of the facies realization (vertical exaggeration=20).

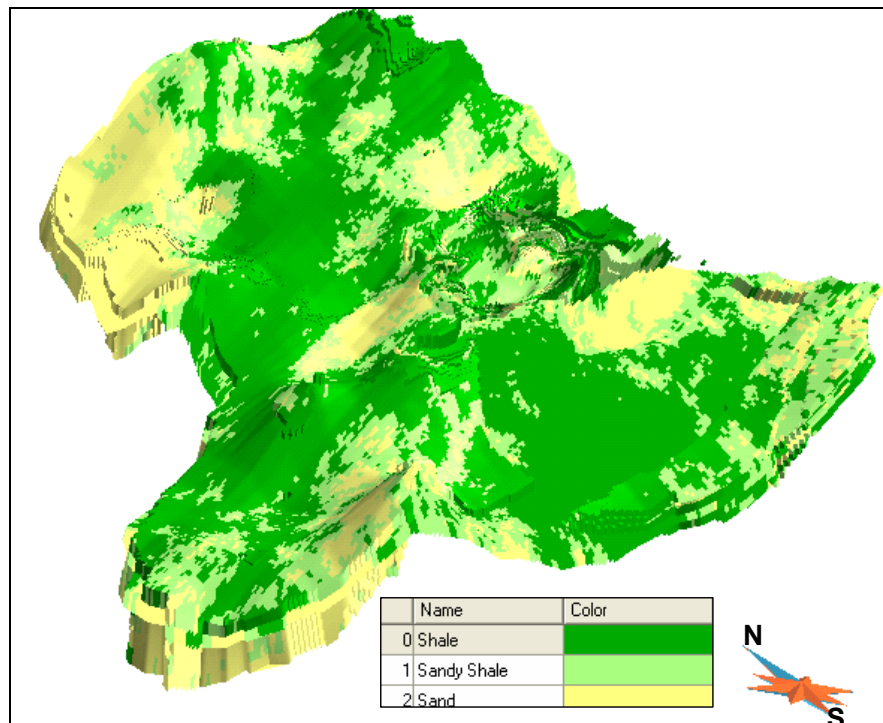


Figure 58. 3-D view of the facies realization in valley fill of Sequence 1 (VF1), lower Cut Bank (vertical exaggeration= 50).

Once satisfactory geological simulations of lithotypes were obtained, they were translated into layers of relevant petrophysical variables (i.e., porosity). Thus, petrophysical values were assigned to each lithotype, given the available measurements performed in the wells.

After completing each facies realization, neutron-density average porosity values calculated from well logs were distributed by facies type. Since the porosity can be treated as a continuous variable, Sequential Gaussian Simulation (SGS) was used. Five reservoir images of the porosity were generated. Figure 59 represents one of the porosity models. Figure 60 shows a 3D view of the porosity model of valley fill of Sequence 1 (VF1). The high dispersion of petrophysical values for a lithofacies is a consequence of the small-scale geological structures existing inside that lithofacies; for example, shale streaks or cross-bedding. Multiple stochastic realizations were constructed by repeating the entire workflow resulting in different lithofacies and petrophysical properties.

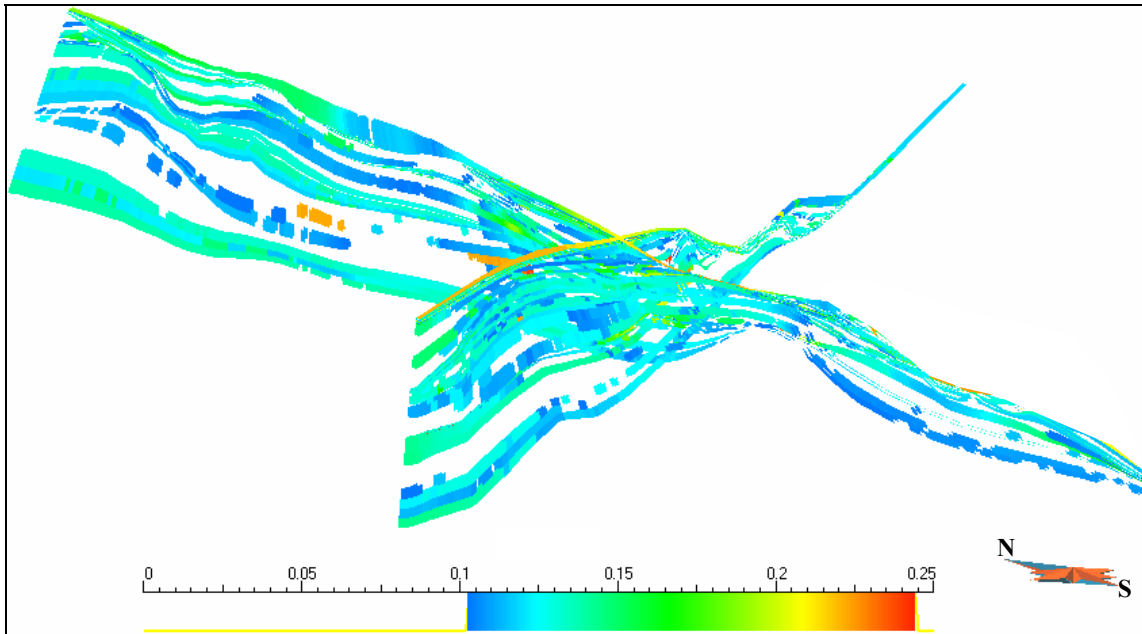


Figure 59. North-south and west-east cross section of the porosity realization (vertical exaggeration=20).

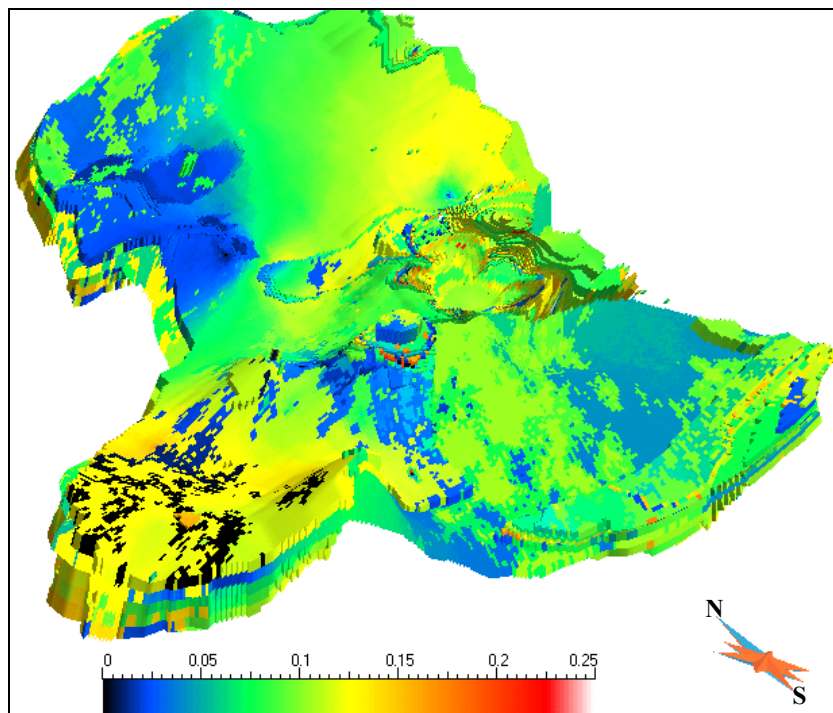


Figure 60. 3-D view of the porosity realization in valley fill of Sequence 1 (VF1), lower Cut Bank (vertical exaggeration=50).

6.2 Vertical Proportion Curve

Geostatistical structural analysis of truncated Gaussian random functions comprises the computation of lithofacies proportion curves and variograms (Matheron et al., 1987; Ravenne et al., 1989).

Vertical proportion curves have proven to be efficient tools to quantify sequential organization and variations of facies. They correspond to the percentage of lithotypes computed in the well at different levels parallel to a given horizontal reference (SB1/Ellis top). This reference horizon is represented on a graph with the percentage of facies along the horizontal and the distance from the reference horizon along the vertical (Fig. 61). The vertical proportion curve allows for a rapid visualization of the vertical organization of lithotypes and can be interpreted from a sedimentological viewpoint. These curves were particularly useful in the case of Cut Bank field. On a curve computed with 169 wells, the cyclic pattern of the fluvial deposits clearly appears with peaks of fluvial sandstones alternating with spikes of flood-plain mudstones. Five fining-upward sequences with a sand-rich layer vertically grading to a shale-rich layer are present (Fig. 61). Each sequence can be correlated with the five base-level cycles delimited in the sequence stratigraphic analysis. The sand-rich layers correspond to the amalgamated fluvial channels, and the shale-rich layers are flooding surfaces. The proportion curves thus confirm the interpretation of layering and, furthermore, allow quantification of the facies distributions within the cycles. Also, the curves can be interpreted qualitatively to roughly estimate the reservoir heterogeneity. The heterogeneity of the fluvial sand sheets, for example, is confirmed by looking at the

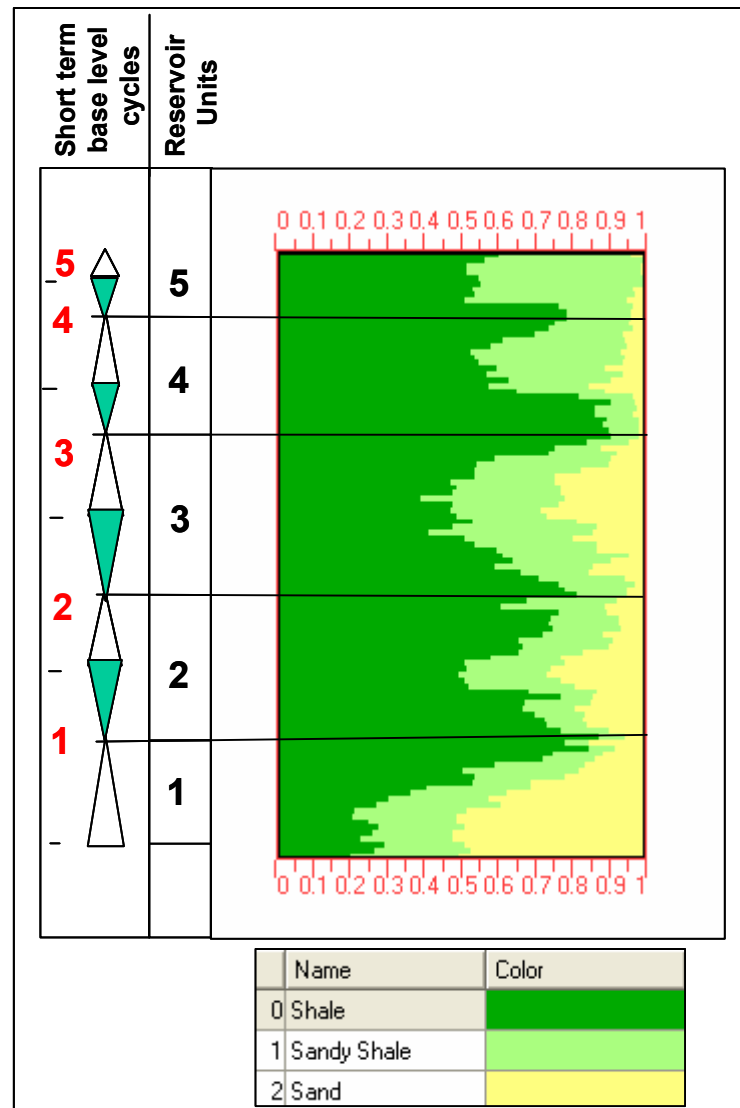


Figure 61. Vertical proportion curve of lithotypes computed with 169 wells for the whole series. The five cycles are clearly shown in the curve, with sandstone peaks grading to mudstone peaks. Reservoir units correspond to the series between two mudstone spikes, corresponding to the maximum flooding surface of the base-level cycles.

relative percentage of lithotypes at different stratigraphic levels in the vertical proportion curves (Fig. 61). The main reservoir units are composed of no more than 50% clean sandstones (lithotype 1) and 30% sandy shales (lithotype 2); 20% non-reservoir

mudstones (lithotype 0) are also present in the amalgamated channel-fill sandstones. Also, we can predict that vertical connection between the different sand sheets is highly probable at field scale, with the presence of porous lithotypes at every stratigraphic level. Local vertical permeability barriers are nevertheless expected with regard to the shale-rich layers, made up of approximately 70% non-reservoir mudstones plus 10–20% non-reservoir sandy shales.

6.3 Variogram Computation

Variograms are used in geostatistical reservoir modeling as a measure of spatial variability. It is essential that variograms be representative of the true heterogeneity present in study area. In this study they have been computed directly with the lithotype database. Variograms describe the increasing difference (or decreasing correlation) between sample values as separation between them increases. Beyond the range of correlation of the variogram, the data are said to be uncorrelated. It is recommended to transform the data to Normal space before performing variogram calculations (Deutsch and Journel, 1997). This has some important advantages: (1) the difference between extreme values is dampened; and (2) the theoretical sill is known (if the data have been transformed, for categorical variables (facies) $\text{sill} = p(1-p)$ where p is the global proportion of the category of interest).

Experimental variograms were first computed from the well data, then fitted with the truncated Gaussian function model (Matheron et al., 1987), which ensures

consistency between variograms and cross-variograms of lithotypes. Vertical and horizontal variograms were directly computed from well data (Fig 62).

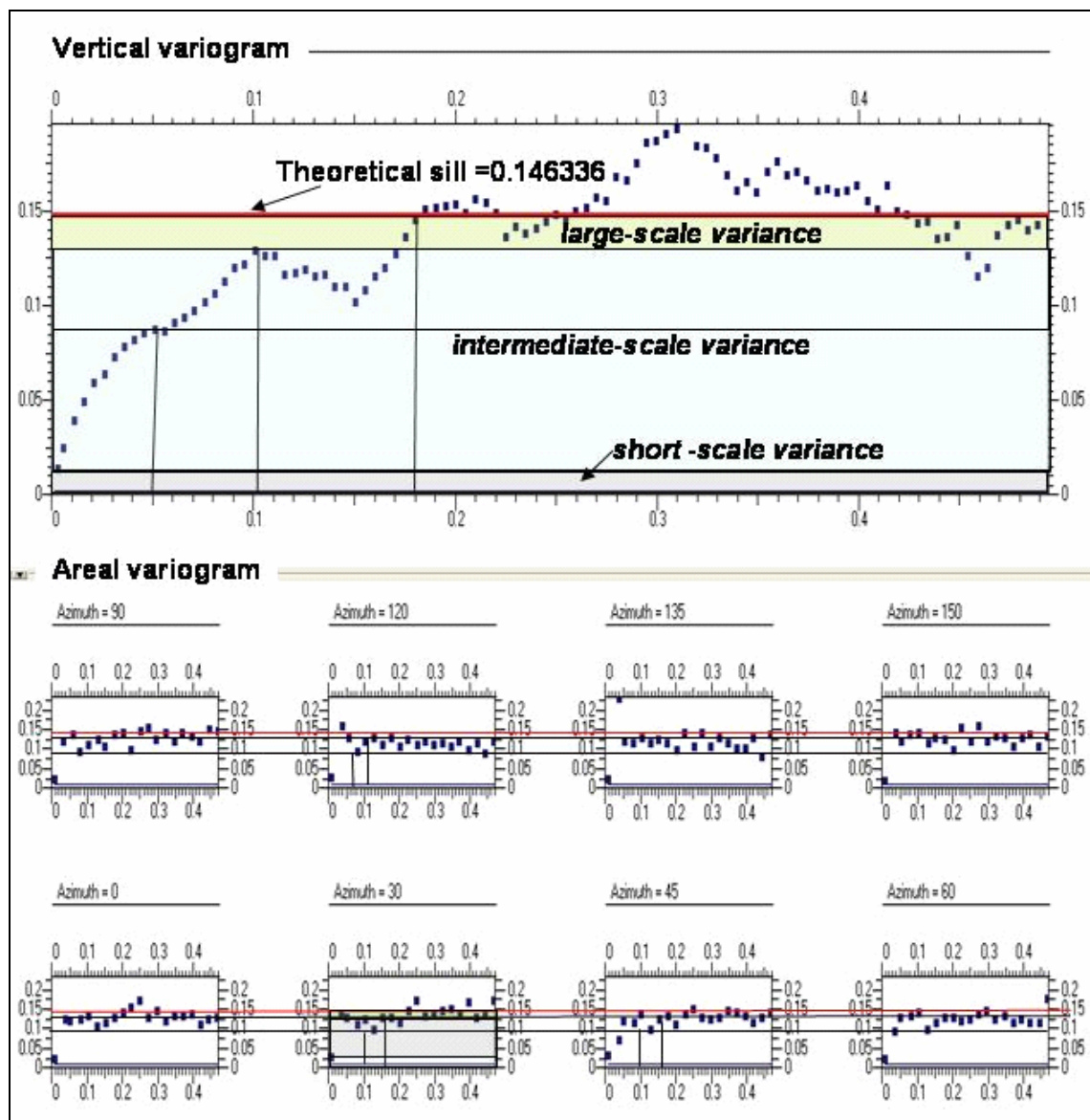


Figure 62. Lithofacies vertical and areal variogram model for study interval (UVW coordinate and indicator transformation applied). UVW transformation was used for SGrid. UVW are local coordinates of SGrid and these coordinates are different than XYZ coordinates. Short-scale variance represents a nugget effect; intermediate-scale variance represents geometric anisotropy; and large-scale variance represents zonal anisotropy.

The dots in Figure 62 show the experimental variogram, which means results from computation of the semi variance. The distance at which data point becomes totally uncorrelated is the Range of the variogram (vertical lines). The variance at that point is called the Sill of the variogram (red horizontal line), which is the statistical semi variance of the data set. The variance where the distance is almost zero is called Nugget. The areal variogram graph shows how reservoir continuity varies in the different directions. Noise in areal variograms is due to scarcity of data in the horizontal direction. The Nugget effect is a discontinuity in the variogram at the origin corresponding to short scale variability. On the experimental variogram, it can be due to measurement errors or geological structures with correlation ranges shorter than the sampling resolution. It must be chosen so as to be equal in all directions. It is picked from the directional experimental variogram exhibiting the smallest nugget. Structure one of the example in Figure 62 with value of 0.012 corresponds to the nugget effect - short-scale variance. Most depositional processes impart spatial correlation to petrophysical properties. The magnitude of spatial correlation decreases with separation distance until a distance at which no spatial correlation exists, the range of correlation. The vertical range of correlation is much less than the horizontal range due to the larger lateral distance of deposition. Geometric anisotropy corresponds to a phenomenon with different correlation ranges in different directions. Each direction encounters the total variability of the structure (Gringarten and Deutsch, 2001). There may exist more than one such variance structure. Structure two in Figure 62, with intermediate-scale variance from 0.086 to 0.146, represents geometric anisotropy with longest correlation range in the

horizontal direction. Highest range is observed in the direction of main axis of the horizontal variogram model, respecting the general southwest-northeast channel orientation. Range in the southeast-northwest direction was 1.4 times smaller than in the perpendicular direction.

Large-scale variance - zonal anisotropy is characterized by directional variograms reaching a plateau at a variance lower than the theoretical sill; i.e., the whole variability of the phenomenon is not visible in those directions. Structure three in Figure 62 corresponds to zonal anisotropy; only the vertical direction contributes to the total variability of the phenomenon at that scale.

Vertical variograms indicate a trend in the petrophysical property distribution—for example, fining or coarsening upward. Repetitive or cyclic variations in the facies in vertical variogram may be linked to geological periodicity.

Thus, geological model populated with reservoir parameters using geostatistical studies provide equiprobable representations of the geological heterogeneity of the main reservoir units. Validation of geological model and confidence in locating the remaining oil in a mature reservoir requires integration of geological and geophysical data with engineering data to accurately identify reservoir architecture, depleted reservoirs, and remaining potential. Therefore, in next chapter I integrate fluid flow trends with reservoir architecture by relating production performance maps with geologic and reservoir-quality maps.

CHAPTER VII

INTEGRATING PRODUCTION TRENDS WITH THE RESERVOIR MODEL

The geological modeling in this work was completed by 1) detailed correlation of stratigraphic units and assessment of facies character; 2) assessment of seismic data for reservoir characterization studies; 3) modeling the stratigraphic framework; and 4) applying geostatistical simulation to produce realizations for each stratigraphic unit.

Characterization of Cut Bank reservoir and recognizing potential compartmentalization in SCCBSU area using seismic data remained challenging due to inconsistent seismic imaging of the target formation. Therefore, I modeled this complex reservoir by combination of stratigraphic models and probabilistic simulations using well log and core data. The sequence stratigraphic conceptual model provided a framework for prediction of facies distributions, and the geostatistical approach filled in estimates of the facies variability within these sequences.

Integrating fluid flow trends with reservoir architecture is critical to identifying heterogeneities within the reservoir and developing three-dimensional flow-unit models that can be used to predict untapped compartments (Hamilton et al., 1998). This task is accomplished by relating production performance maps with geologic and reservoir-quality maps. Coincidences among the spatial positions of reservoir quality, structural setting, and production trends are key to recognizing heterogeneities and controls on production. Areas of high production, for example, overlap fairways of high-quality reservoir facies as predicted by the geological analysis, whereas disruption in production trends may indicate facies changes or structural discontinuities. For Cut Bank field, this

comparison was accomplished by relating production performance maps with geologic and reservoir-quality maps. Even though average thickness of the study interval is 120 ft, lower Cut Bank (lowest 40 ft interval) is the major reservoir and the most complete data are available from this interval. Therefore, focus in this chapter is on lower Cut Bank sands. Production performance maps in Cut Bank field shows that reservoir quality controls production, because fluid flow trends (oil production) coincide with reservoir quality (net thickness, reservoir facies and porosity) maps. Continuous zones of high reservoir quality predicted by the net sand maps coincide with areas of high transmissivity of fluids and high production rates. Also, breaks in production trends that correspond to facies changes, identify heterogeneity and confirm the integrity of the model (McVay et al., 2004). In Figure 63, the QRI/BEG net thickness map is overlain by a cumulative production bubble map. Cumulative production map highlights important trends in fluid flow. Areas of best production (sweet spots) as well as areas showing impedance to fluid flow are readily identifiable from these maps. Wells 33-1 and 18A-1 record high cumulative oil production where BEG/QRI net reservoir thickness is very low which is inconsistent with other. There are no logs available for these wells, precluding any direct determination of sand thickness. These 2 wells coincide with sand zone on lithofacies map realization of the amalgamated sand valley fill part of Sequence 1 (VF1), which corresponds to lower Cut Bank (Fig. 64). There is no production around wells 49-14, 49-4 and 49-8 where QRI/BEG net thickness map shows high net thickness. Lower Cut Bank interval is shaly zone in Well 49-14. This is one of the inconsistent

areas of QRI/BEG net thicknesses map with well log data. In the lithofacies realization map (Fig. 64), Well 49-14 is in shale zone, whereas the other two wells are in sand zone.

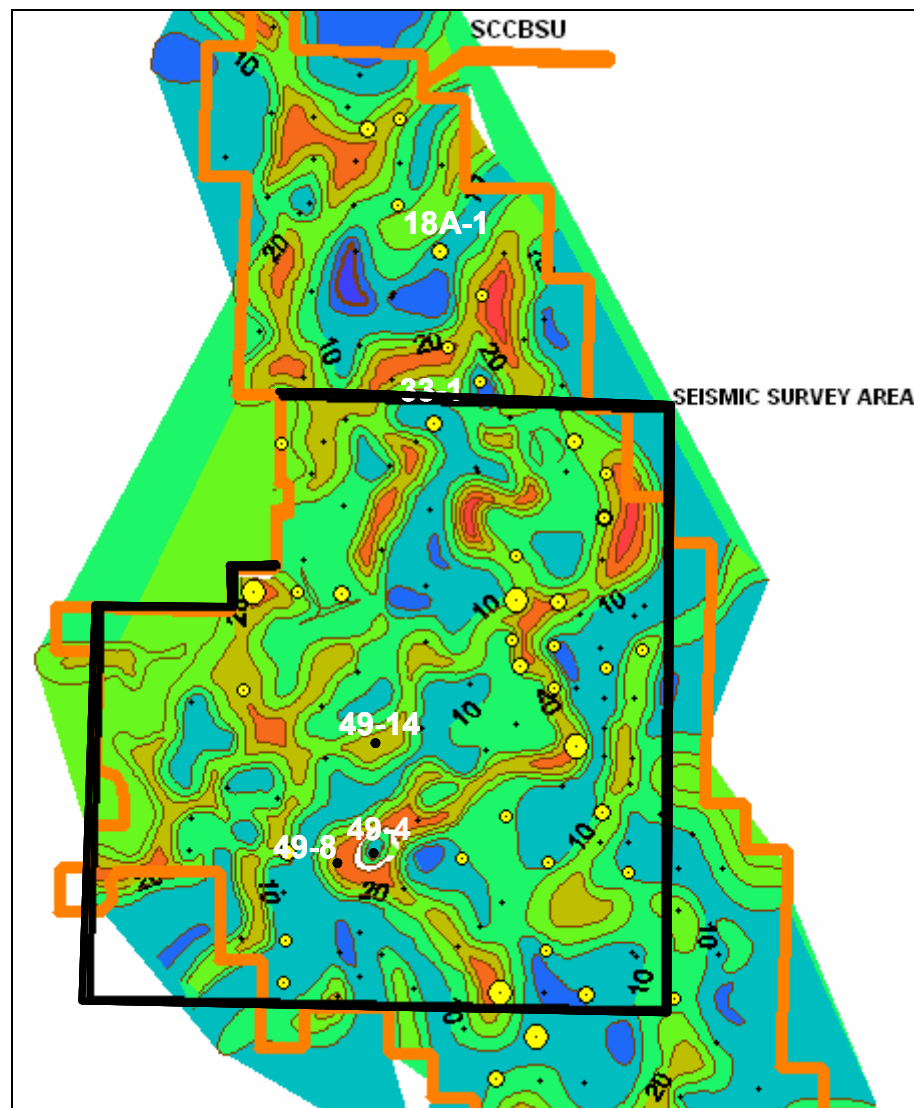


Figure 63. Lower Cut Bank net sand thickness map (QRI/BEG) (from Quicksilver Resources, 2002) overlain by cumulative production bubble map (McVay et al., 2004). There is a clear correlation between cumulative production and reservoir net thickness, i.e. high production trend correspond to high net-reservoir thickness in most areas excluding the highlighted wells

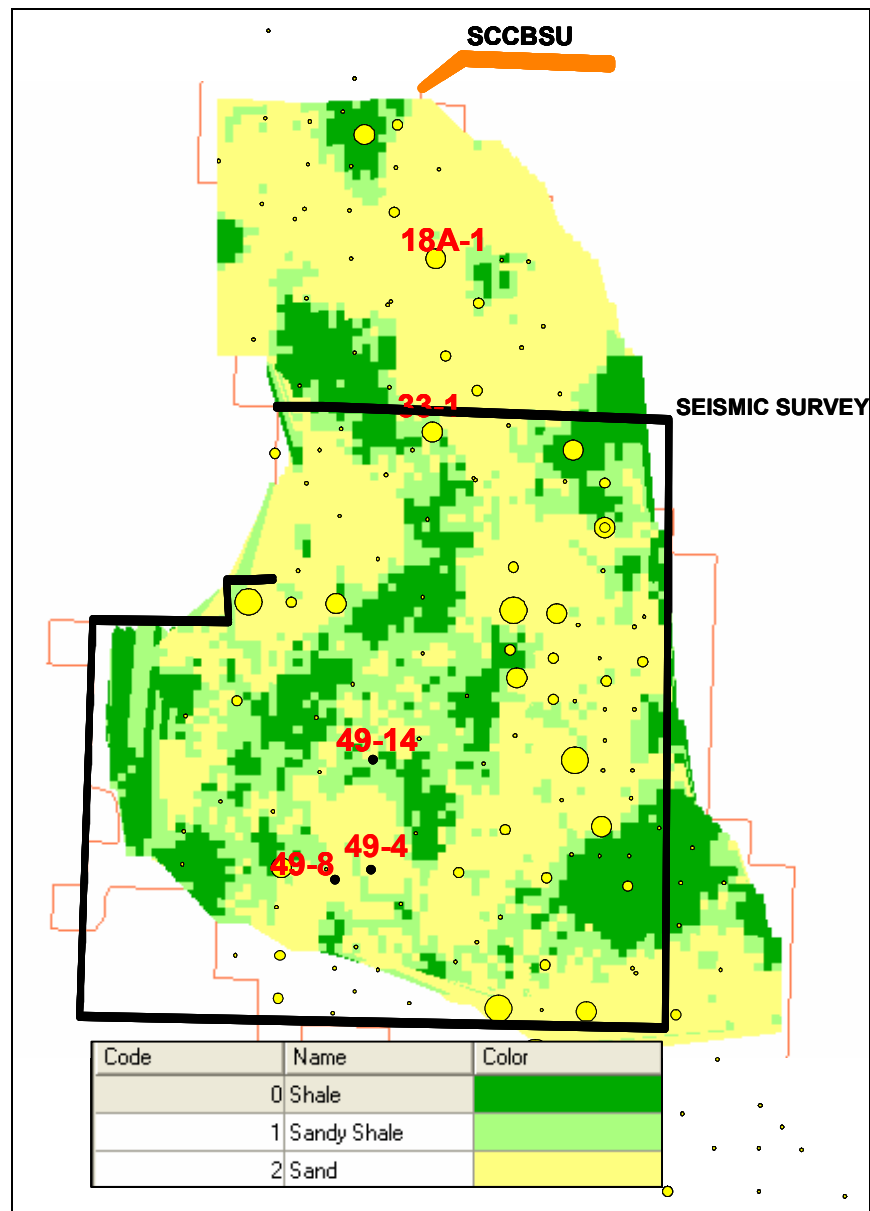


Figure 64. Lithofacies map realization at valley fill of Sequence 1 (VF1) overlain by cumulative production bubble map.

However, all three wells are in low porosity zone (<10%) on porosity realization map (Fig. 65).

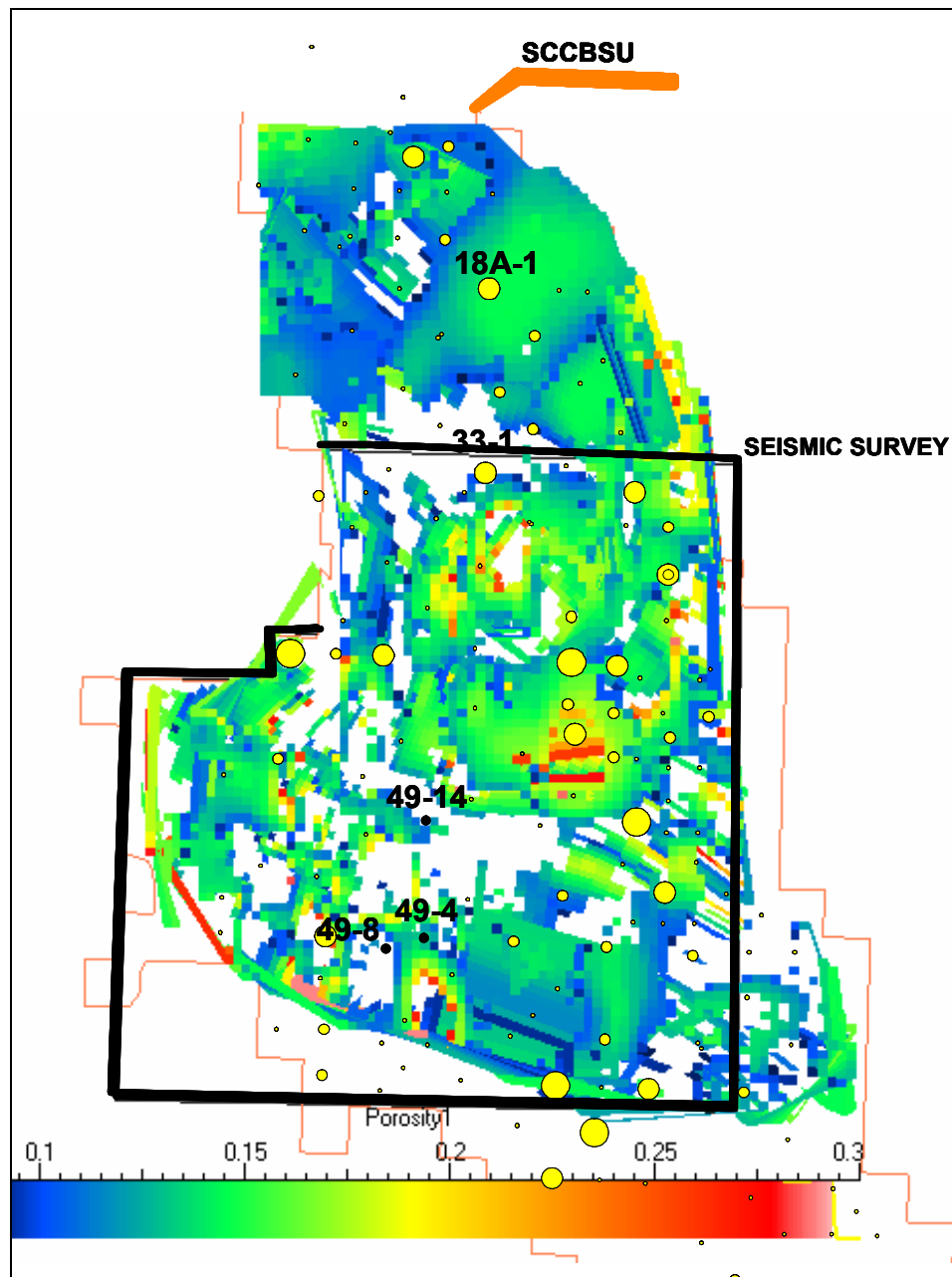


Figure 65. Porosity map realization of valley fill of Sequence 1 (VF1) overlain by cumulative production bubble map. White areas correspond to porosity values less than 8%.

Correspondence between geostatistical simulation results (facies and porosity realization) and patterns of production were assessed quantitatively by cross plotting facies realization times porosity realization (facies*porosity) of VF1 at each well against cumulative production of Lower Cut Bank interval (Fig. 66). There is a general increasing trend of cumulative production with the increase of facies*porosity product. However, there is large scatter. The general trend between QRI/BEG (2002) net thicknesses and lower Cut Bank cumulative production is expressed weaker and the scatter is larger (Fig.67).

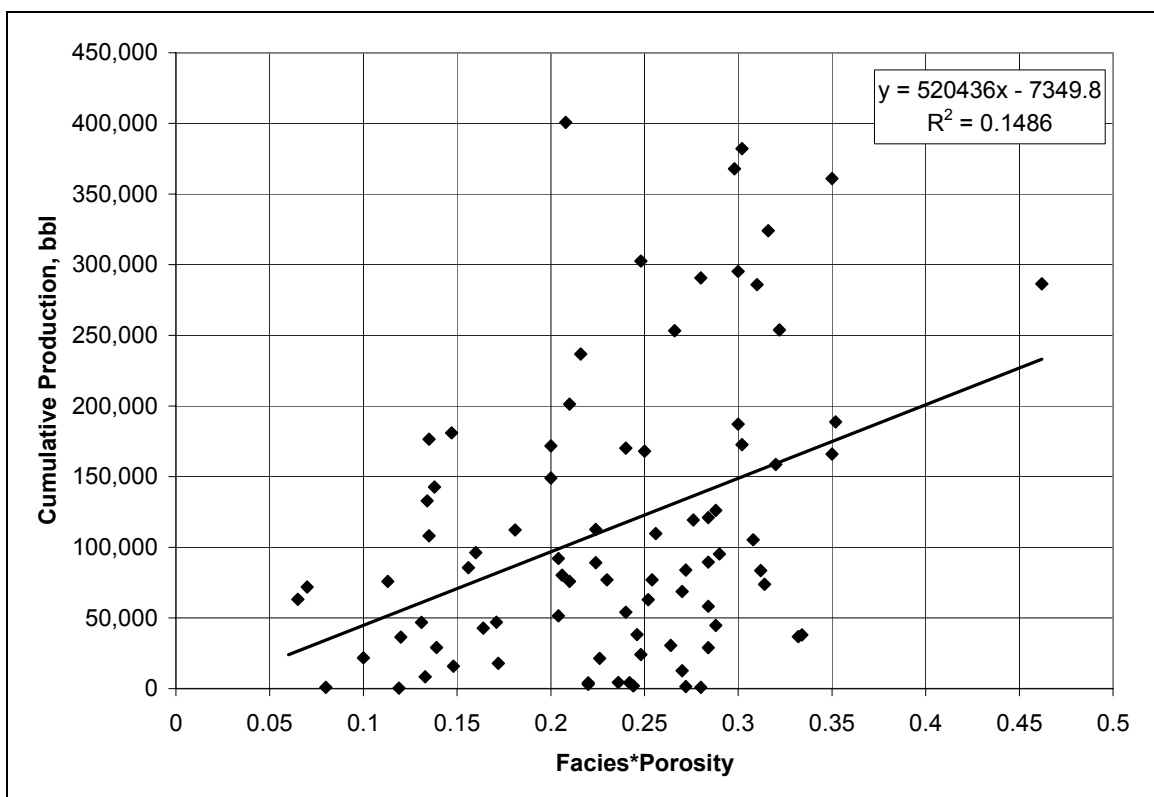


Figure 66. Lower Cut Bank cumulative production vs VF1 facies realization times porosity realization (facies*porosity). There is a general increasing trend of cumulative production with the increase of facies*porosity, with a large scatter.

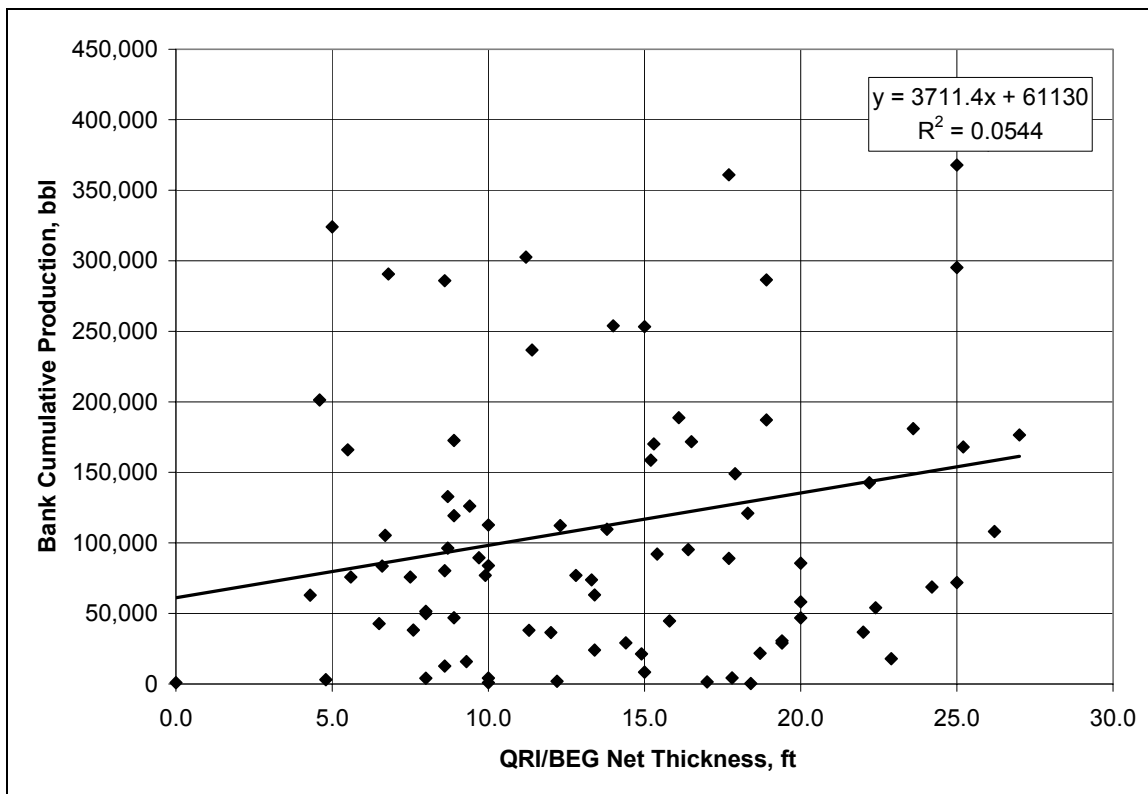


Figure 67. Lower Cut Bank cumulative production vs QRI/BEG net thickness [(net thickness data were estimated from QRI/BEG net thickness map (Quicksilver Resources, 2002)]. The general trend between QRI/BEG net thicknesses and lower Cut Bank cumulative production is expressed weaker and the scatter is larger than lower Cut Bank cumulative production vs facies*porosity (Fig. 66).

Figures 68 and 69 are arrow plots (McVay et al., 2004) overlain on the lithofacies and porosity maps realizations of valley fill of Sequence 1 (VF1). Arrow plot represents magnitudes and directions of fraction of flow in a producer attributable to flow at an injector (λ). λ is a vector quantity and its magnitude is represented by the arrow length. The arrow points from the injection well towards the producer for which the λ is calculated. There is a generally good correspondence between the calculated λ

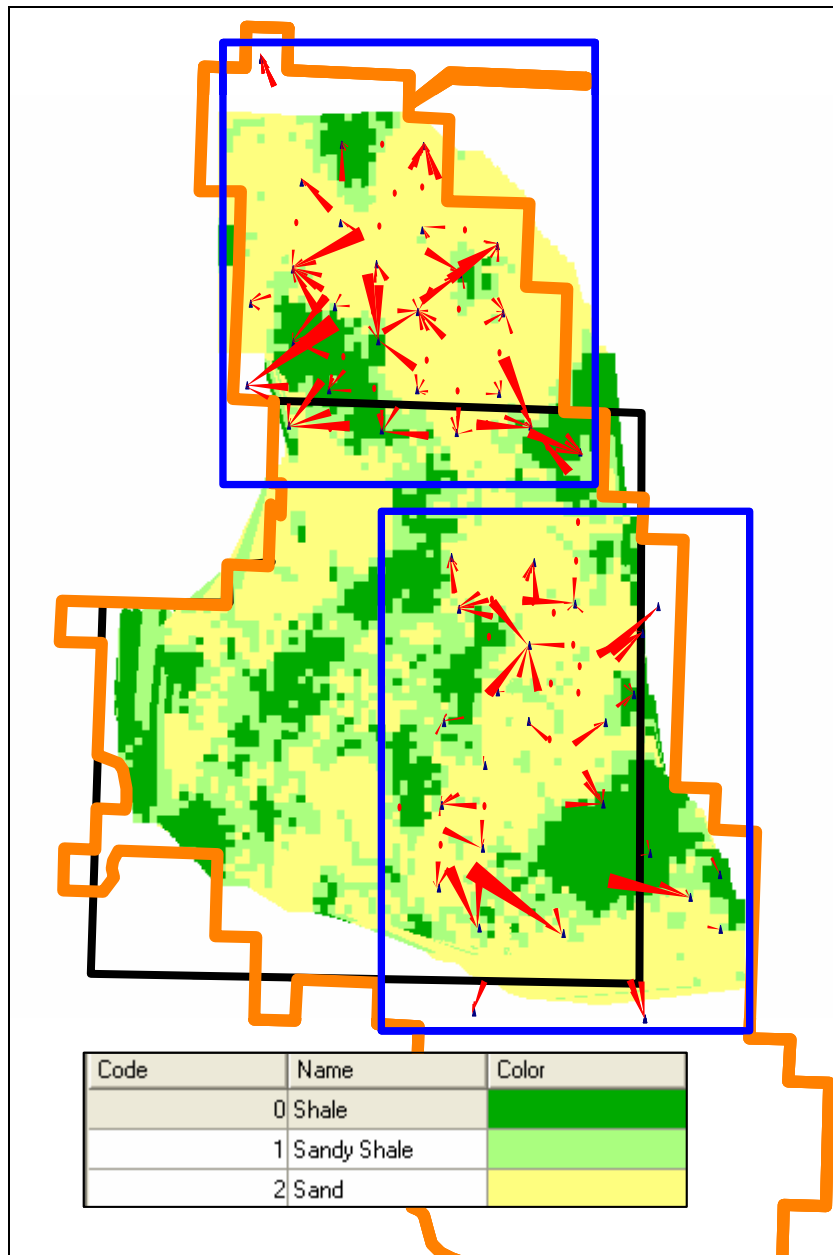


Figure 68. Lithofacies map realization at valley fill of Sequence 1 (VF1) overlain by arrow plots. λ (fraction of flow in a producer attributable to flow at an injector) is large in sand zones and small in shale zone.

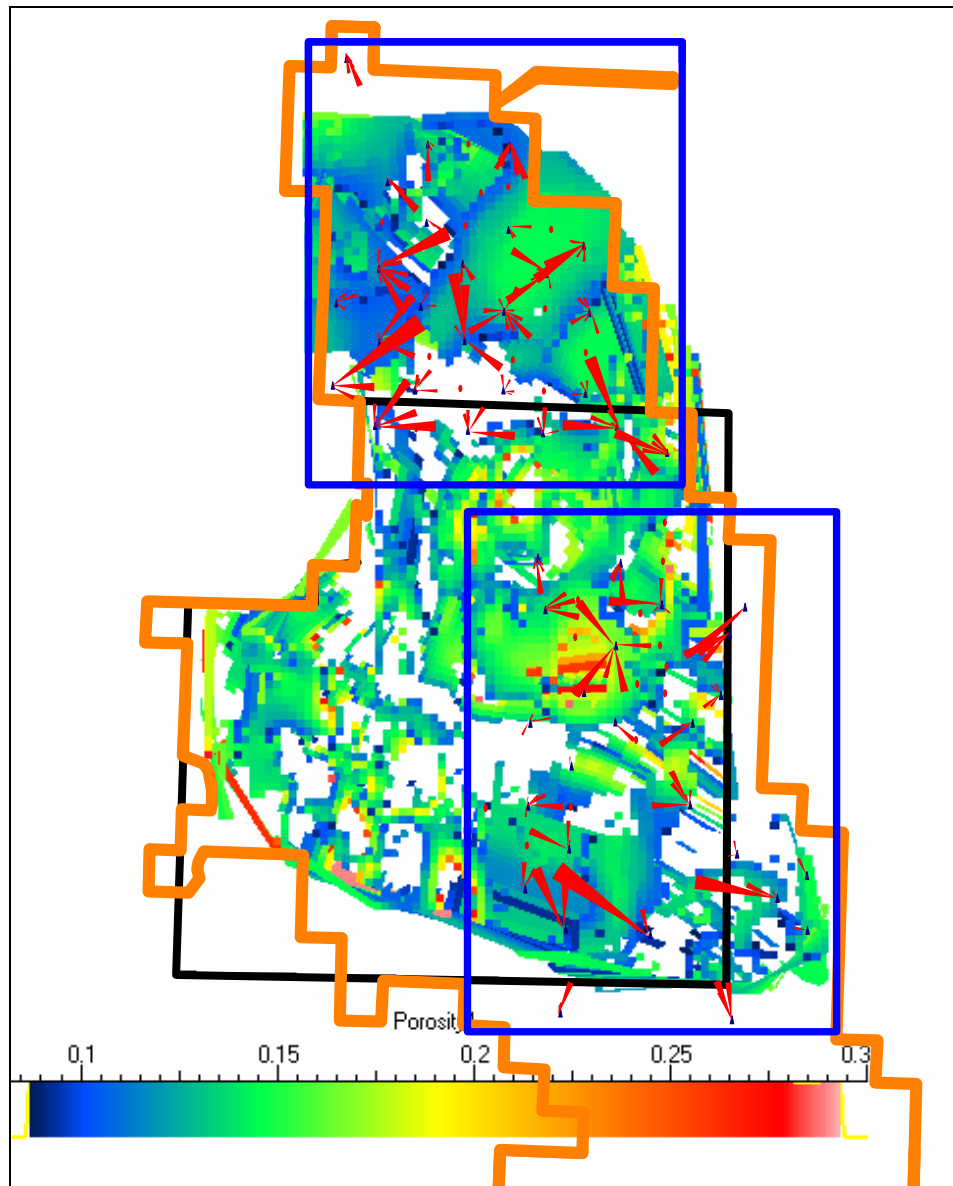


Figure 69. Porosity map realization at valley fill of Sequence 1 (VF1) overlain by arrow plots. White area corresponds to porosity values less than 8%.

and the lithofacies and porosity realizations as indicated on the maps; λ is large in sand zones and small in shale zones. The variability of the arrow lengths with direction suggests the connectivity is strongly anisotropic, favoring the orientations of the channel

axes. The presence of distant injector-producer pairs with strong connectivity appears to reflect the channel orientation of the reservoir.

It appears there is generally good correlation between net-to-gross ratio and lithofacies realization at valley fill of Sequence 1 (VF1) (Fig. 70). In the central part of SCCBSU the highest net-to-gross areas correspond to northeastward-trending sand-rich lithofacies that reflect alluvial channels orientation. The possibility is great that there is connection among the wells along this trend. Zero net-to-gross contours fall in shale zones. It is difficult to obtain exact coincidence because computer generated contours usually are smoothed and sometimes cut through grids of various values. However, this comparison still is useful because it gives the general trend.

Thus, comparison with production data is a way to validate the geological modeling. The case of Cut Bank was particularly demonstrative. The good fit of the total production and arrow plots with the geological model validated the geological interpretation and demonstrated that trends in fluid flow were definitive in the lower Cut Bank reservoir, because oil production closely follows the reservoir quality (net thickness, reservoir facies and porosity), with the most productive wells coinciding with the high reservoir quality.

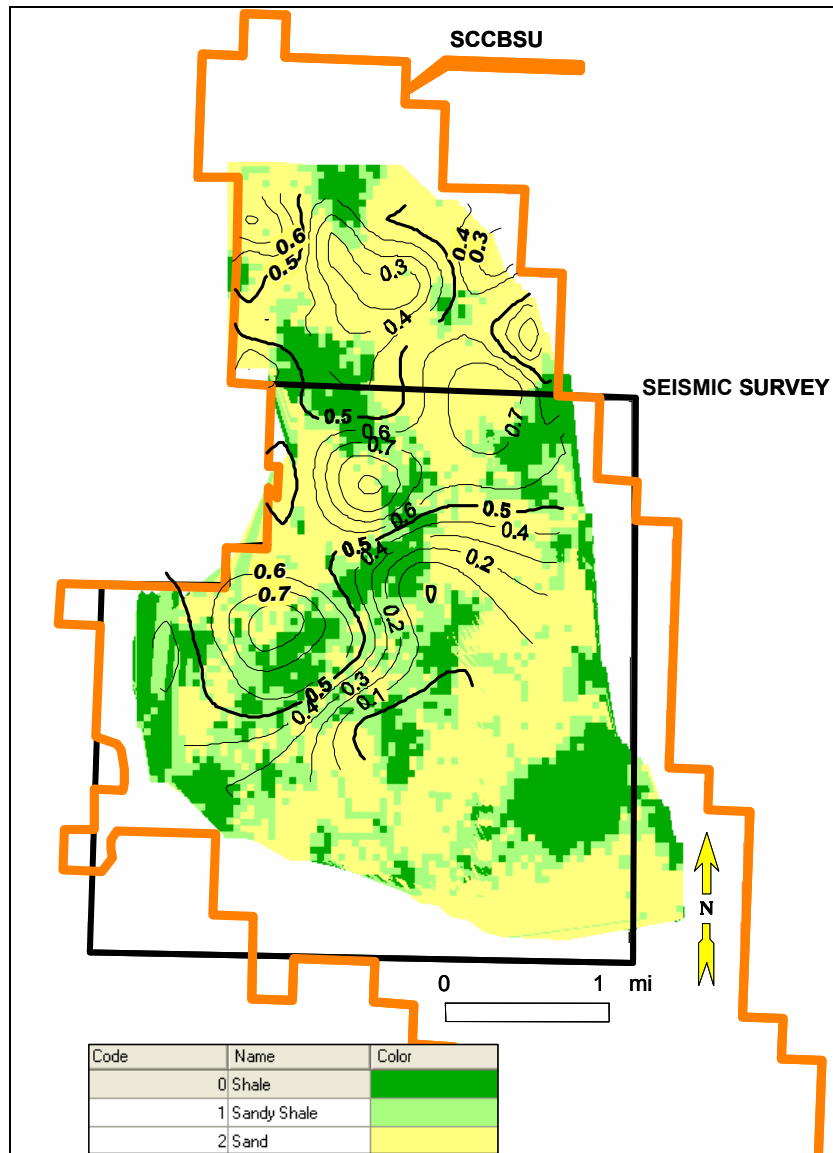


Figure 70. Lithofacies map realization at valley fill of Sequence 1 (VF1) overlain by net-to-gross ratio contours of VF1 constructed using well logs.

CHAPTER VIII

DISCUSSION

Effective field development requires detailed reservoir models. Lithologic maps of genetic stratigraphic units, accurately depicting the facies architecture, can be useful guides in delineating remaining oil and identifying areas of strategic infill wells, recompletions, redrilled wells, and candidates for future water injection and secondary oil recovery. High-resolution stratigraphic correlation permits accurate representation of reservoir compartmentalization in a spatial and temporal framework. In alluvial systems the boundaries of the main reservoir compartments coincide with stratigraphic boundaries of genetic sequences.

Channel-fill sandstones in the Cut Bank field range transitionally from vertically amalgamated (multi-storied), areally continuous sandstones to isolated sandstone bodies embedded in floodplain mudstones. Channel sandstones exhibit regular, recurring motifs that are associated with changes in A/S conditions. Lowest accommodation conditions resulted in amalgamated channel-fill sandstones, up to 18 ft thick, with intraclast-rich bases; they are capped by up to 2 ft thick floodplain mudstones. At higher A/S conditions, slightly amalgamated channel sandstones have lateral accretion surfaces and are capped by a thicker unit of floodplain mudstones. Channel sandstones in the highest A/S conditions are single-storied, possess conspicuous lateral accretion surfaces with thick mud drapes, and have a thick cover of overbank and floodplain deposits. Detailed well log correlations and oil production data support that the amalgamated, multistory sandstones are more laterally continuous.

Petrophysical properties are closely associated with subtle variations in facies, and both are stratigraphically sensitive. Petrophysical properties of identical sedimentological facies change regularly as a function of stratigraphic position because of variations in the rates of accumulation and degree of preservation of the sediments. In the case of fluvial strata deposited during an increase in A/S, porosity and permeability are highest in trough cross-stratified sandstones, immediately above channel scour bases, and both properties decrease upward to the next scour base. Successive channel-fill sandstones within the same stratigraphic sequence and channel-fill sandstones from one sequence to the next have progressively lower porosity and permeability values related to an overall increase in the A/S. An inverse trend is observed during a decrease in A/S.

Geostatistical modeling of lithotypes is a flexible way to account for the small-scale heterogeneities. By using a geostatistical approach in a sequence stratigraphic framework, cross correlation across major unconformities is avoided, and the subtle variability of spatial distribution of facies in the different sequences is preserved. A sedimentological analysis combined with a sequence stratigraphic study and a geostatistical analysis provides a qualitative estimation of the reservoir geometry and of its internal architecture. Also, it helps to better define the relevant lithotypes, their sequential organization, the lithostratigraphic units within which the simulation has to be performed.

Three lithologic facies (sand, shale, and sandy shale) were distributed throughout the GOCAD model. Although the suite of depositional facies (1-7) were not distributed

throughout the GOCAD model, the facies description/discretization effort was nonetheless critical for appreciation of reservoir facies.

Proportion curves allowed recognition of cyclic facies arrangements with the end-result being a higher resolution, higher confidence correlation framework.

Properties from the wells were geostatistically distributed using variograms describing the spatial relationship of the reservoir properties. The benefits of a variogram analysis are to provide a useful tool for summarizing spatial data, to provide a measure of spatial dependence between samples and to use it to estimate data values at unsampled locations.

The final stage of the reservoir characterization is a 3D reservoir model populated with rock properties based on a prior petrophysical, geological and geophysical study of the field. Construction of the 3D reservoir model consisted of two main parts: (1) stratigraphic framework; and (2) reservoir property modeling.

Stochastic models of reservoir porosity and lithofacies were iteratively generated.

Fine-scale reservoir model were constructed for SCCBSU so that all geologically significant units could be captured.

CHAPTER IX

CONCLUSIONS AND RECOMMENDATIONS

This research was conducted to improve ultimate recovery of oil from Cut Bank field, Montana. The research was completed by building an integrated reservoir model that was based on high-resolution sequence stratigraphy and combine both deterministic and geostatistical approaches. The reservoir model was validated by integrating production trends with the reservoir model. The following are conclusions and recommendations from this study.

- Characterization of Cut Bank reservoir and recognition of potential compartments in SCCBSU area using seismic data was problematic due to inconsistent past interpretations of seismic data, including (1) seismic horizons that were incorrectly picked due to a crossing channel system, and (2) reservoir sandstones that are much thinner (~30 ft) than seismic resolution (110 ft).
- Complex, thin reservoir, such as Cut Bank sandstones can be modeled using combination of high-resolution stratigraphic models and probabilistic simulation.
- Identification and delineation of sequences and their bounding surfaces within a very low accommodation alluvial setting was possible; well log correlations show a relationship between base-level variations and channel amalgamation.
- Systems tracts were identified on the basis of sequential position, facies association and systematic changes in architectural style and sediment body geometry. Five cycles that constituted the reservoir framework layers were identified.

- Analysis of stacking patterns – predominantly fining and thinning upward – allowed the prediction of reservoir rock quality. Within every cycle the best quality reservoir rocks were strongly concentrated in the lowstand systems tract.
- The low-accommodation, alluvial paleogeography triggered the development of high-frequency sequences in which the erosional contacts between sandstones allowed communication among different reservoirs.
- The lowermost lower Cut Bank sand is a series of braided stream parasequences are areally extensive and have highest reservoir quality of all reservoirs in Cut Bank field.
- The basal lower Cut Bank sand has the highest average net-to-gross ratio (0.6) of all reservoir sands in Cut Bank field. We can expect little additional stratigraphically untapped sand from this interval.
- Over most of SCCBSU field, the Sunburst Member and the upper Cut Bank Sandstone are a valley fill complex with interfluvial sands that may laterally compartmentalize valley-fill sands.
- Upper Cut Bank net-to-gross ratio values are greater than zero only in the north part of SCCBSU. The average net-to-gross ratio value of the basal Sunburst sand (Sunburst 1) is 0.3, and this sand occurs throughout the SCCBSU. The basal Sunburst sand has better reservoir quality than other Sunburst sands or the upper Cut Bank sand, but its reservoir quality is not nearly as good as that of the lower Cut Bank sand.

- There may be the potential for undrilled compartments in upper Cut Bank and Sunburst sands in some areas of the field, owing to poor connectivity.
- Geostatistics provided equiprobable representations of the geological heterogeneity within the main reservoir units. The simulated reservoir geometries provided improved descriptions of reservoir distribution, connectivity and flow barrier distribution. Uncertainty in the reservoir architecture was accounted for by generating multiple realizations.
- Thus, high-resolution sequence stratigraphy and geostatistical simulation resulted in improved reservoir description that provided a better basis to predict reservoir performance.
- Although there may be opportunities for recompletions in Cut Bank field, a major challenge in such older fields is the integration of the geology-driven options with engineering and economic realities.
- I recommend incorporating engineering analyses such as fluid flow simulation, history matching, pressure communication and decline-curve analysis results into the reservoir model. The interpretations of the geological analysis and fluid flow simulation results should be consistent with calculated engineering parameters. Compartment dimensions may be verified by history matching and decline-curve analysis, compartment boundaries can be estimated by flow simulation, and pressure communication across the reservoir may be assessed using pressure tests. Results of these analyses will provide a basis for refining the working geologic model and selecting locations for infill, recompletion, and redrill wells,

as well as candidates for future water injection to recover additional volumes of remaining oil and extend the productive life of Cut Bank field.

- The technical approaches and tools from this study can be used to improve reservoir description of other oil and gas fields with similar depositional systems.

REFERENCES CITED

- Aitken, J. F., and S. S. Flint, 1995, The application of high resolution sequence stratigraphy to fluvial systems: a case study from the Upper Carboniferous Breathitt Group, eastern Kentucky, USA: *Sedimentology*, v. 42, p. 3-30.
- Ardies, G. W., R. W., Dalrymple, and B. A. Zaitlin, 2002, Controls on the geometry of incised valleys in the Basal Quartz Unit (Lower Cretaceous), western Canada Sedimentary Basin: *Journal of Sedimentary Research*, v. 72, no. 5, p. 602-618.
- Balster, C. A., M. Sokaski, G. McIntyre, R. B. Berg, H. G. McClellan, and M. Hansen, 1976, Status of Mineral Resource Information for the Blackfeet Indian Reservation, Montana: Administrative Report BIA-24, 69 p.,
<http://www.eere.energy.gov/tribalenergy/guide/pdfs/blackfeet_24.pdf>
(Accessed November 1, 2006).
- Berkhouse, G. A., 1985, Sedimentology and diagenesis of the Lower Cretaceous Kootenai Formation in the Sun River Canyon Area, Northwestern Montana: M.S. thesis, Indiana University, Bloomington, Indiana, 152 p.
- Blair, T. C., and J. G. McPherson, 1994, Alluvial fans and their natural distinction from rivers based on morphology, hydraulic processes, sedimentary processes, and facies assemblages: *Journal of Sedimentary Research*, v. 64, no. 3, p. 450-489.
- Blixt, J. E., 1941, Cut Bank oil and gas field, Glacier County, Montana, *in* A. I., Levorsen, ed., Stratigraphic type oil fields: AAPG Special Publication 11, p. 327-381.

- Blum, M. D., 1994, Genesis and architecture of incised valley fill sequences: a late Quaternary example from the Colorado River, Gulf Coast plain of Texas, *in* P. Weimer and H. W. Posamentier, eds., *Siliciclastic sequence stratigraphy: recent developments and applications: AAPG Memoir 88*, p. 259–283.
- Bridge, J. S., and S. D. Mackey, 1993, A theoretical study of fluvial sandstone body dimensions, *in* Flint, S., and Bryant, I. D., eds., *Quantitative description and modeling of clastic hydrocarbon reservoirs and outcrop analogues: International Association of Sedimentologists Special Publication 15*, p. 213–236.
- Burnett, M., 1996, 3-D seismic expression of a shallow fluvial system in west central Texas, *in* P. Weimer and T. L. Davis, eds., *Applications of 3-D seismic data to exploration and production: AAPG Studies in Geology 42 and SEG Geophysical Developments Series no. 5*, p. 45–56.
- Busch, D. A., 1971, Genetic units in delta prospecting: *AAPG Bulletin*, v. 55, no. 8, p. 1137–1154.
- Callagher, A. V., 1957, Geology of the Lower Cretaceous Cut Bank conglomerate in Northwest Montana: M.S. Thesis, Michigan State University of Agriculture and Applied Science, East Lansing, Michigan, 40 p.
- Conybeare, C. E. B., 1976, Geomorphology of oil and gas fields in sandstone bodies: *Developments in Petroleum Science*, 4, p. 84-88.
- Cupps, C. Q., and J. Fry, 1967, Reservoir oil characteristics, Cut Bank field, Montana: U.S. Department of Interior, Bureau of Mines, 36 p.

- Currie, B. S., 1997, Sequence stratigraphy of non-marine Jurassic-Cretaceous rocks, Central Cordilleran foreland-basin system: GSA Bulletin, v. 109, p. 1206-1222.
- Davies, D. K. I., B. P. J. Williams, and R. K., Vessel, 1992, Models for meandering and braided fluvial reservoirs with examples from the Travis Peak Formation, East Texas: SPE Paper 24692, 67th Annual Technical Conf., Washington, D.C., p. 321-329.
- DeAngelo, M. V., and B. A. Hardage, 2001, Using 3-D seismic coherency and stratal surfaces to optimize redevelopment of waterflooded reservoirs, Cut Bank field, Montana: Bureau of Economic Geology, Austin, Texas, 23 p.
- DOE, 2005, Fossil energy: marginal & stripper well revitalization: DOE's Marginal/Stripper Well Revitalization Programs, <<http://www.fossil.energy.gov/programs/oilgas/marginalwells/index.html>> (Accessed October 3, 2006).
- Deutsch, C. V., and A. G., Journel, 1997, GSLIB: Geostatistical software library and user's guide, 2nd Edition: New York, Oxford University Press, 369 p.
- Dolson, J. C. and J. Piombino, 1994, Giant proximal foreland basin non-marine wedge trap: Lower Cretaceous Cut Bank sandstone, Montana, *in* J. C. Dolson, Hendricks, M. L., and Wescott, W. A., eds., Unconformity related hydrocarbons in sedimentary sequences: Rocky Mountain Association of Geologists Guidebook, Cutbank, Montana, p. 135-148.

- Fielding, C. R. and R. C. Crane, 1987, An application of statistical modeling to the prediction of hydrocarbon recovery factors in fluvial reservoir sequences: Society of Economic Paleontologists and Mineralogists Special Publication 39, p. 321-327.
- Galloway, W. E., Williams, T. A., 1991, Sediment accumulation rates in time and space: Paleogene genetic stratigraphic sequences of the northwestern Gulf of Mexico Basin: *Journal of Geology*, no 19, p. 986–989.
- Gardner, G. H. F. , L. W. Gardner, and A. R. Gregory, 1974, Formation velocity and density-the diagnostic basics for stratigraphic traps: *Geophysics*, v. 39, no. 6 p. 770-780.
- Gardner, M. H., and Cross, T. A., 1994, Middle Cretaceous paleogeography of Utah, *in* M. V. Caputo, J. A. Peterson, and K. J. Franczyk, eds., *Mesozoic systems of the Rocky Mountain region, USA: Rocky Mountain Section SEPM (Society for Sedimentary Geology)*, Denver, p. 471-502.
- Gringarten E. and C. V. Deutsch, 2001, Variogram interpretation and modeling: *Mathematical Geology*, v. 33, no. 4, p. 507-534.
- Gully, T. G., 1984, Cut Bank field, *in* J. Tonnsen ed., *Montana Oil and Gas Fields Symposium: Montana Geological Society, Billings, Montana*, v. 1, p. 397-409.
- Haldorsen, H. H., and E. Damsleth, 1990, Stochastic modeling: *Journal of Petroleum Technology*, v. 42, no. 4, p. 404–412.
- Hamilton D. S., M. H. Holtz, P. Ryles, T. Lonergan, and M. Hillyer, 1998, Approaches to identifying reservoir heterogeneity and reserve growth opportunities in a

- continental-scale bed-load fluvial system: Hutton Sandstone, Jackson Field, Australia: AAPG Bulletin, v. 82, no. 12, p. 2192–2219.
- Hardage, B. A., R. A. Levey, V. Pendleton, J. Simmons, and R. Edson, 1994, A 3-D seismic case history evaluating fluvially deposited thin-bedded reservoirs in a gas-producing property: Geophysics, v. 59, p. 1650–1665.
- Hardage, B. A., R. A. Levey, V. Pendleton, J. Simmons, and R. Edson, 1996, 3-D seismic imaging and interpretation of fluvially deposited thin-bed reservoirs, *in* P. Weimer and T. L. Davis, eds., Applications of 3-D seismic data to exploration and production: AAPG Studies in Geology 42 and SEG Geophysical Developments Series no. 5, AAPG/SEG, p. 27–34.
- Hayes B. J. R., 1990, A perspective on the Sunburst Member of Southern Alberta: GEOLOGICAL NOTE, Bulletin of Canadian Petroleum Geology, v. 38, no. 4, p. 483-484.
- Hayes B. J. R., 1986, Stratigraphy of the basal Cretaceous Lower Mannville Formation, Southern Alberta and North-central Montana: Bulletin of Canadian Petroleum Geology, v. 34, p. 30-48.
- Henriquez, A., K. J. Tyler, and A. Hurst, 1990, Characterization of fluvial sedimentology for reservoir simulation modeling: SPE Formation Evaluation, SPE 18323, p. 211-216.
- Hill, R. B., 1989, Geologic evaluation of S.C.C.B.S.U. and recommendations for future development: In-house Report, Union Oil Company of California, El Segundo, California.

- Hirst, J. P., C. R. Blackstock, and S. Tyson, 1993, Stochastic modeling of fluvial sandstone bodies: International Association of Sedimentologists Special Publication 15, p. 237-252.
- Hopkins, J. C., 1993, Mesozoic depositional environments, Great Falls, Montana: Caesar Geological Consultants Ltd., Field Trip Report, Great Falls, Montana.
- Horkowitz, K. O., 1987, Direct and indirect control of depositional fabric on porosity, permeability, and pore size and geometry. Differential effect on sandstone subfacies on fluid flow, Cut Bank sandstone, Montana: PhD dissertation, University of South Carolina, Columbia, South Carolina, 136 p.
- Kalkomey C. T., 1997, Potential risks when using seismic attributes as predictors of reservoir properties: The Leading Edge, p. 247-251.
- Lemouzy, P., J. Parpant, R. Eschard, C. Bacchiana, I. Morelon, and B. Smart, 1995, Successful history matching of Chaunoy field reservoir behavior using geostatistical modeling: Proceedings of the Society of Petroleum Engineers Annual Technical Conference and Exhibition, SPE Paper 30707, p. 23–38.
- Lorenz, J. C., D. M. Heinze, J. A. Clark, and G. A. Searls, 1985, Determination of widths of meander-belt sandstone reservoirs from vertical downhole data, Mesaverde Group, Piceance Creek Basin, Colorado: AAPG Bulletin, v. 69, no.5, p.710-721.
- Lukie, T. D., G. W. Ardies, R. W. Dalrymple, and B. A. Zaitlin, 2002, Alluvial architecture of the Horsefly Unit (Basal Quartz) in Southern Alberta and Northern

- Montana: Influence of accommodation changes and contemporaneous faulting:
Bulletin of Canadian Petroleum Geology, v. 50, no. 1, p. 73-91.
- MacDonald, A. C., L. Fält, and A. Hektoen, 1998, Stochastic modeling of incised valley geometries: AAPG Bulletin, v. 82, no. 6, p. 1156–1172.
- Matheron, G., H. Beucher, C. Fouquet, A. Galli, D. Guerillot, and C. Ravenne, 1987, Conditional simulation of the geometry of fluvio-deltaic reservoirs: Proceedings of the Society of Petroleum Engineers Annual Technical Conference and Exhibition, SPE Paper 16753, p. 591-596
- Matthies, P. E., 1962, Evaluation of future operations south central area of Cut Bank field, Glacier County, Montana: In-house Report, Union Oil Company of California, El Segundo, California.
- McVay, D. A., W. B. Ayers, Jr., R. Gibson, J. L. Jensen, 2004, Advanced technology for infill and recompletion candidate well selection: DOE Report, Department of Petroleum Engineering, Texas A&M University, 86 p.
- Miall, A. D., 1996, The geology of fluvial deposits: Berlin, Springer-Verlag, 582 p.
- Nanson, G. C., 1980, Point bar and floodplain development of the meandering Beatton River, northeastern British Columbia, Canada: Sedimentology, v. 27, p. 3-29.
- Nilsen, T. H., 1982, Alluvial fan deposits sandstone depositional environment, *in* P. A. Scholle and D. Spearing, eds., Sandstone depositional environments: AAPG Memoir 31, p. 49–86.

- Peterson, J. A., 1986, General stratigraphy and regional paleotectonics of the western Montana overthrust belt, *in* J. A. Peterson, ed., Paleotectonics and sedimentation in the Rocky Mountain region, United States: AAPG Memoir 41, p. 57-86.
- Posamentier, H. W., M. T. Jervey, and P. R. Vail, 1988, Eustatic control on clastic deposition I-conceptual framework, *in* C. K. Wilgus, B. S. Hastings, C. G. St. C. Kendall, H. W. Posamentier, C. A. Ross, and J. C. Van Wagoner, eds., Sea-level changes: an integrated approach: SEPM Special Publication 42, p. 109–124.
- Quicksilver Resources, 2002, Cut Bank field database: Quicksilver Resources Inc., Fort Worth, Texas.
- Ravenne, C., R. Eschard, A. Galli, Y. Mathieu, L. Montadert, and J. L. Rudkiewicz, 1989, Heterogeneities and geometry of sedimentary bodies in a fluvio-deltaic reservoir: Society of Petroleum Engineers Journal Formation Evaluation, v. 4, p. 239–246.
- Remson, D. J., 2005, A forecast of marginal natural gas and oil well data: Topical report, U.S. Department of Energy National Energy Technology Laboratory, Work Performed Under Contract No. DE-AD26-01NT00612, <www.netl.doe.gov/publications/AP/MarginalWellData_Topical.pdf> (Accessed October 3, 2006).
- Robinson, J. W., and P. J. McCabe, 1997, Sandstone-body and shale-body dimensions in a braided fluvial system: Salt Wash sandstone (Morrison Formation), Garfield County, Utah: AAPG Bulletin, v. 81, no. 8, p. 1267-1291.

- Schumm, S. A., 1993, River response to base-level change: implications for sequence stratigraphy: *Journal of Geology*, no. 101, p. 279–294.
- Shanley, K. W., and P. J. McCabe, 1991, Predicting facies architecture through sequence stratigraphy-an example from the Kaiparowitz plateau, Utah: *Geology*, v. 19, p. 742–745.
- Shanley, K. W. and P. J. McCabe, 1994, Perspectives on the sequence stratigraphy of continental strata: *AAPG Bulletin*, v. 78, no. 4, p. 544–568.
- Shelton, J. W., 1967, Stratigraphic models and general criteria for recognition of alluvial, barrier-bar, and turbidity-current sand deposits: *AAPG Bulletin*, v. 51, no. 12, p. 2441-2461.
- Suttner, L. J., 1969, Stratigraphic and petrographic analysis of Upper Jurassic-Lower Cretaceous Morrison and Kootenai Formations, Southwest Montana: *AAPG Bulletin*, v. 53, no. 7, p. 1391-1410.
- Treckman, J. F., 1996, Geological evaluation of Cut Bank field, Montana: In-house Report, MSR Exploration Ltd., Fort Worth, Texas.
- Vail, P. R., Mitchum, R. M., Jr., Todd, R. G., Widmeri, J. W., Thompson, S., III, Sangree, J. B., Bubb, J. N., Hatelid, W. G., 1977, Seismic stratigraphy and global changes of sea-level, *in* C. E. Payton, ed., *Seismic stratigraphy-applications to hydrocarbon exploration*: AAPG Memoir 26, p. 49–212.
- Van Wagoner, J. C., H. W. Posamentier, R. M. Mitchum, P. R. Vail, J. F. Sarg, T. S. Loutit, and J. Hardenbol, 1988, An overview of the fundamentals of sequence stratigraphy and key definitions, *in* C. K. Wilgus, B. S. Hastings, C. G. St. C.

- Kendall, H. W. Posamentier, C. A. Ross, and J. C. Van Wagoner, eds., Sea-level changes: an integrated approach: SEPM Special Publication 42, p. 39–45.
- Van Wagoner, J. C., R. M. Mitchum, K. M. Campion, and V. D. Rahmanian, 1990, Siliciclastic sequence stratigraphy in well logs, cores and outcrops: concepts for high-resolution correlation of time and facies: AAPG Methods in Exploration 7, 55 p.
- Walker, T. F., 1974, Stratigraphy and depositional environments of the Morrison and Kootenai Formations in the Great Falls area, Central Montana: PhD dissertation, University of Montana, Missoula, Montana, 195 p.
- Weber, K. J., 1993, The use of 3-D seismic in reservoir geological modeling, *in* S. S. Flint and I. D. Bryant, eds., The geological modeling of hydrocarbon reservoirs and outcrop analogues: International Association of Sedimentologists Special Publication 15, p. 181–188.
- Weimer, R. J. and R. W. Tillman, 1982, Sandstone reservoirs: SPE Paper 10009.
- Wescott, W. A., 1993, Geomorphic thresholds and complex response of fluvial systems—some implications for sequence stratigraphy: AAPG Bulletin, v. 77, no.7, p. 1208–1218.
- Wheeler, H. E., and H. H. Murray, 1957, Base-level control patterns in cyclothermic sedimentation: AAPG Bulletin. no. 41, p. 1985–2011.
- Wood, J. M., 1996, Sedimentology and sequence architecture of incised-valley fills and interfluvial deposits: Upper Mannville interval (Lower Cretaceous), Little Bow-

Turin area, Southern Alberta: Bulletin of Canadian Petroleum Geology, v. 44, no. 4, p. 632-653.

Zaitlin, B. A., M. J. Warren, D. Potocki, L. Rosenthal and R. Boyd, 2002, Depositional styles in low accommodation foreland basin setting: an example from Basal Quartz (Lower Cretaceous), Southern Alberta: Bulletin of Canadian Petroleum Geology, v. 50, no.1, p. 31-72.

VITA

Rahila Ramazanova holds a Ph.D. in geology from Texas A&M University (2006), a M.S. in geology from Texas A&M University (2001), and a B.S. in geology from Azerbaijan Oil Academy (1990). During her graduate studies she served as a graduate research assistant working on a number of projects and as a graduate teaching assistant of interactive integrated reservoir studies course (GEOL 400 and 685 and PETE 400 and 685) taken by both senior undergraduate and graduate students. She worked as a geoscientist intern during the summer of 1999 for EXXON, Houston-USA, spring of 2001 for Anadarko Petroleum Corp., Houston-USA and fall of 2004 for Amerada Hess Corp., Houston-USA. Previously, she worked as a geoscientist for State Oil Company of Azerbaijan Republic, Baku-Azerbaijan (1994-1998), and as a geoscientist research assistant for Institute of Geology, Azerbaijan Academy of Sciences, Baku-Azerbaijan (1990-1994).

She is a member of the American Association of Petroleum Geologists, the Society of Petroleum Engineers and the Honor Society Phi Kappa Phi.

She can be reached c/o Dr. Walter B. Ayers, Jr., Department of Petroleum Engineering, Texas A&M University, College Station, TX 77843-3116.